

Supporting Information

for

Photocontrolled synthesis of n-type conjugated polymers

Eliot F. Woods, Alexandra J. Berl, and Julia A. Kalow*

Department of Chemistry, Northwestern University, 2145 Sheridan Rd, Evanston, IL 60208

E-mail: jkalow@northwestern.edu

Table of Contents

General information	2
Measured LED emission profiles.....	3
Procedures for monomer synthesis	6
Polymerization details.....	17
Yield duplications of monomers.....	19
Polymerization mass balance	19
GPC traces.....	25
Lithium chloride equivalents screen	38
Conversion assay details	38
Statistical copolymerization details.....	45
Block copolymerization details.....	50
Polymerization wavelength variation details.....	52
ICP-MS and control reaction details.....	55
UV-Vis spectra	63
NMR spectra	70
MALDI-TOF MS spectra.....	75
References	82

General information

General procedures. Unless otherwise noted, reactions were performed under Ar atmosphere in oven-dried (150 °C) glassware. Reaction progress was monitored by thin layer chromatography (EMD 250 μm silica gel 60-F254 plates) and visualized with potassium permanganate stain, or ceric ammonium molybdate stain and heat. Automated column chromatography was performed using SiliCycle SiliaFlash F60 (40-63 μm , 60 Å) in SNAP cartridges on a Biotage Isolera One. Organic solvents were removed in vacuo using a rotary evaporator (Büchi Rotovapor R-100, ~20–200 torr) and residual solvent was removed under high vacuum (<0.1 torr).

Materials. Commercial reagents were purchased from Sigma-Aldrich, Acros, Alfa Aesar, TCI, or Oakwood and used as received. 2-Ethylhexyl bromide was purchased from Sigma-Aldrich and distilled over calcium hydride prior to use. N-bromosuccinimide was recrystallized from water prior to use. All solvents were purified and dried using a solvent-purification system that contained activated alumina. Additionally, THF and Toluene were degassed before being stored in a nitrogen-filled glove box over activated 3Å sieves.

Instrumentation. Proton nuclear magnetic resonance (^1H NMR) spectra and carbon nuclear magnetic resonance (^{13}C NMR) spectra were recorded on Bruker AVANCE-500 spectrometers at 500 MHz, 600 MHz, and 125 MHz, and referenced to the solvent residual peaks. NMR data are represented as follows: chemical shift (δ ppm), multiplicity (s = singlet, d = doublet, t = triplet, q = quartet, m = multiplet), coupling constant in Hertz (Hz), integration. UV-vis spectra were collected on a Cary 5000 UV-vis-NIR spectrophotometer with an Hg lamp; cuvettes were 10-mm path length quartz cells (Starna 23-Q-10). Size exclusion chromatography (SEC) measurements were performed in stabilized, HPLC-grade tetrahydrofuran using an Agilent 1260 Infinity II system with variable-wavelength diode array (254, 400, 480, 530, and 890 nm) and refractive index detectors, guard column (Agilent PLgel; 5 μm ; 50 x 7.5 mm), and three analytical columns (Agilent PLgel; 5 μm ; 300 x 7.5 mm; 105 , 104 , and 103 Å pore sizes). The instrument was calibrated with narrow dispersity polystyrene standards between 640 g/mol and 2300 kg/mol (Polymer Standards Service GmbH). All runs were performed at 1.0 mL/min flow rate and 40 °C. Molecular weight values are calculated based on the refractive index signal. UV LED strip lights (wavelength = 400 nm, power = 6.1 W), blue LED strip lights (wavelength = 470 nm, power = 6.6 W) green LED

strip lights (wavelength = 525 nm, low power = 5.7 W, high power = 16 W), red LED strip lights (wavelength = 626 nm, power = 6.6W), and 4000 K white LEDs (power = 16.2 W) were purchased from superbrightleds.com. Emission spectra of LEDs was measured with an Ocean Optics Fiber coupled CCD spectrometer model number ADC1000-USB. Matrix-assisted laser desorption/ionization time of flight mass spectrometry (MALDI-TOF-MS) was performed on Bruker rapiflex MALDI-TOF Tissue typer in linear positive mode. Samples were prepared by dissolving 0.5 μL of a 2 g/mL solution of sample in THF with 10-100 μL 1,1,3,3-tetraphenylbutadiene (25 mg/mL in THF). The sample:matrix ratios were varied to achieve good signal to noise. The glove box in which specified procedures were carried out was an MBraun Unilab Pro with N_2 atmosphere. Inductively coupled plasma mass spectrometry (ICP-MS) measurements were made using a Thermo iCAP Q ICP-MS.

Measured LED emission profiles

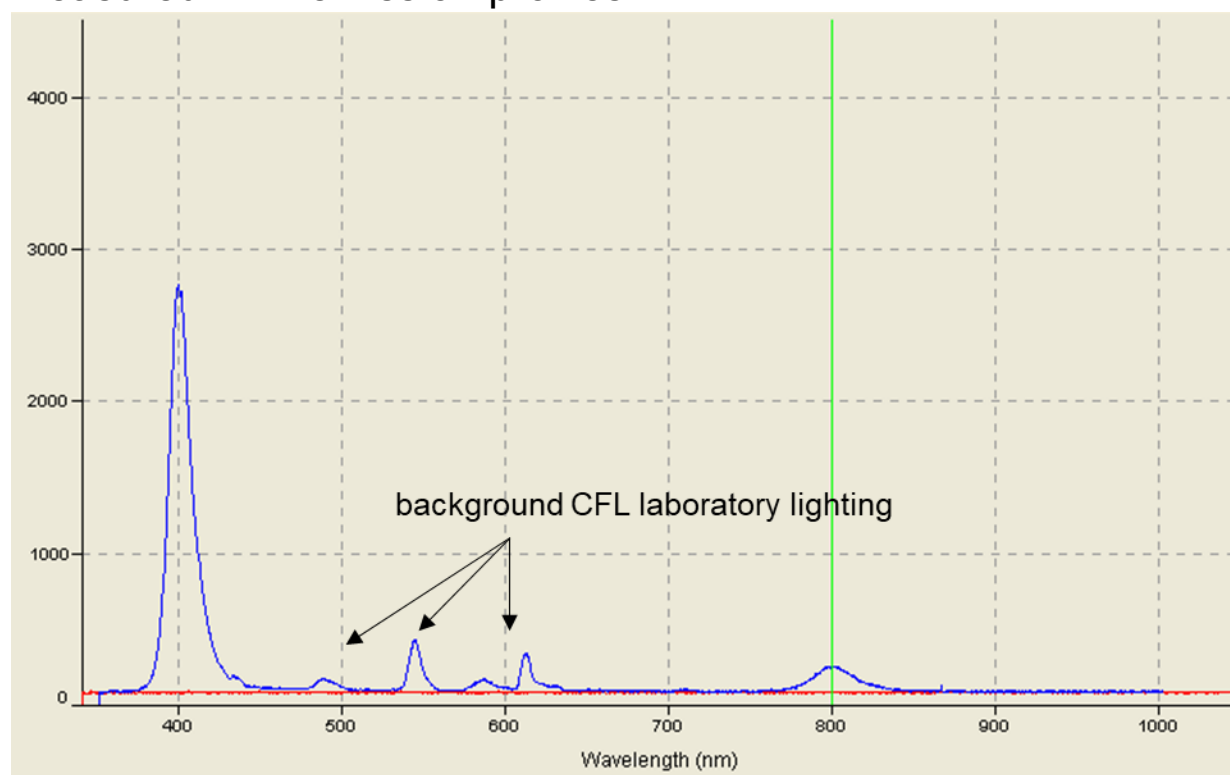


Figure S1. Measured emission spectra of "400 nm" LEDs used.

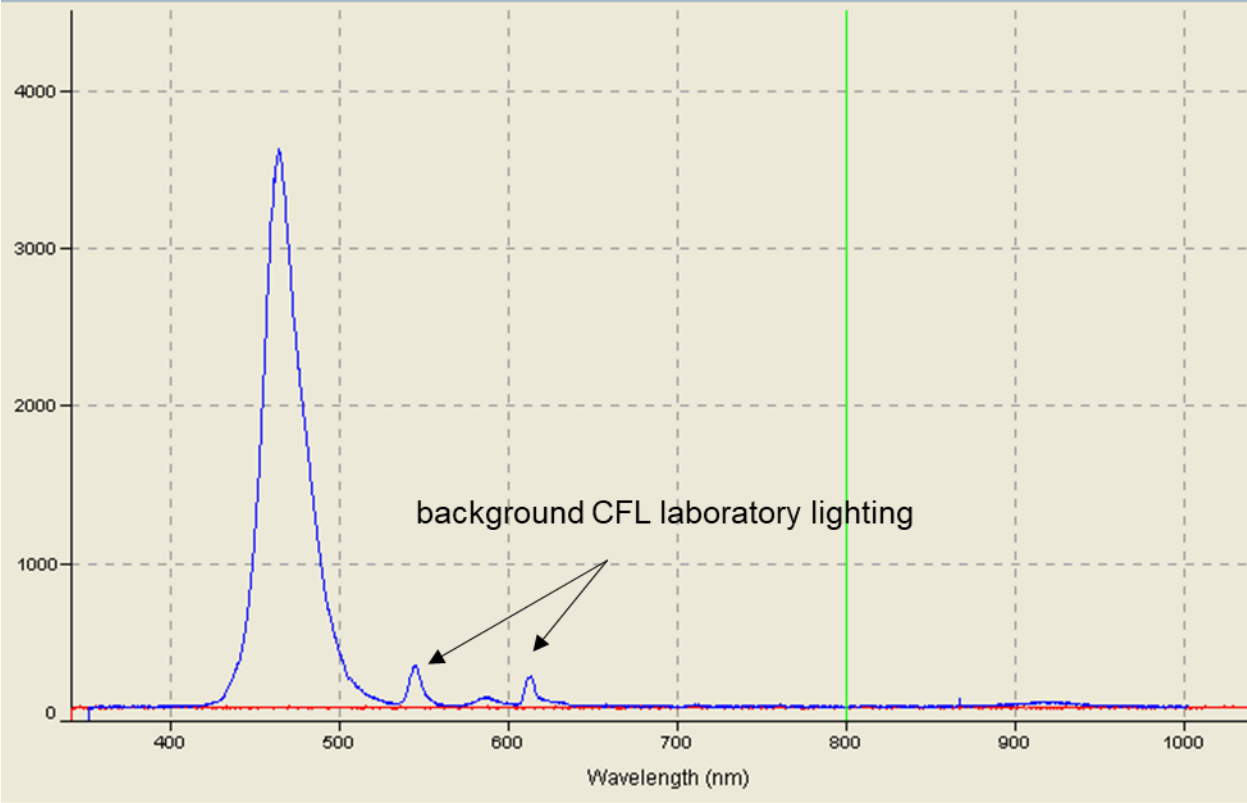


Figure S2. Measured emission spectra of "470 nm" LEDs used.

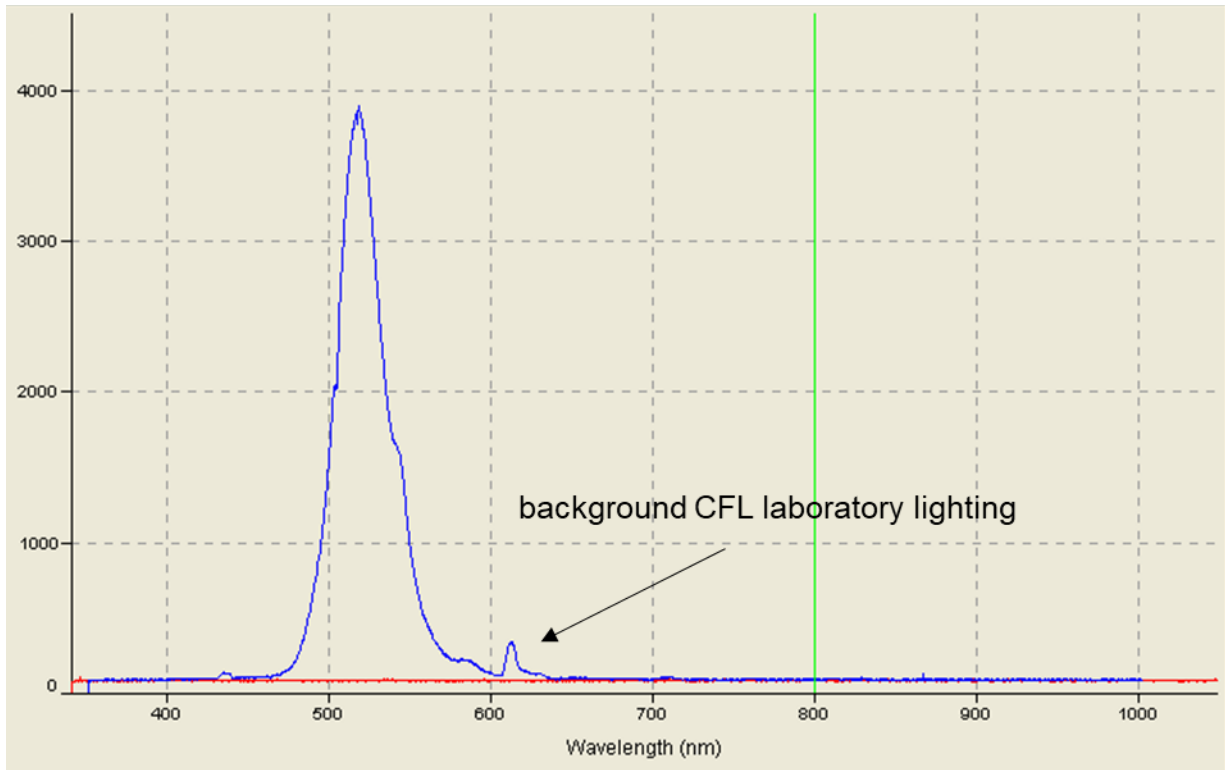


Figure S3. Measured emission spectra of "525 nm" LEDs used.

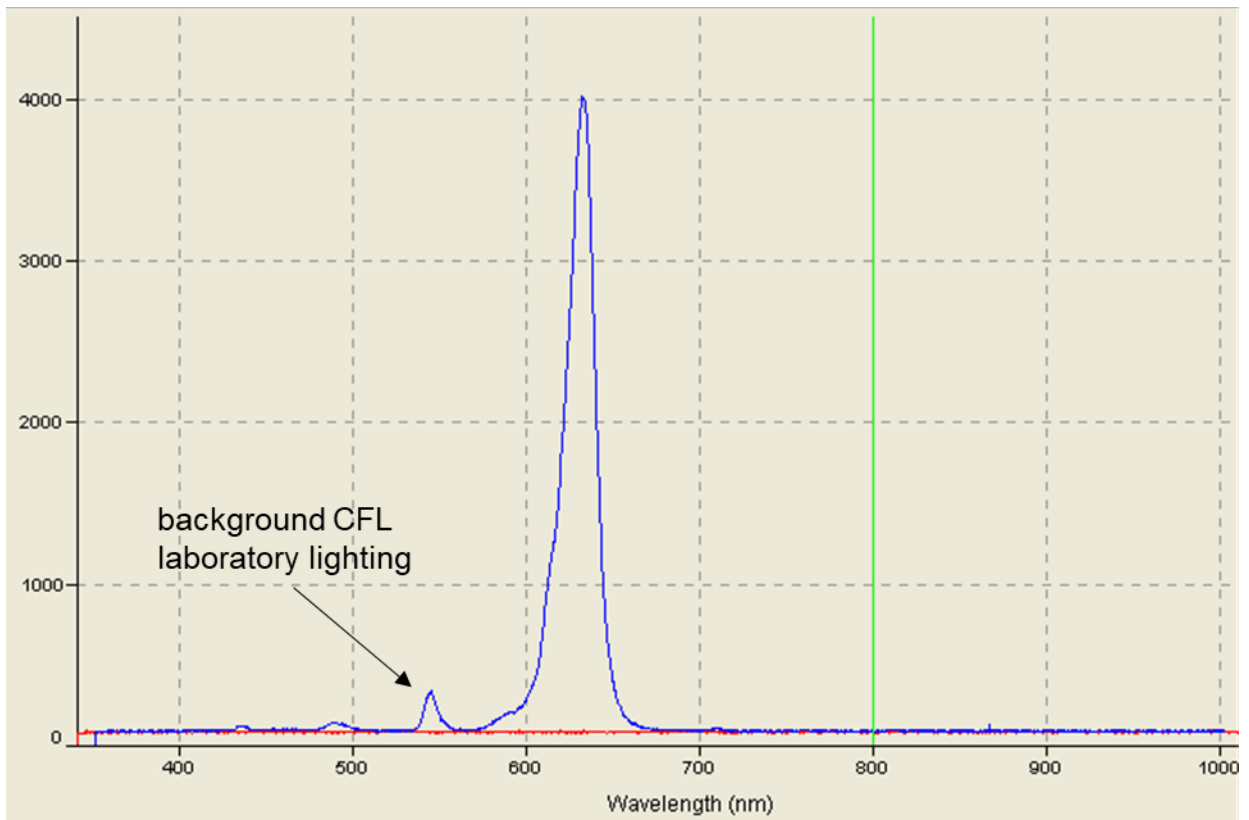


Figure S4. Measured emission spectra of "626 nm" LEDs used.

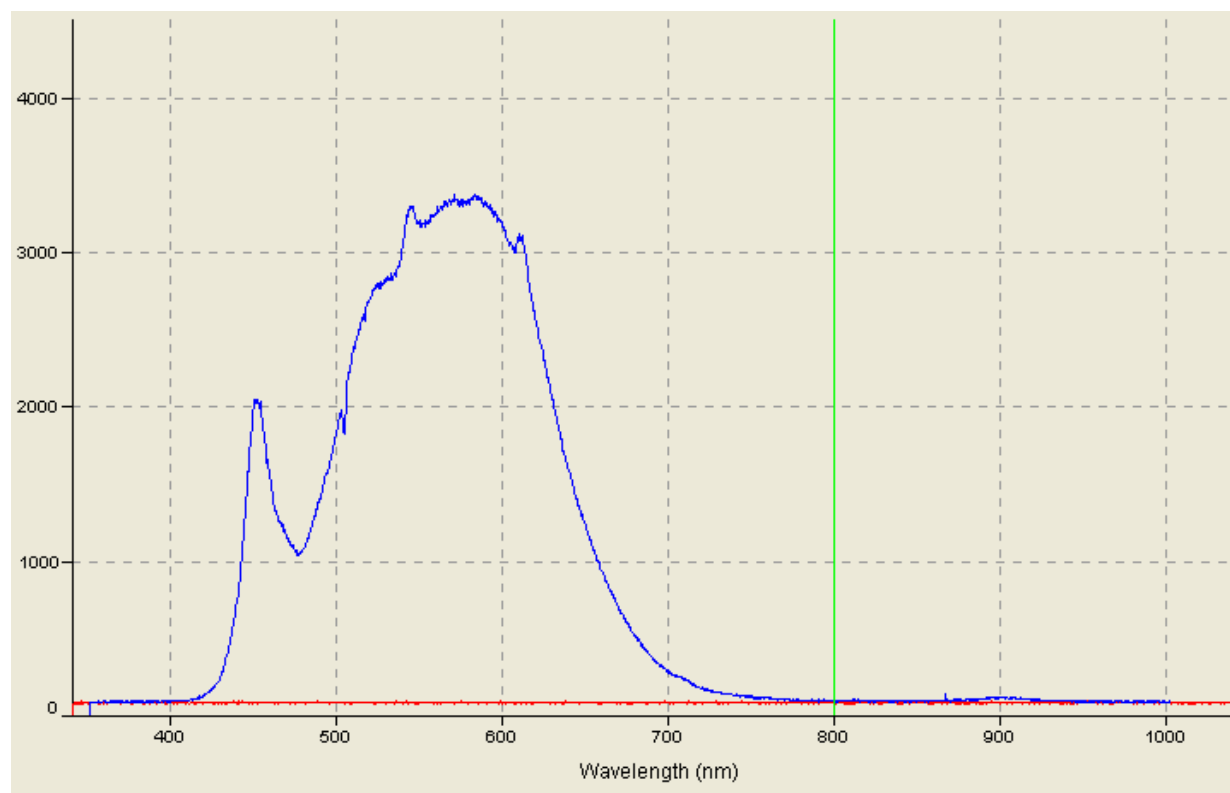
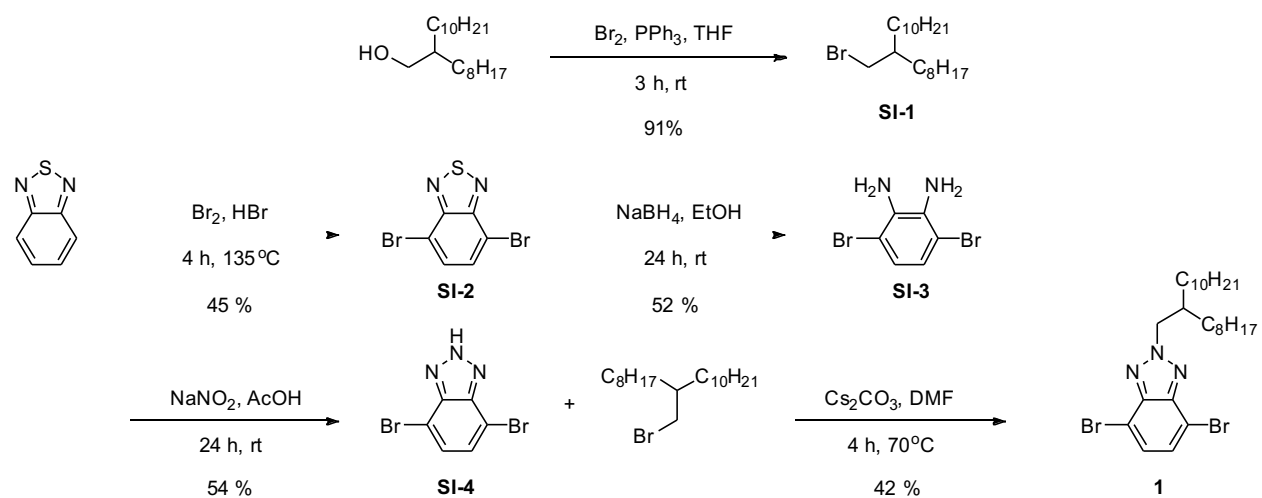
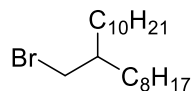


Figure S5. Measured emission spectra of “4000 K” white LEDs used.

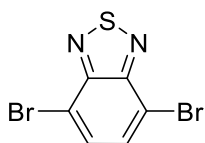
Procedures for monomer synthesis



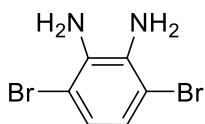
Scheme S1. Synthetic route of benzotriazole monomer for polymerization studies



9-(bromomethyl)nonadecane (SI-1) : Based on a modified literature procedure, 2-octyldodecan-1-ol (23.3 g, 78 mmol) and triphenylphosphine (91.9 g, 350 mmol) were dissolved in 1100 mL of THF in a 2000 mL round bottom flask equipped with stir bar. The solution was set to stir before bromine (16.1 mL, 312 mmol) was charged dropwise via addition funnel over the course of an hour. The reaction was stirred for 3 hours before 15 mL of MeOH was injected to quench the reaction. The reaction was concentrated *in vacuo* to produce white residue. This residue was washed with hexanes. The hexanes were removed *in vacuo* to produce a clear oil. The oil was passed through a four inch silica plug with hexanes to afford 9-(bromomethyl)nonadecane (**SI-1**, 25.8 g, 91%) as a clear oil. The spectral data were consistent with the literature report.¹



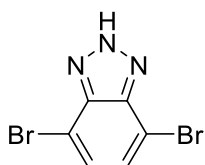
4,7-dibromobenzo[c][1,2,5]thiadiazole (SI-2) : Based on a modified literature procedure, benzo[c][1,2,5]thiadiazole (25.0 g , 183.7 mmol) was charged into 55 mL of hydrobromic acid in 250 mL round bottom flask equipped with stir bar. The solution was heated to 135 °C before bromine (24 mL, 459 mmol) was slowly injected into the reaction. The solution was refluxed for 2.5 hours before being allowed to cool to room temperature and diluted with water (100 mL). The red solid was collected *via* filtration and washed with 1000 mL of water before being recrystallized in chloroform to afford 4,7-dibromobenzo[c][1,2,5]thiadiazole (**SI-2**, 24.39 g 45%) as tan needles. The product was used in the subsequent step without further purification. The spectral data were consistent with the literature report.²



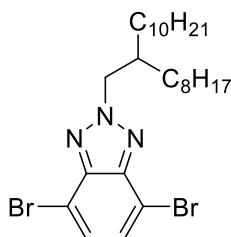
3,6-dibromobenzene-1,2-diamine (SI-3) : Based on a modified literature procedure, 4,7-dibromobenzo[c][1,2,5]thiadiazole (**SI-2**, 9.46 g, 32.2 mmol) was dissolved in 300 mL of ethanol in a 500 mL round bottom flask equipped with stir bar. The solution was cooled to 0 °C in an ice water bath. Under argon sodium borohydride (11.1 g, 293 mmol) was added portion-wise over the course 30 minutes. After 18 hours the solution was concentrated *in vacuo* to afford a tan

paste. The paste was taken up in water and extracted with diethyl ether (3x). The combined organic layers were dried over sodium sulfate, filtered and concentrated *in vacuo* to afford 3,6-dibromobenzene-1,2-diamine (**SI-3**, 4.48 g, 52%) as a tan solid. The product was used in the subsequent step without further purification. The spectral data were consistent with the literature report.²

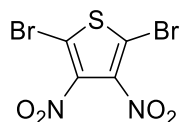
NOTE: The diamine is unstable under ambient conditions and should be stored under inert atmosphere.



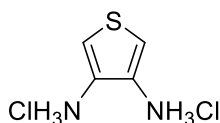
4,7-dibromo-2H-benzo[d][1,2,3]triazole (SI-4) : Based on a modified literature procedure, 3,6-dibromobenzene-1,2-diamine (**SI-3**, 24 g, 90 mmol) was dissolved in acetic acid (125 mL) in a 500 mL beaker equipped with stir bar. A solution of sodium nitrite (6.8 g, 99 mmol) dissolved in 140 mL of water was added into the beaker resulting in a beige precipitate. The suspension was then stirred for 15 minutes before the solid was collected *via* filtration and washed with water (400 mL) to afford 4,7-dibromo-2H-benzo[d][1,2,3]triazole (**SI-4**, 13.4 g, 54%). The product was used in the subsequent step without further purification. The spectral data were consistent with the literature report.³



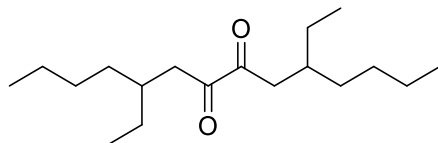
4,7-dibromo-2-(2-octyldodecyl)-2H-benzo[d][1,2,3]triazole (1): To a flame-dried 100 mL round bottom flask equipped with stir bar, 4,7-dibromo-2H-benzo[d][1,2,3]triazole (**SI-4**, 4.31 g, 11.9 mmol) and cesium carbonate (10.584 g, 32.5 mmol) and anhydrous DMF (50mL) were added. The reaction mixture was then heated to 70 °C for 30 minutes before 9-(bromomethyl)nonadecane (**SI-1**, 3.00 g, 10.9 mmol) was charged into the reaction. The reaction was stirred at 70 °C for 3 hours before being cooled to room temperature and diluted with water (100 mL). It was then extracted with ethyl acetate (3x). The combined organic layers were washed with brine (1x), dried



2,5-dibromo-3,4-dinitrothiophene (SI-5): Based on a modified literature procedure, concentrated sulfuric acid (20 mL) and fuming sulfuric acid (20 mL) were charged into a 100 mL round bottom flask equipped with stir bar. The solution was cooled in an ice water bath before 2,5-dibromothiophene (10 g, 41.3 mmol) was slowly charged into the flask. Concentrated nitric acid (6.5 mL) was slowly added to the solution dropwise. The reaction was stirred for 1 hour at 0°C before the solution was poured over crushed ice. The mixture was filtered cold and the orange solid was recrystallized in methanol to give 2,5-dibromo-3,4-dinitrothiophene (**SI-5**, 5.51 g 40%) as a green solid. The product was used in the subsequent step without further purification. The spectral data were consistent with the literature report.⁴

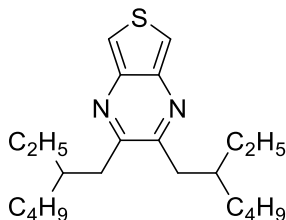


Thiophene-3,4-diaminium chloride (SI-6) : In a 250 mL round bottom flask equipped with a stir bar, 2,5-dibromo-3,4-dinitrothiophene (**SI-5**, 5.51 g, 16.6 mmol) was dissolved into 100 mL of ice cold hydrochloric acid. To it tin (powder) (14.5 g, 122.3 mmol) was added portion-wise over 2 hours at 0 °C, after which the reaction was allowed to warm to room temperature. The reaction was then stirred for more 2.5 hours after which the reaction was moved into a -20 °C freezer overnight. The next day the solution was filtered and to produce a yellow powder that was washed with acetonitrile and diethyl ether to afford thiophene-3,4-diaminium chloride (**SI-6**, 2.24 g, 72%) as a gray powder. The free base diamine is extremely sensitive to oxidation and is best stored as the salt. The diamine was collected and characterized by extraction of an aqueous solution of thiophene-3,4-diaminium chloride with ether and dried to afford white needles. The spectral data were consistent with the literature report.⁴

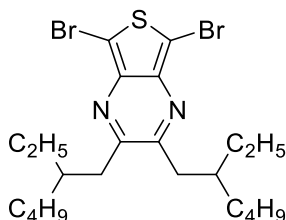


5,10-diethyltetradecane-7,8-dione (SI-7) : In a 100 mL schlenk flask, lithium bromide (4.44 g, 51.2 mmol) was heated under vacuum to melt, cooled and purged with argon and anhydrous tetrahydrofuran (40 mL) was added to it. In another separate 500 mL schlenk flask equipped with stir bar, anhydrous copper (I) bromide (6.71 g 46.8 mmol) and 40 mL of anhydrous tetrahydrofuran were added. The schlenk flask was then sealed, cycled with argon (3x). The lithium bromide solution was then charged into the 500 mL schlenk flask containing copper (I) bromide solution *via* cannula and cooled to -90 °C.

Meanwhile, in another separate 100 mL three neck round bottom flask equipped with stir bar, magnesium turnings (1.41 g, 58.3 mmol) and catalytic iodine was added, followed by addition of anhydrous tetrahydrofuran (40 mL). The solution was then stirred for 10 minutes at room temperature and a solution of 2-ethylhexyl bromide (10.0 g, 102 mmol) was added dropwise to the reaction mixture. The Grignard reaction was stirred for 20 mins at the same temperature before being cannula-transferred into the initial 500 mL schlenk flask containing copper (I) bromide solution. The flask was then cooled to -90 °C and oxalyl chloride (2.63 g, 20.7 mmol) was then added to it and stirred for more 1 hour. The reaction mixture was then allowed to warm to room temperature over 30 minutes and quenched with saturated ammonia chloride solution (20 mL). The solution was extracted with ethyl acetate (3x) and brine (1x). The combined organic layers were dried over sodium sulfate and concentrated *in vacuo* to produce a green residue. Crude material was purified *via* column chromatography (40-50% DCM : Hexanes) to afford the 5,10-diethyltetradecane-7,8-dione (**SI-7**, 3.33 g, 23%) as a yellow oil. The spectral data were consistent with the literature report.⁵

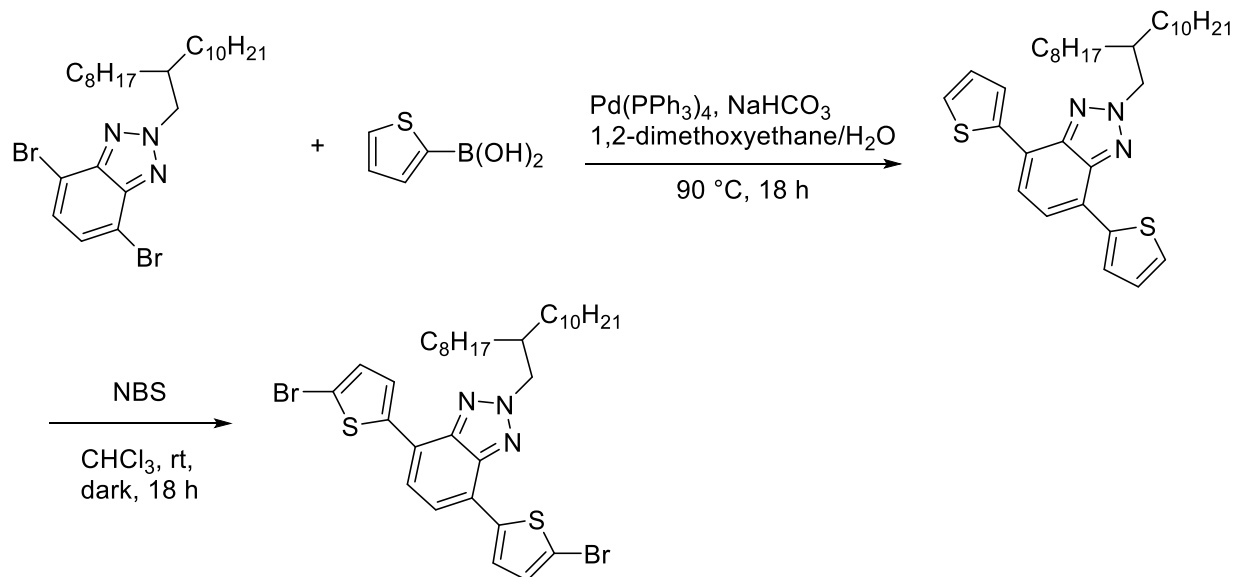


2,3-bis(2-ethylhexyl)thieno[3,4-b]pyrazine (SI-8) : Based on a modified literature procedure, thiophene-3,4-diaminium chloride (1.07 g, 5.74 mmol) and sodium carbonate (1.07 g, 10.2 mmol) were charged into a 500 mL round bottom flask equipped with stir bar followed by addition of anhydrous, degassed ethanol (350 mL). To it, 5,10-diethyltetradecane-7,8-dione (1.7 g, 6.1 mmol) was added and the reaction mixture was heated to 40 °C for 4 hours. The reaction was then cooled to room temperature and passed through a silica plug. The filtrate was concentrated and purified *via* column chromatography (40-50% DCM:Hexanes) to afford 2,3-bis(2-ethylhexyl)thieno[3,4-b]pyrazine (**SI-8**, 1.41 g, 71%) as a dark oil. The spectral data were consistent with the literature report.⁶

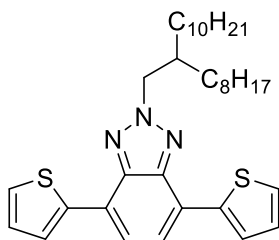


5,7-dibromo-2,3-bis(2-ethylhexyl)thieno[3,4-b]pyrazine (2) : In a 100 mL round bottom flask equipped with a stir bar, 2,3-bis(2-ethylhexyl)thieno[3,4-b]pyrazine (0.92 g, 2.54 mmol) was dissolved in into 50 mL of anhydrous dimethylformamide (DMF). The solution was then cooled to -40 °C and *N*-bromosuccinimide (1.21 g, 6.80 mmol) was added. The reaction was stirred at -40 °C for 2 hours before being poured into 150 mL water . The reaction mixture was then extracted using ethyl acetate (3x). The combined organic fractions were washed with brine, dried over sodium sulfate, filtered and concentrated *in vacuo*. Crude material was purified via column chromatography (100% hexanes) to afford 5,7-dibromo-2,3-bis(2-ethylhexyl)thieno[3,4-b]pyrazine (**2**, 0.44 g, 34%) as a red oil.⁶

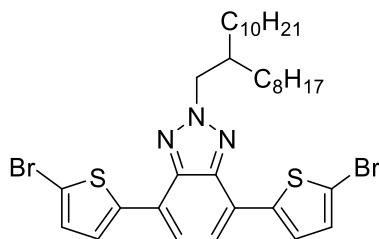
NOTE: The compound should be stored cold (-20°C) in the dark.



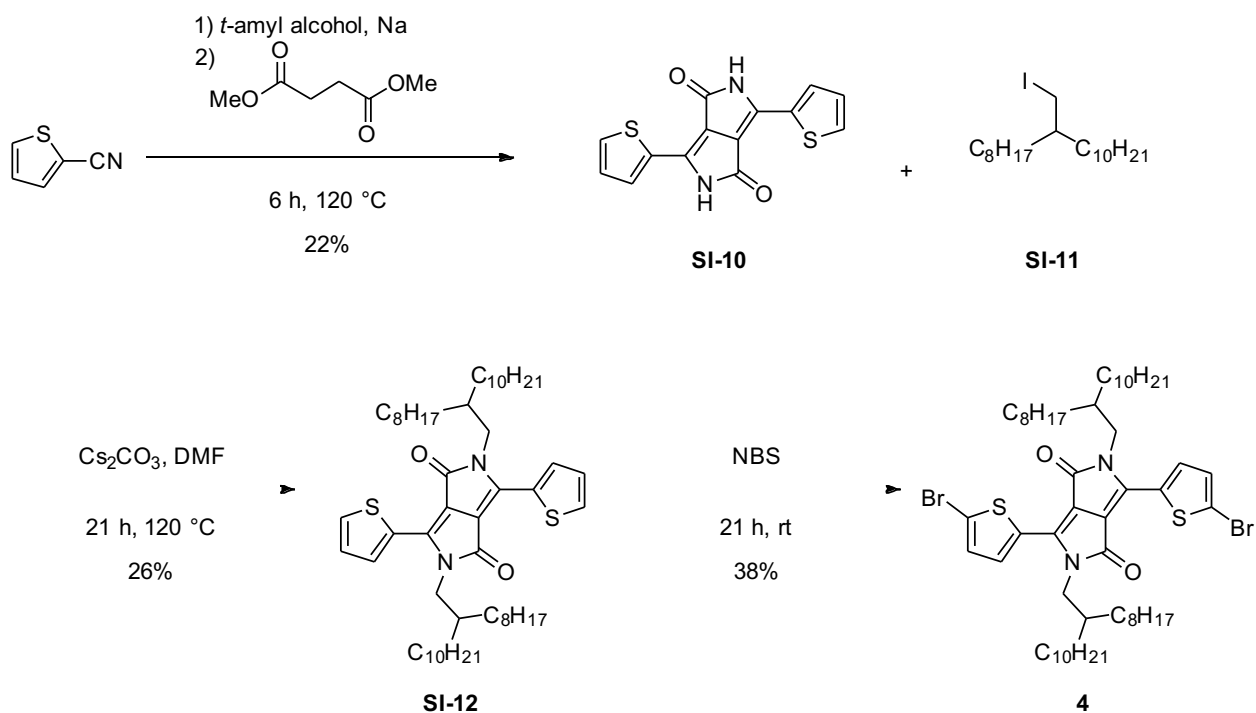
Scheme S3. Synthetic route of benzotriazole ABA monomer for polymerization studies



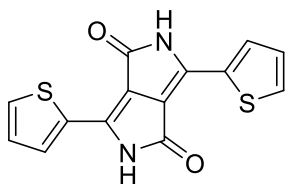
2-(2-(8-oxydodecyl)-4,7-di(thiophen-2-yl)-2H-benzo[d][1,2,3]triazole (SI-9) : A 50 mL flame-dried flask equipped with a stir bar was charged with **1** (1.06 g, 1.90 mmol), thiophene-2-boronic acid (2.20 g, 18.8 mmol), sodium bicarbonate (159 mg, 1.90 mmol), tetrakis(triphenylphosphine)palladium(0) (43.9 mg, 38.0 μ mol), 1,2-dimethoxyethane (18 mL) and water (19 mL). The solution was degassed and the reaction was stirred at 90 °C overnight. The crude product was extracted in DCM (3x), washed with water (2x) and brine (1x), dried over magnesium sulfate and concentrated. The product was purified by flash column chromatography on silica gel (20% PhMe in hexanes) and concentrated to afford (**SI-9**, 0.79 g, 74%) a light yellow solid. The spectral data were consistent with the literature report.⁷



4,7-bis(5-bromothiophen-2-yl)-2-(2-octyldodecyl)-2H-benzo[d][1,2,3]triazole (SI-10) : A 250 mL RBF with stir bar was charged with **SI-10** (402 mg, 713 μ mol) and CHCl_3 (140 mL) and stirred in the dark for 10 minutes. Then NBS (634 mg, 3.56 mmol) was added in one portion and the reaction was stirred in the dark at room temperature overnight. The crude product was extracted with DCM (3x), washed with water (2x) and brine (1x), dried over magnesium sulfate, and concentrated. The crude product was purified by flash column chromatography on silica gel (30% DCM in hexanes) and concentrated to afford (SI-10, 0.43 g, 84%) a bright yellow solid. The spectral data were consistent with the literature report.⁷

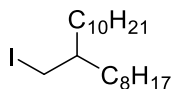


Scheme S4. Synthetic route of 4,7-bis(5-bromo-3-octylthiophen-2-yl)benzo[c][1,2,5]thiadiazole monomer for polymerization studies



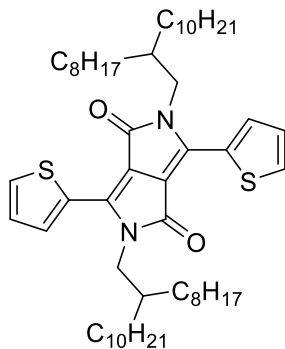
3,6-di(thiophen-2-yl)-2,5-dihydropyrrolo[3,4-c]pyrrole-1,4-dione (SI-11) :

Based on a modified literature procedure, in a 250 mL flame-dried round bottom flask equipped with a stir bar was charged with *t*-amyl alcohol (105 mL) and sodium metal (1.05 g, 45.8 mmol) was added and the reaction was stirred at 120 °C for 2 h until all the sodium had dissolved. To it, Thiophene-2-carbonitrile (5.00 g, 45.8 mmol) was added followed by addition of dimethyl succinate (2.24 g, 15.3 mmol) *via* syringe pump over 1 hour. The reaction was stirred at 120 °C for 3 hours, then precipitated into acidic methanol (200 mL methanol + 10 mL conc. hydrochloric acid) to form a purple suspension. The solid product was filtered and dried *in vacuo* overnight to yield 3,6-di(thiophen-2-yl)-2,5-dihydropyrrolo[3,4-c]pyrrole-1,4-dione (2.99 g, 65%) as a maroon solid. The spectral data were consistent with the literature report.⁸



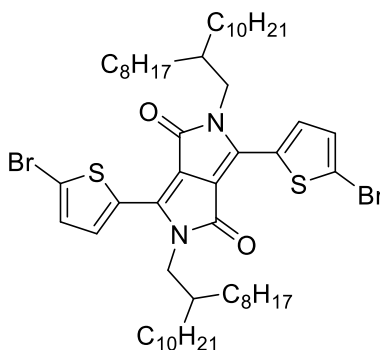
9-(iodomethyl)nonadecane (SI-12) :

Based on a modified literature procedure, 2-octyldodecyl-1-ol (9.30 g, 31.2 mmol), imidazole (2.62 g, 38.5 mmol), and triphenylphosphine (9.06 g, 34.6 mmol) were dissolved in anhydrous dichloromethane (70 mL) in a 250 mL round bottom flask equipped with stir bar. The solution was stirred at 0 °C for 15 minutes before metallic iodine (9.54 g, 37.6 mmol) was added in portions over 15 minutes. The reaction was stirred at 0 °C for 2 hours and concentrated *in vacuo*. The crude product was taken up in sodium thiosulfate (10 mL), extracted in hexanes (3x), washed with water (2x) and brine (1x), then dried over sodium sulfate and concentrated. The crude product was purified *via* flash column chromatography on silica gel (100% hexanes) to yield 9-(iodomethyl)nonadecane (9.01 g, 71%) as a clear oil. The spectral data were consistent with the literature report.⁹



2,5-bis(2-octyldodecyl)-3,6-di(thiophen-2-yl)-2,5-dihydropyrrolo[3,4-c]pyrrole-1,4-dione (SI-13) :

In a flame-dried 100 mL round bottom flask equipped with stir bar 3,6-di(thiophen-2-yl)-2,5-dihydropyrrolo[3,4-c]pyrrole-1,4-dione (**SI-11**, 1.00 g, 3.34 mmol), and cesium carbonate (3.26 g, 10.0 mmol) and anhydrous dimethylformamide (40 mL) were added. The solution was stirred at 120 °C for 3 hours, then 9-(iodomethyl)nonadecane (**SI-12**, 3.39 g, 8.31 mmol) was added dropwise and the reaction was stirred at 140 °C for 18 hours. The reaction was then cooled to 0 °C, filtered and washed with chloroform. The filtrate was concentrated *in vacuo* and the crude material was purified *via* column chromatography (40-45% DCM : Hexanes) to yield 2,5-bis(2-octyldodecyl)-3,6-di(thiophen-2-yl)-2,5-dihydropyrrolo[3,4-c]pyrrole-1,4-dione (737 mg, 26%) as a purple solid.⁸



3,6-bis(5-bromothiophen-2-yl)-2,5-bis(2-octyldodecyl)-2,5-dihydropyrrolo[3,4-c]pyrrole-1,4-dione (SI-14):

A 20 mL scintillation vial equipped with a stir bar was charged with 2,5-bis(2-octyldodecyl)-3,6-di(thiophen-2-yl)-2,5-dihydropyrrolo[3,4-c]pyrrole-1,4-dione (**SI-13**, 361 mg, 4.19 mmol) and CHCl₃ distilled over calcium hydride (12.5 mL). The solution was stirred in the dark at room temperature for 20 minutes, then *N*-bromosuccinimide (187 mg, 1.05 mmol) was added and the reaction was stirred in the dark for 18 hours. The solution was diluted with water, then extracted

in CHCl₃ (3x), washed with water (2x) and brine (1x) and dried over sodium sulfate. The organic phase was concentrated *in vacuo* and purified by flash column chromatography on silica gel (10-12% Et₂O : Hexanes) to yield 3,6-bis(5-bromothiophen-2-yl)-2,5-bis(2-octyldodecyl)-2,5-dihydropyrrolo[3,4-c]pyrrole-1,4-dione (170 mg, 52%) as a purple solid. The spectral data were consistent with the literature report.⁸

NOTE: The compound should be stored cold (−20 °C) in the dark.

Polymerization details

General experimental considerations:

Monomer, LiCl, and magnesium bromide solutions were prepared inside of a glove box with H₂O detector reading below 5 ppm and O₂ level readings below the limit of detection, <0.1 ppm. It is essential to the polymerization that O₂ levels be as low as possible in the glove box before removing the solutions for *n*-BuLi or *i*-PrMgBr addition and irradiation outside the glovebox. We observed that glovebox O₂ levels at or above 0.3 ppm O₂ during reaction set-up resulted in inconsistent initiation of polymerization reactions. Stir bars used were cleaned with piranha acid before use to minimize batch variation between polymerizations. Syringes were purged with Ar before injection of any reagent into the polymerization reaction vials.

When the polymerizations were conducted entirely in the glovebox, using either method, long initiation times (> 6 hours) were observed. Additionally, polymerizations produced lower molecular weight species when conducted under an active flow of argon as opposed to static argon. While these observations suggest a mechanistic role for molecular oxygen in the initiation step of polymerization, detailed mechanistic understanding is beyond the scope of this study.

General procedure A: Polymerization using *n*-butyllithium and magnesium bromide diethyl etherate to generate Grignard monomer

Vial 1- Into a 2 dram vial equipped with a stir bar, 1 equivalent monomer and 15 equivalents lithium chloride were charged. THF was added to reach a solution concentration of 66 mM with respect to the monomer.

Vial 2- Into a separate vial, magnesium bromide diethyletherate (1 equiv.) and THF to reach a solution concentration of 190 mM.

Both vials were then sealed with septum caps and taped before being removed from the glove box.

The monomer solution (**Vial 1**) was then cooled to $-78\text{ }^{\circ}\text{C}$ before *n*-butyllithium (2.5 M in hexanes, 0.9 equiv.) was added to the solution. The vial was then covered with foil to protect from light. After stirring for 10 minutes, the magnesium bromide diethyl etherate solution from **Vial 2** (sonicated for homogeneity) was injected into the monomer **Vial 1**. The vial was stirred for 20 minutes before being removed from the dry ice bath acetone ($-78\text{ }^{\circ}\text{C}$) bath and stirred for an additional 30 minutes at room temperature. The vial is then placed under LED irradiation with high stirring, and overhead fan to prevent heating. After 24 hours of irradiation the solution was precipitated into methanol. If solubility of the polymer allowed, the sample was then reprecipitated into acetone (2X).

General procedure B : Polymerization using *i*-PrMgBr to generate Grignard monomer

Into a 2 dram vial equipped with a stir bar, 1 equivalent monomer and 15 equivalents lithium chloride were charged. THF was added to reach a solution concentration of 50 mM with respect to the monomer. The vial was then sealed with a septum cap and tapped before being removed from the glove box.

The vial was covered with foil before *iso*-propylmagnesium bromide (*i*-PrMgBr, 0.70 M in THF, 1.0 equiv.) was injected into the vial. The vial was stirred for 20 minutes before being placed under LED irradiation with high stirring and overhead fan to prevent heating. After 24 hours of irradiation, the solution was precipitated into methanol. If solubility of the polymer allowed, the sample was then reprecipitated into acetone (2X).

Yield duplications of monomers

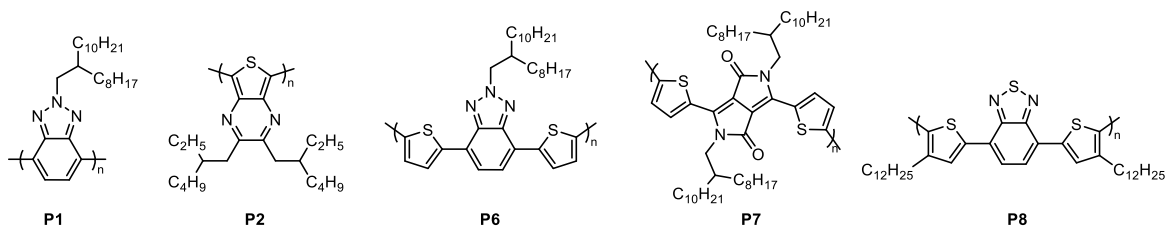


Table S1. Full yield and GPC characterization of polymer scope.

Polymer	M_n (kg/mol)	\bar{D}	Yield (%)
P1 Run 1	13.7	1.61	39
P1 Run 2	11.6	1.60	35
P2 Run 1	7.9	1.99	75
P2 Run 2	7.6	1.56	67
P6 Run 1	1.6	1.19	37 ^a
P6 Run 2	1.9	1.18	21 ^a
P7^b Run 1	3.3	1.43	46
P7^b Run 2	3.5	1.61	38
P8^c Run 1	2.4	1.16	19
P8^c Run 2	2.3	1.19	31

^a Characterization of THF soluble fraction. ^bPrevious reports of a similar diketopyrroloepyrrole ABA monomer by Janssen and coworkers showed higher molecular weights but used required elevated temperatures for the polymerization (80°C toluene) and elevated temperature GPC conditions (80 °C o-dichlorobenzene SEC) for characterization.¹⁰ ^bPrevious reports of a similar benzothiadiazole ABA monomer by Janssen and coworkers showed higher molecular weights but used required halogenated solvents (25 °C chloroform) for the polymerization and halogenated solvent for GPC conditions (25 °C chloroform SEC) for characterization.¹¹

Polymerization mass balance

To better understand the fate of **1** after the polymerization, we conducted a mass balance experiment to identify and quantify all produced species. A polymerization was performed using **1** (30.5 mg) using *general procedure A*. After the crude material was precipitated into methanol, the supernatant was concentrated and extracted in chloroform to remove salts, and concentrated. The solids were then precipitated into acetone, and the supernatant was concentrated and extracted in chloroform. The final polymer **P1** was isolated in 36% overall yield. The results are shown in Table S2, and spectral data used to characterize each fraction (NMR and MALDI-TOF) are shown in Figures S6-S10.

Table S2. GPC results of **P1** from the mass balance experiment. Molecular weights determined relative to polystyrene standards.

Product	Dry Mass (mg)	Mass (%)	M _n (kg/mol)	Đ	Contents
MeOH supernatant	11.0	38	N/A ^a	N/A	Debrominated monomer
Acetone supernatant	10.4	36	1.6	1.3	Oligomers
Polymer (P1)	7.6	26	13.7	1.5	Polymer

^aMolecular weight below the polystyrene calibration limit of the instrument (800 g/mol PS standard)

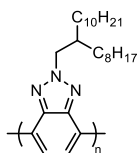
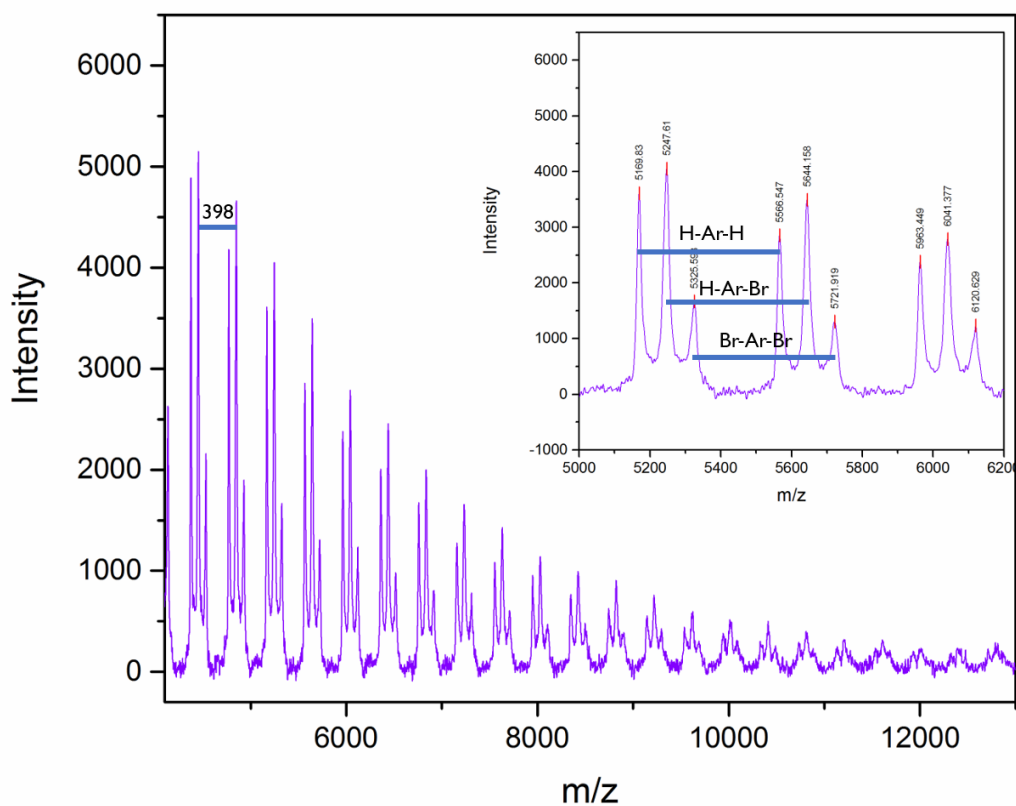


Figure S6: MALDI-TOF of the polymer from the mass balance experiment. Peaks separated by 398 are **P1** repeat units. Inset: magnified spectrum to show H-Ar-H species, H-Ar-Br species, and Br-Ar-Br. See figure S50 for ¹H NMR of **P1**

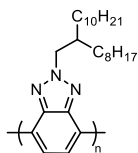
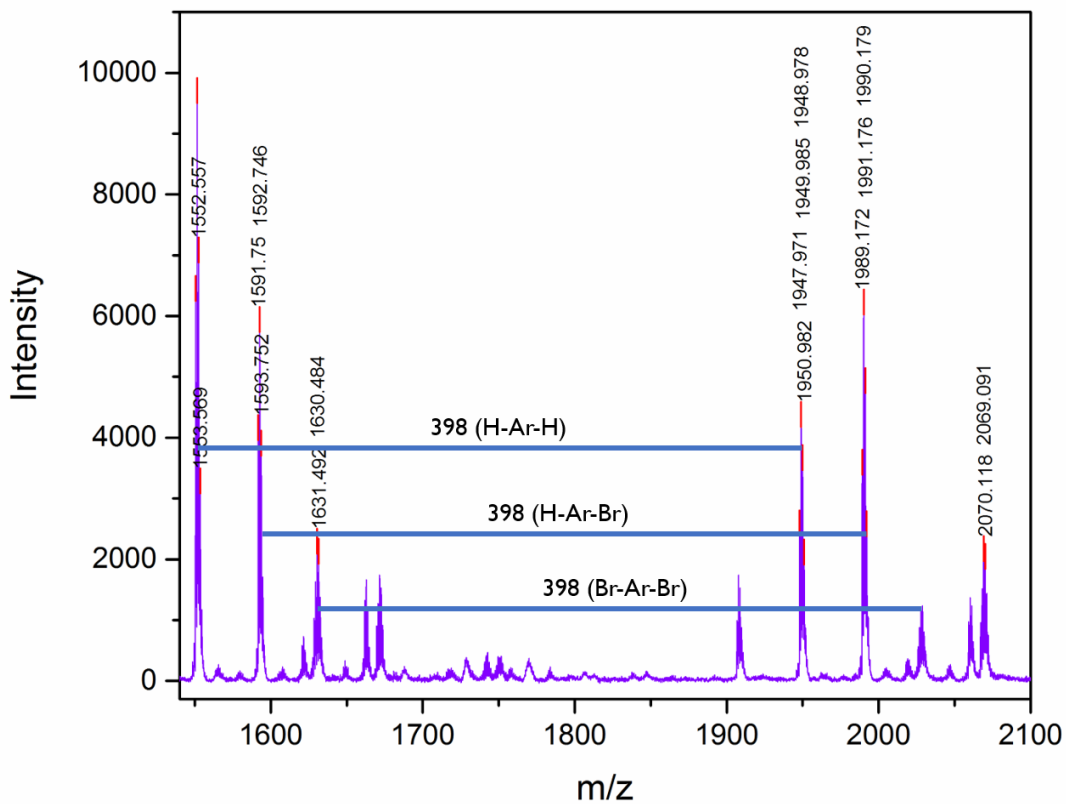


Figure S7: MALDI-TOF of the oligomers collected from the acetone fraction. Peaks separated by 398 are BTz repeat units (H-Ar-H), and the peaks 80 and 160 m/z higher are singly (H-Ar-Br) and doubly brominated (Br-Ar-Br) oligomers, respectively. Major peaks are DP = 4 (left) and 5 (right).

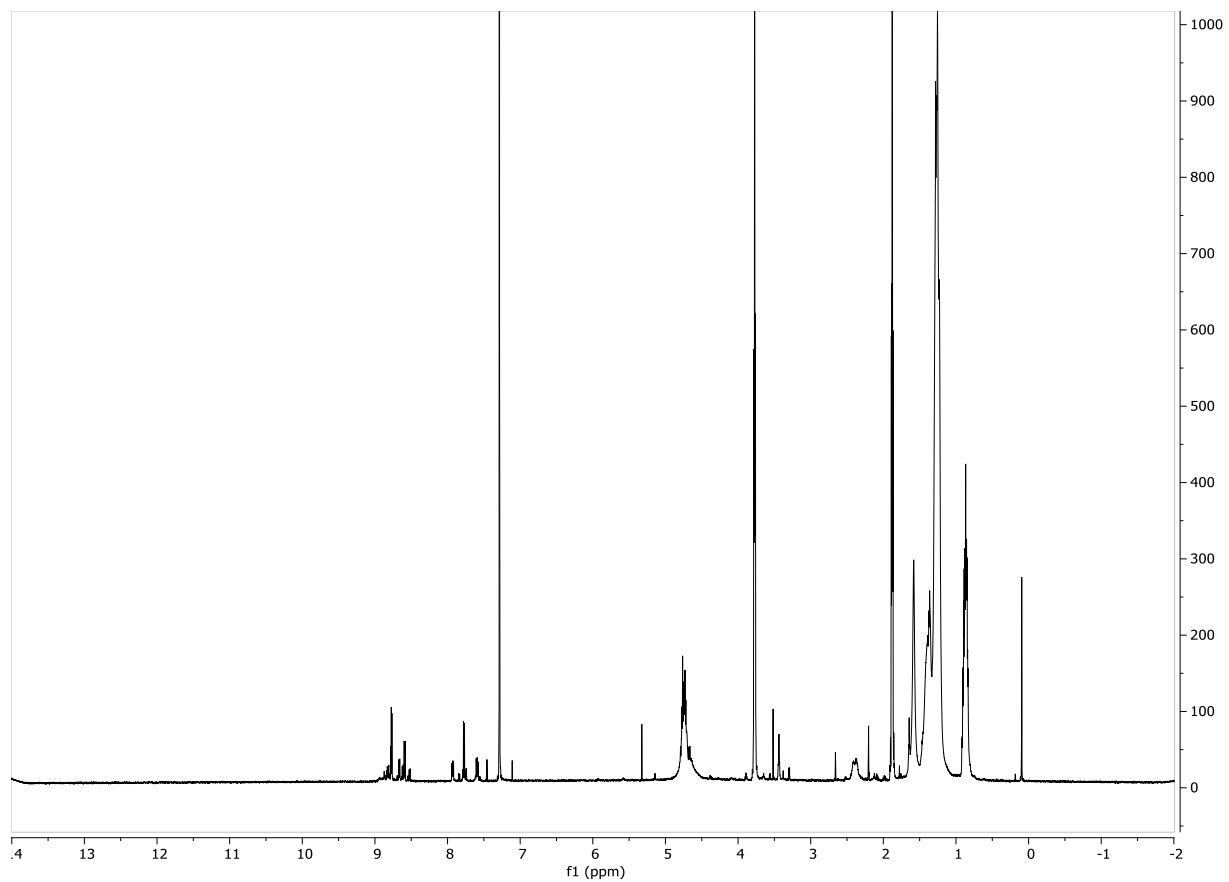


Figure S8: $^1\text{H-NMR}$ (500 MHz, CDCl_3) spectrum of the acetone fraction.

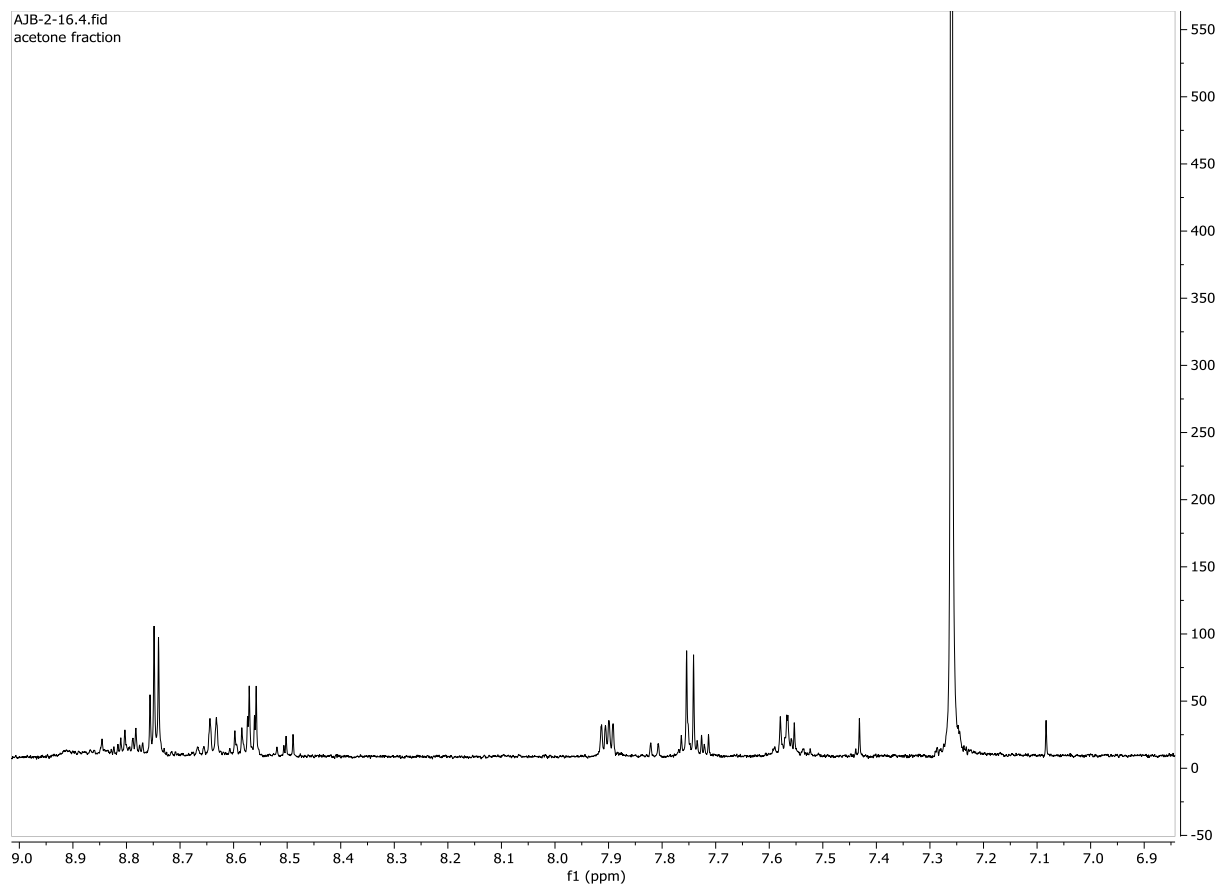


Figure S9: Aromatic region of the ^1H -NMR (500 MHz, CDCl_3) spectrum of the acetone fraction.

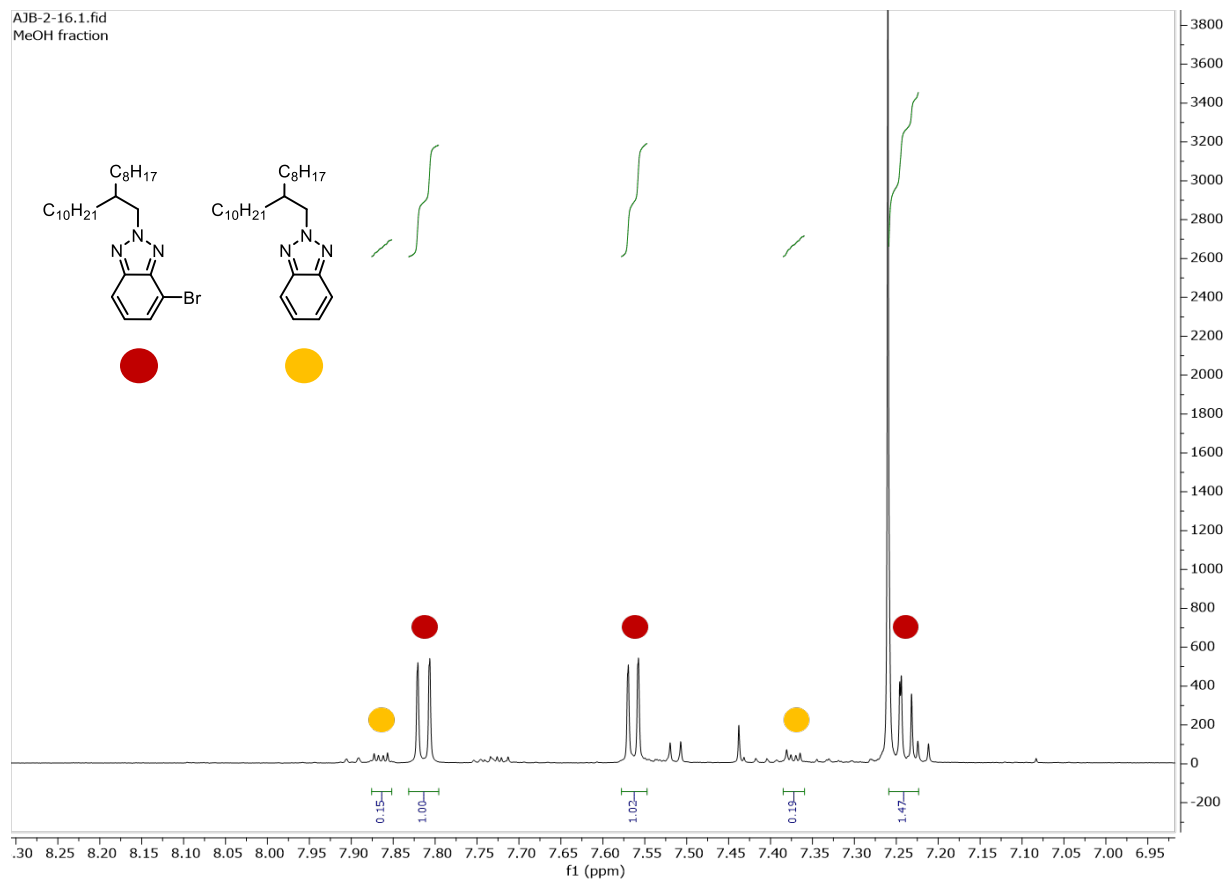


Figure S10: ^1H NMR of the MeOH fraction from the mass balance experiment, with red dots denoting the singly debrominated **1** and yellow dots denoting the doubly debrominated **1**.

GPC traces

Note: For reactions where precipitation of the polymer was not possible, crude reactions mixtures were submitted. In these cases the RI signal is dominated by the recovered monomer in the sample, and thus the trace polymer seen by UV-vis detection at 480 nm is not observed in the RI (e.g., Figure S12).

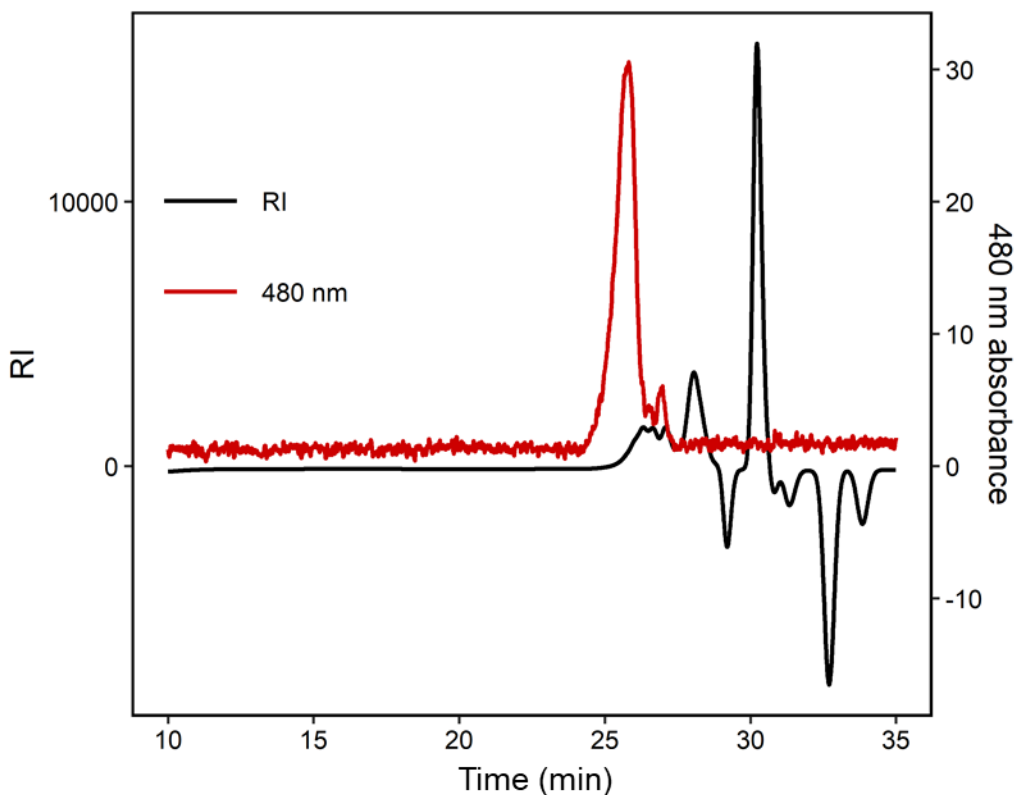


Figure S11. GPC traces of reaction solution for Table 1, entry 1. GPC sample was obtained from chloroform extraction of crude material.

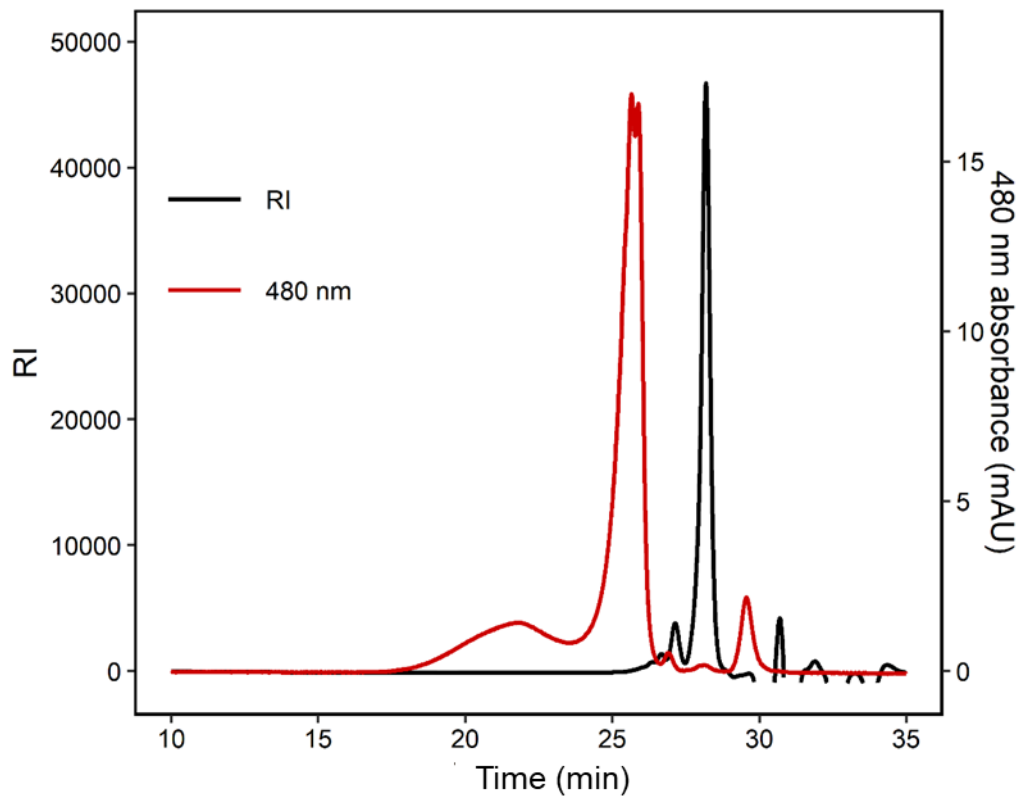


Figure S12. GPC traces of reaction solution for Table 1, entry 2. GPC sample was obtained from chloroform extraction of crude material.

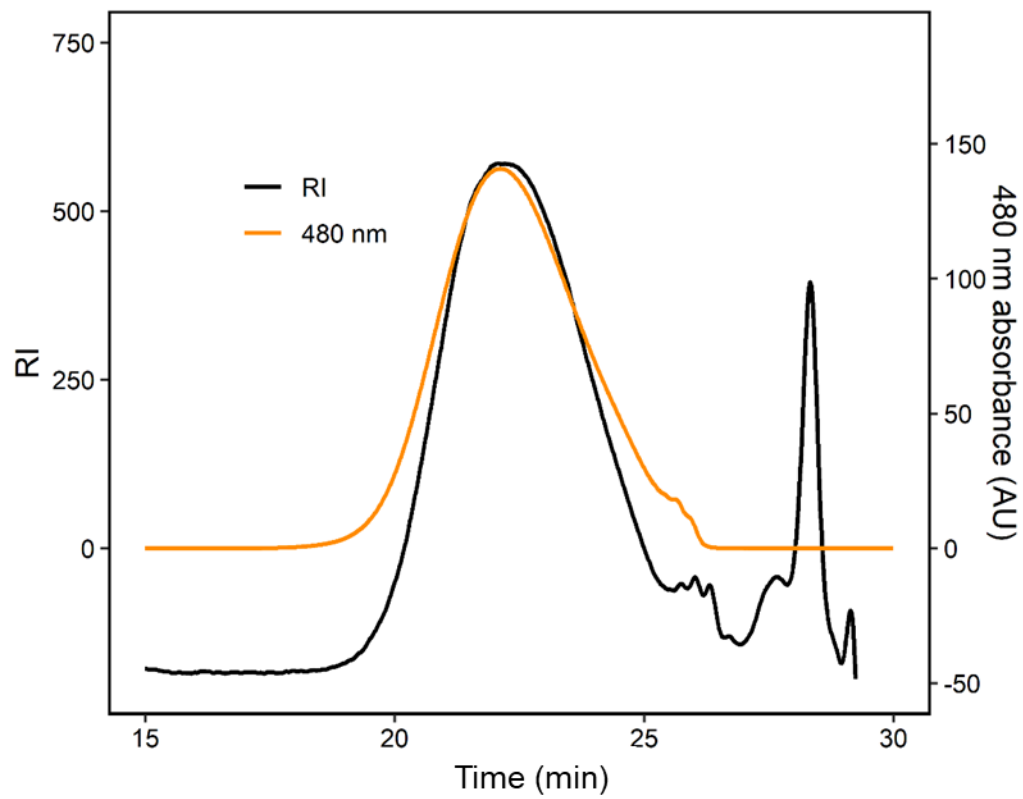


Figure S13. GPC traces of **P1** from Table 1, entry 3.

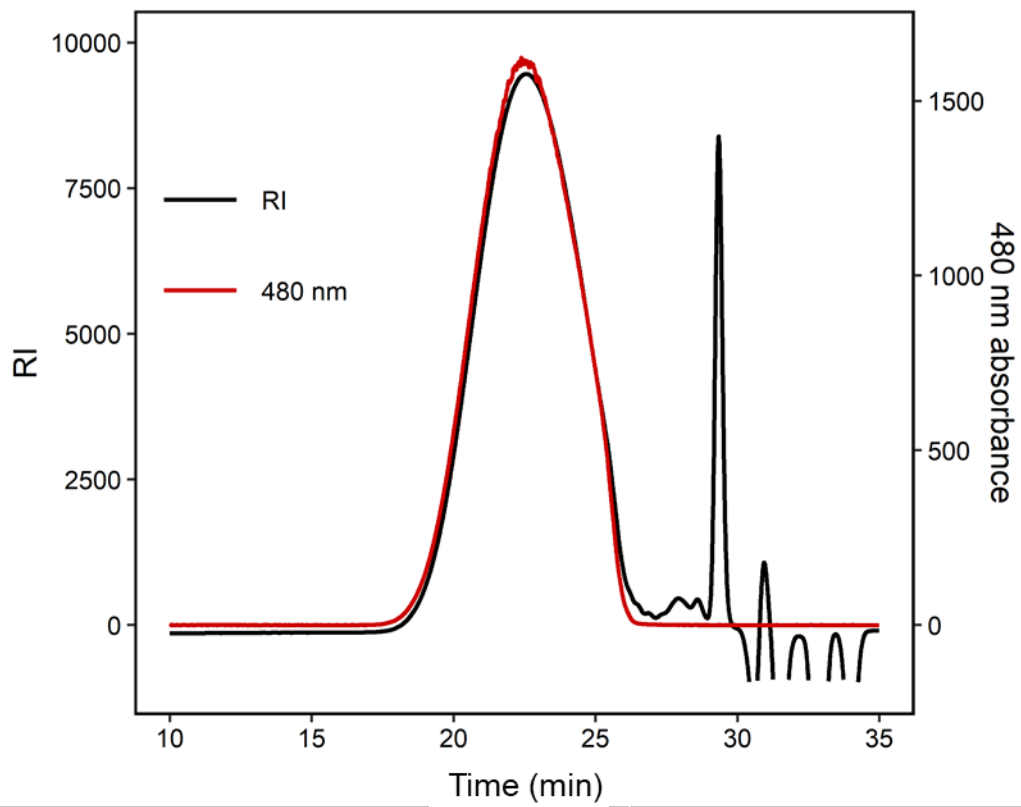


Figure S14. GPC traces of **P1** from Table 1, entry 4.

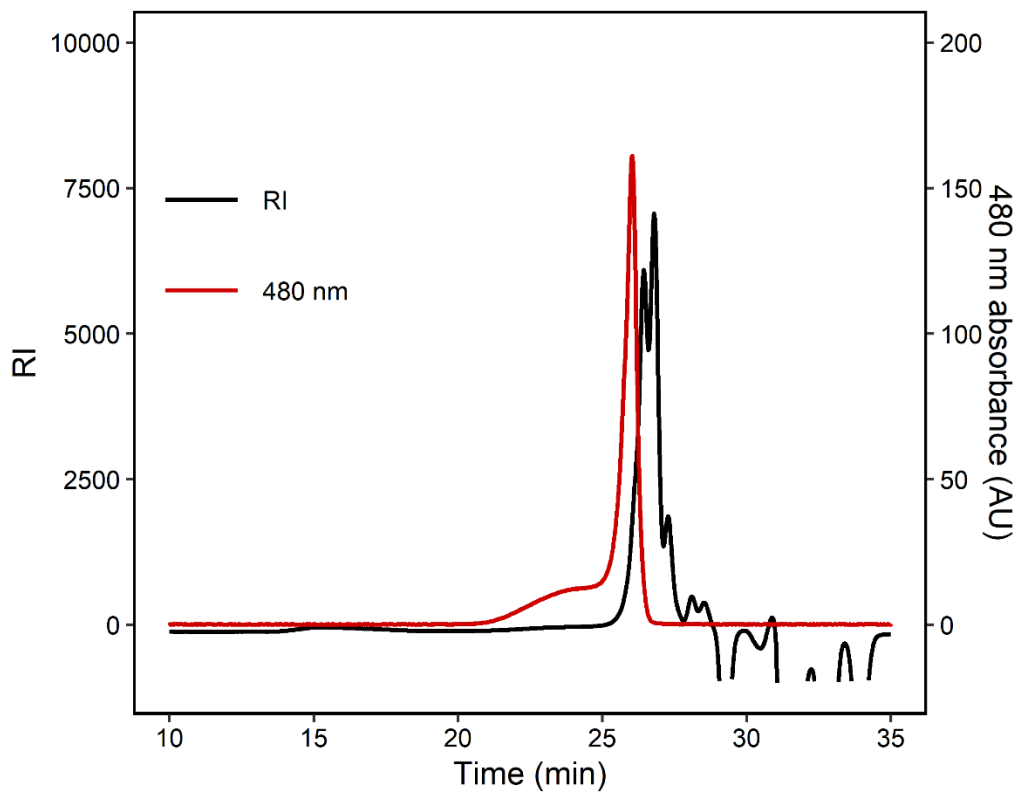


Figure S15. GPC traces of **P1** from Table 1, entry 5. M_n 3.2 kg/mol, \bar{D} 1.57 vs polystyrene standards. GPC sample was obtained from chloroform extraction of crude material to remove Li salts.

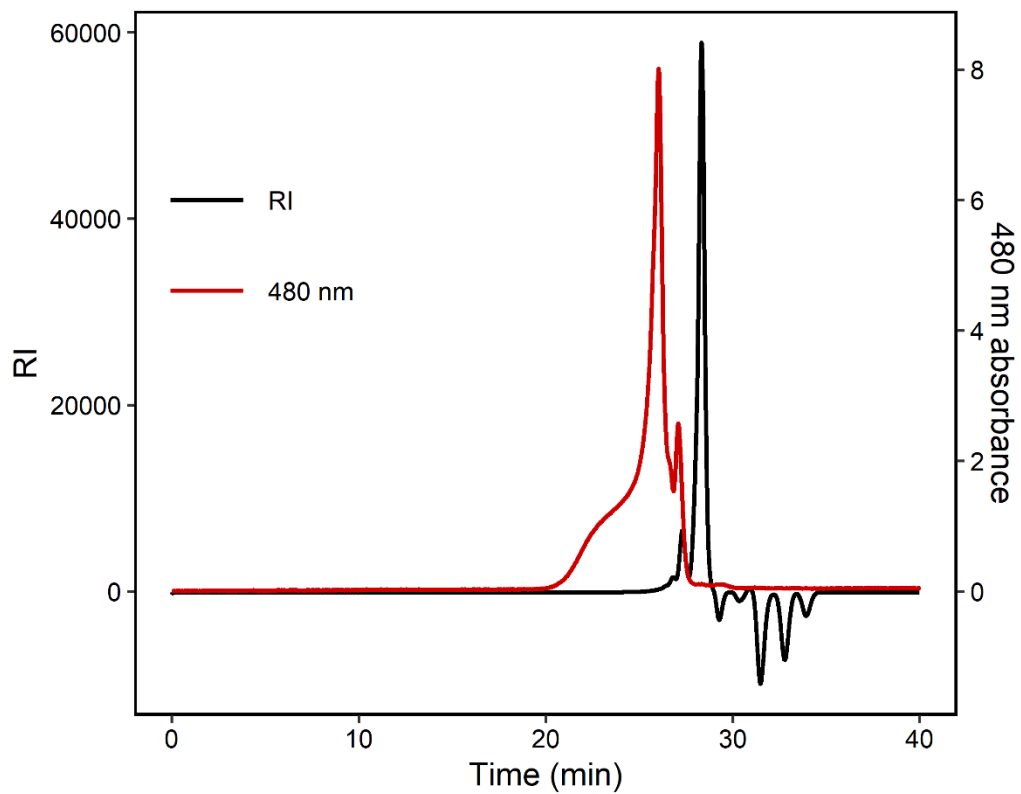


Figure S16. GPC traces of **P1** from dark control replication (Table 1, entry 5 conditions). M_n 2.9 kg/mol, \bar{D} 2.15 vs polystyrene standards. GPC sample was obtained from chloroform extraction of crude material to remove Li salts.

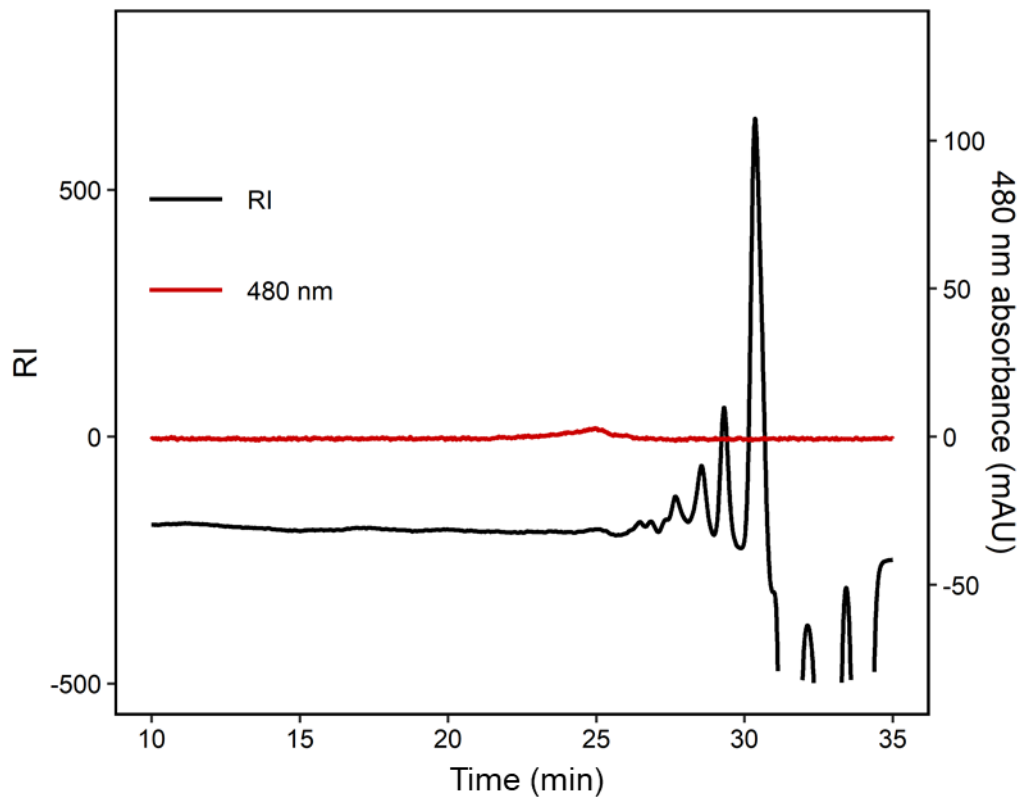


Figure S17. GPC traces of **P1** from Table 1, entry 6. GPC sample was obtained from chloroform extraction of crude material.

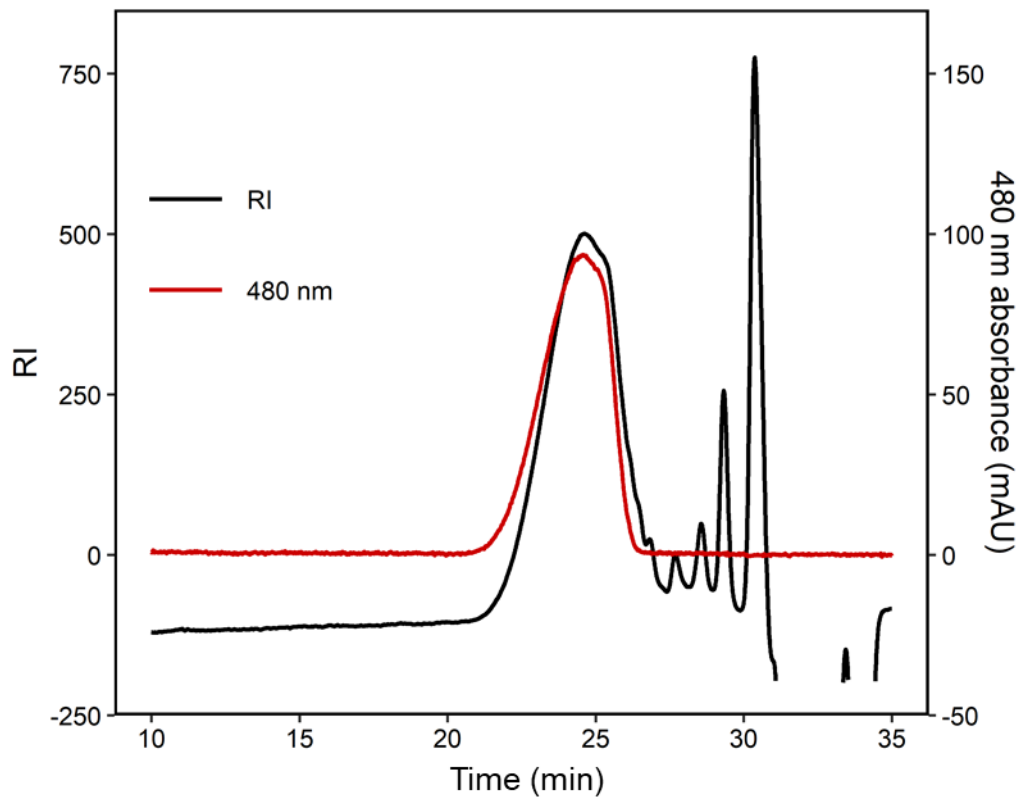


Figure S18. GPC traces of **P1** from Table 1, entry 7.

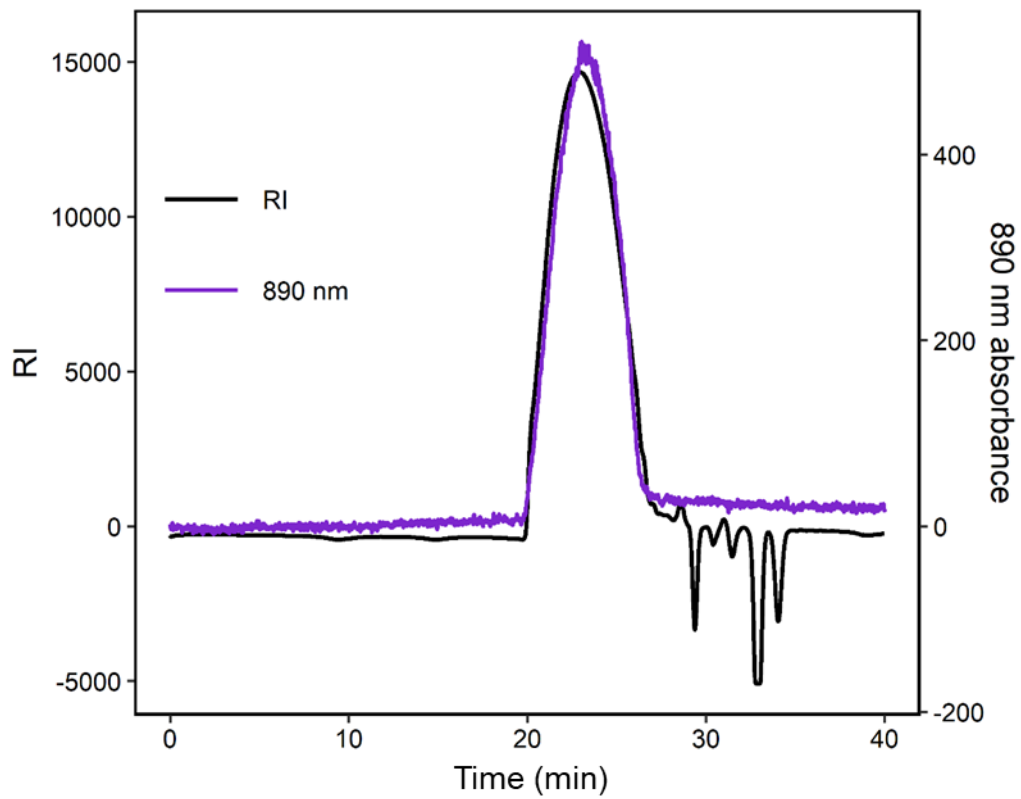


Figure S19. GPC traces of **P2** from general procedure B.

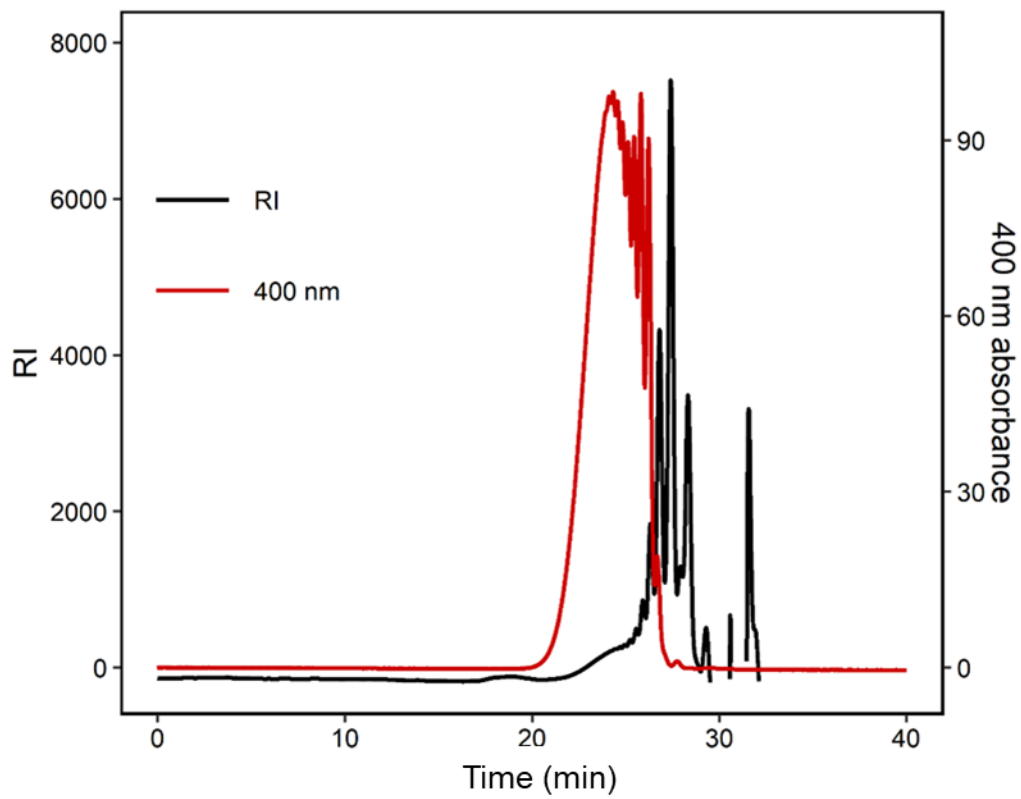


Figure S20. GPC traces of **P3** from general procedure A.

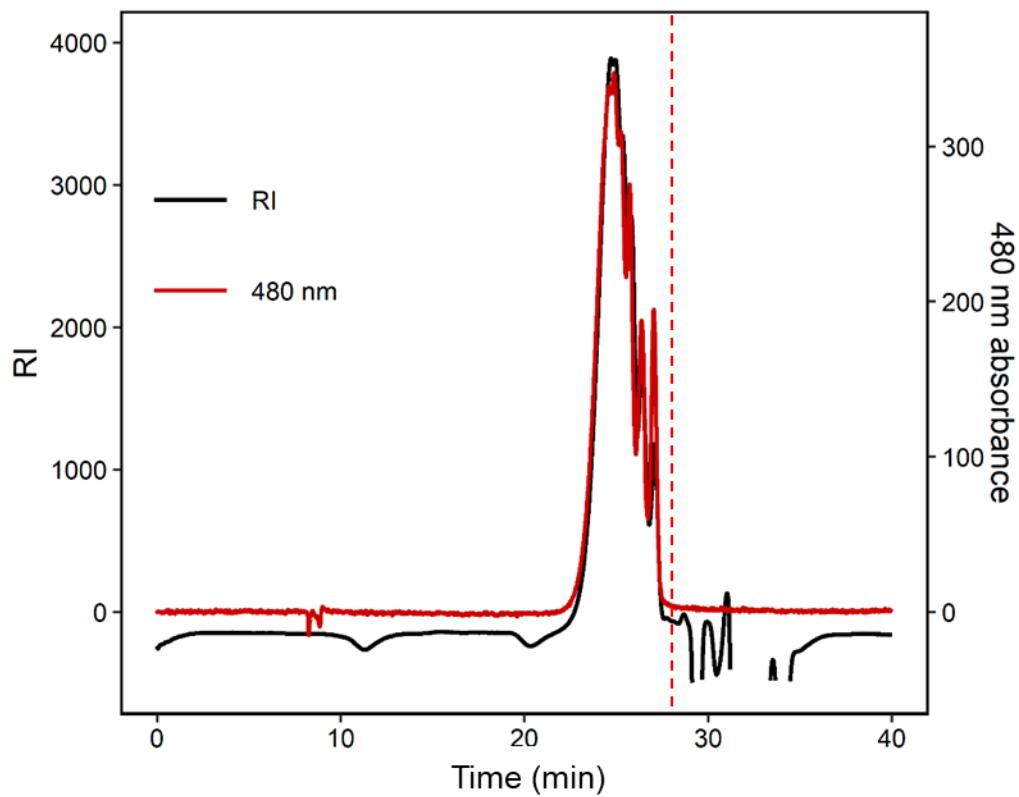


Figure S21. GPC traces of **P6** (soluble fraction) from general procedure A. Dashed red line shows lower calibration limit of polystyrene MW calibration curve.

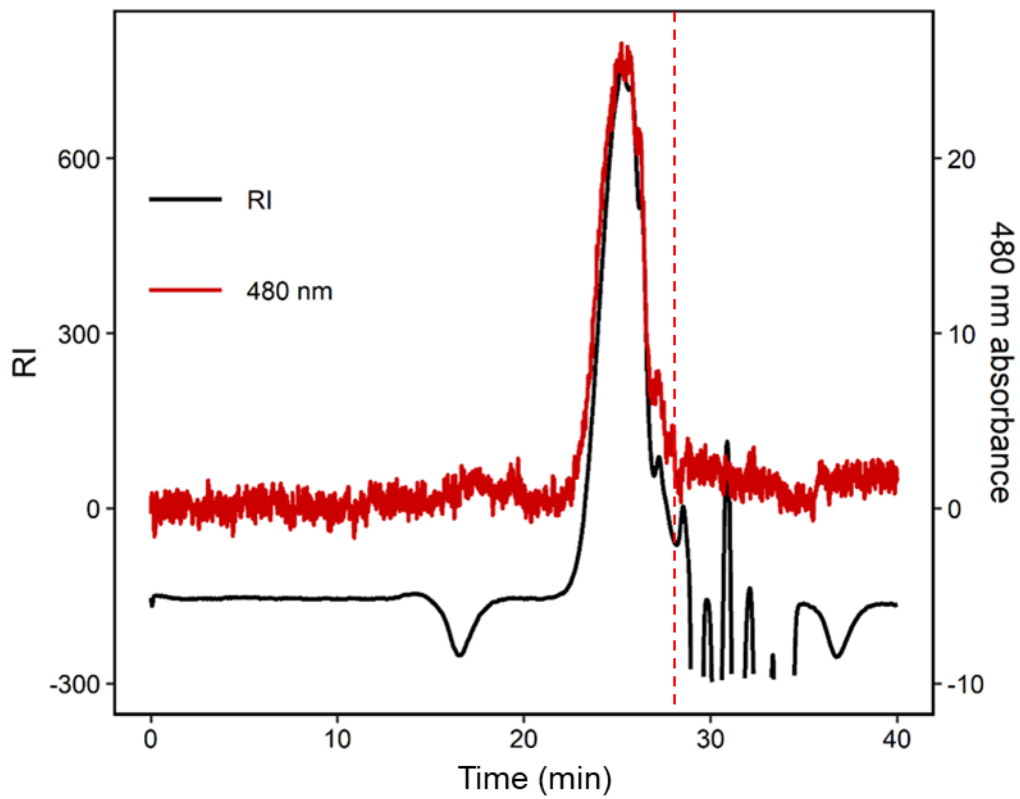


Figure S22. GPC traces of **P7** from general procedure A. Dashed red line shows lower calibration limit of polystyrene MW calibration curve.

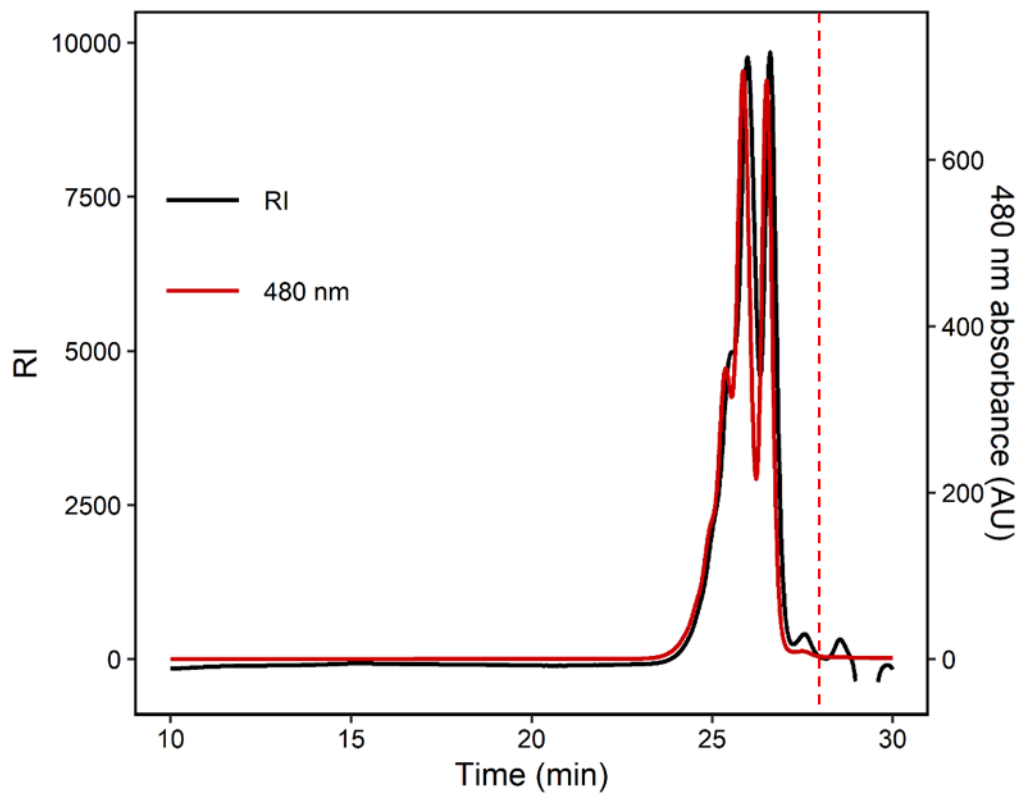


Figure S23. GPC traces of **P8** from general procedure A. Dashed red line shows lower calibration limit of polystyrene MW calibration curve.

Lithium chloride equivalents screen

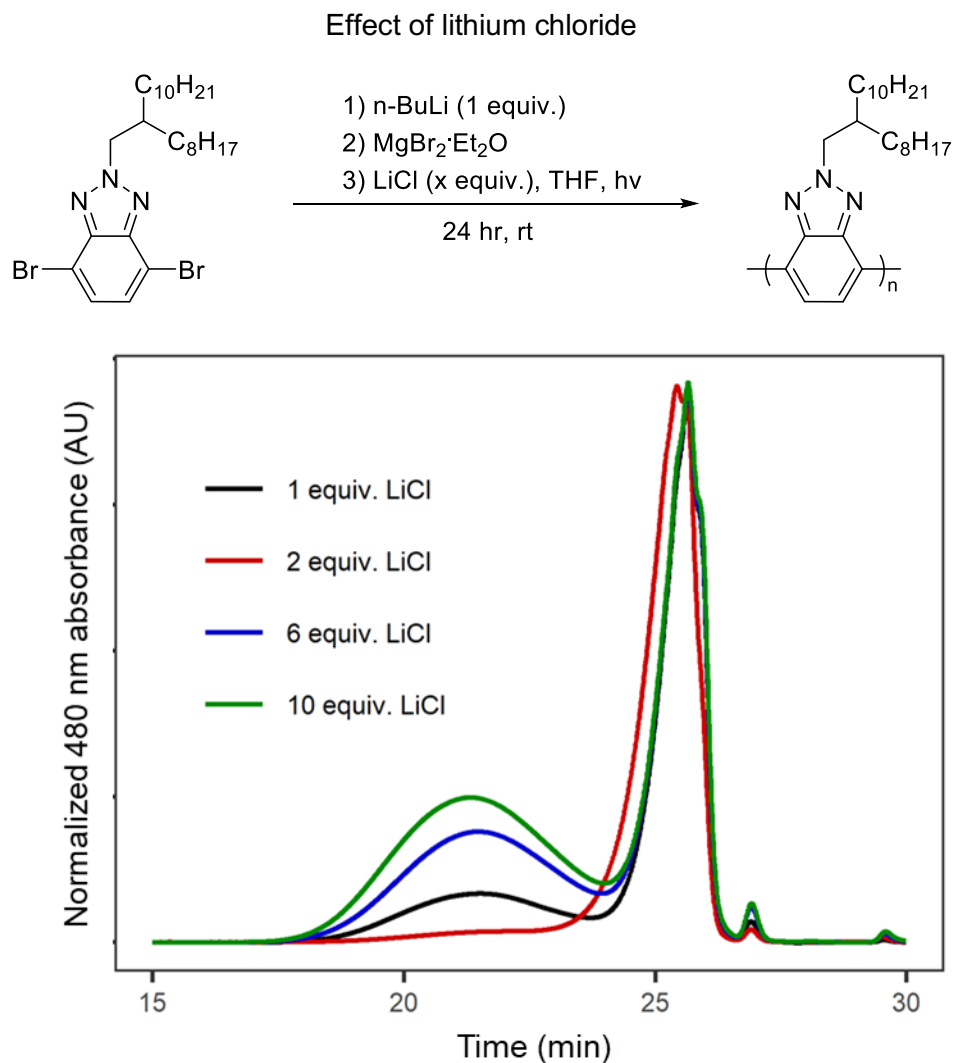


Figure S24. GPC traces of **P1** polymerized using different equivalents of lithium chloride.

Conversion assay details

Conversion assay experiments of **1** were conducted using a modified variant polymerization *general procedure A* wherein the polymerization was conducted with 0.5 equivalents of 1,3,5-trimethoxybenzene as internal ¹H NMR (500 MHz) standard.

Aliquots were removed with argon purged syringe and precipitated into methanol-d₄. The aliquots were centrifuged, and supernatant analyzed via ¹H NMR (500 MHz). Solids were dissolved in tetrahydrofuran and analyzed via THF-GPC analysis.

Note: The molecular weight plateau seen in the conversion assay is below the solubility limit of **P1** in THF (see table 1, entry 3). The lower molecular weights obtained for the time point experiments are the result repeatedly puncturing the septa to remove aliquots for analysis, which introduces oxygen and requires a positive pressure of argon (see Polymerization details for information on the effect of oxygen).

While there is conversion of **1-MgBr** in the dark, *this conversion does not produce polymer*. The dark control reaction of **1-MgBr** in the shows only oligomers and unreacted starting material (figure S25). This suggests that the dark reaction consumes monomer but is not a productive pathway towards polymerization.

The increase in 550 nm absorbance over the course of the polymerization (Figure 2c, Figure S26 for full absorption data) cannot be attributed to the unproductive background reaction. A dark control reaction of **1-MgBr**, prepared through *general procedure A*, showed no absorbance at 550 nm (figure S49).

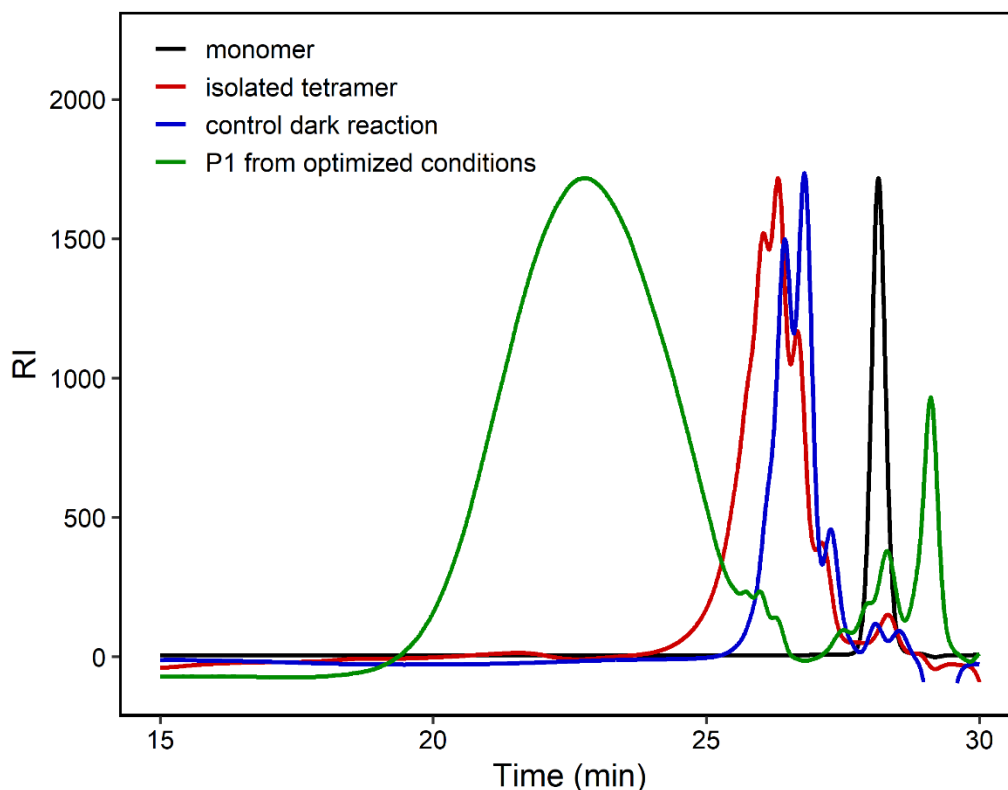


Figure S25. GPC traces of **1** (black), isolated oligomer of **1** (red), material obtained from dark control reaction (blue), and **P1** obtained using *general procedure A*. See figure S56 for MALDI-TOF MS of oligomer fraction.

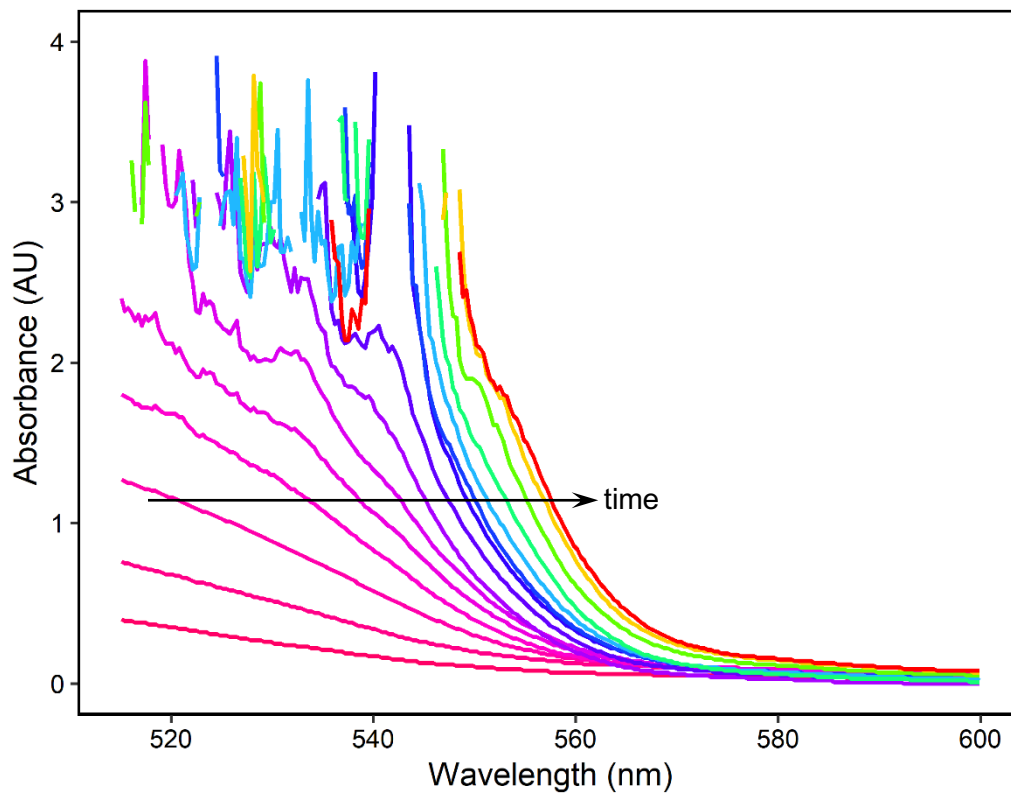


Figure S26. UV-Vis absorption over the course monitored over the course of **P1** polymerization. The absorbance values at 550 nm were used to construct Figure 2c.

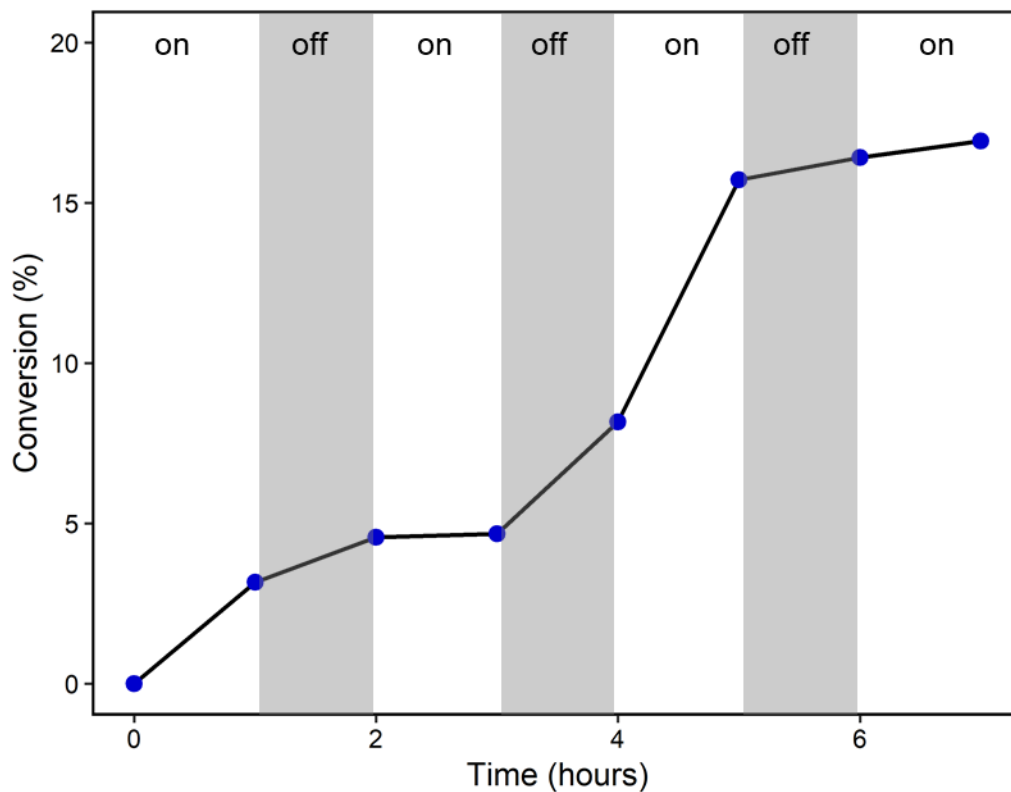


Figure S27. Corrected conversion of **1-MgBr** during “on-off” polymerization study determined via ^1H NMR relative to 1,3,5-trimethoxybenzene internal standard. Due to incomplete conversion of **1** to **1-MgBr** (0.9 equiv *n*-BuLi are used to minimize formation of the bis-Grignard monomer), the conversion was corrected to shift conversion at time 0 to 0% conversion. Note: dark conversion is not due to polymerization of **1-MgBr**.

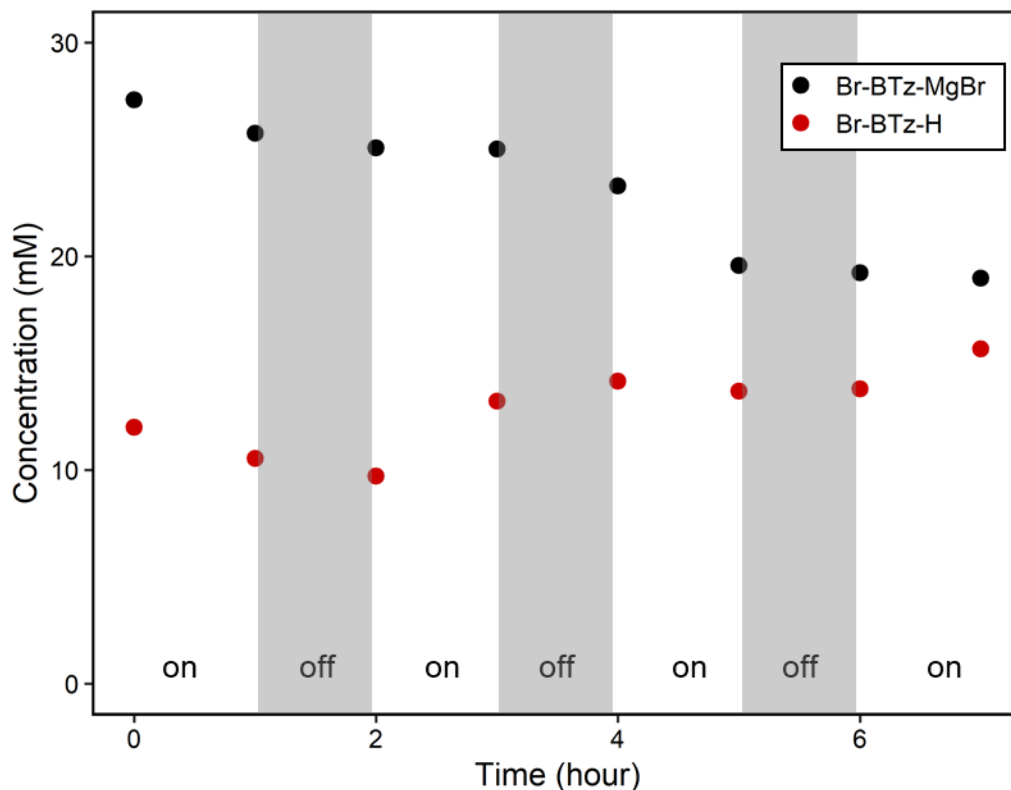


Figure S28. Concentration of benzotriazole species during polymerization of **1-MgBr** generated via *general*. Concentrations determined via ^1H NMR relative to 1,3,5-trimethoxybenzene internal standard.

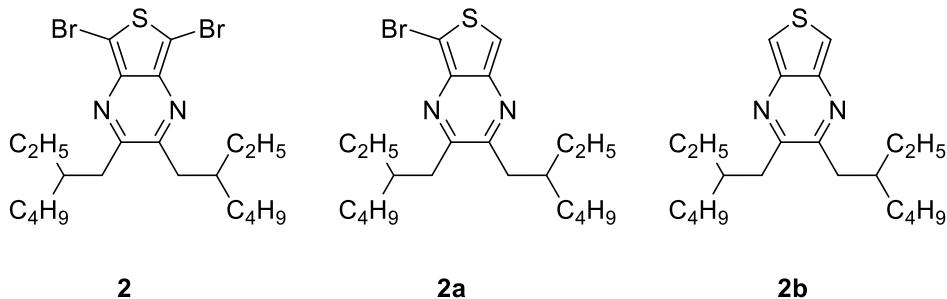
In order to ensure block fidelity during chain extension polymerization, a truncated conversion assay was conducted (as described below) to determine when polymerization of **2-MgBr** is complete under 626 nm irradiation. In order to perturb the reaction as little as possible, conversion assay data was collected beginning after 12 hours of irradiation.

Conversion assay of P2 polymerization

The lack of aromatic protons in **2-MgBr** makes determining monomer concentrations by ^1H -NMR challenging. This is further complicated by our findings of quenched **1-MgBr** over the course of the polymerization of **P1** (figure 2a), suggesting that we must also be able to distinguish between active Grignard monomer and monomer adventitiously quenched during the course of the reaction. To accomplish this, we devised a dual-quench protocol wherein aliquots were divided between a methanol and methanol- d_4 quench. A suppression in the integration of the monodebrominated signal of **2** in the methanol- d_4 quenched aliquot relative to the methanol quench

was used to determine remaining **2-MgBr**. We then defined the end point of the polymerization as the time at which no difference between the H and D quenched spectra was seen.

Conversion assay experiments of **2** were conducted using a modified variant of *general procedure B* wherein the polymerization was conducted with 0.5 equivalents of 1,3,5-trimethoxybenzene as internal ^1H NMR (500 MHz) standard. After 12 h, the reaction was placed under dynamic argon and aliquots were removed with an argon purged syringe and precipitated into methanol or methanol-d4. For each timepoint, one aliquot was divided; half the aliquot volume was precipitated into methanol (CH_3OH quench) and the other half was precipitated into methanol-d4 (CD_3OD quench). Both aliquots were concentrated and submitted for ^1H NMR (500 MHz) in CDCl_3 . Monomer reactivity was determined by examining the differences between integrations of **2a** and **2b** (figure S29) in each spectrum.



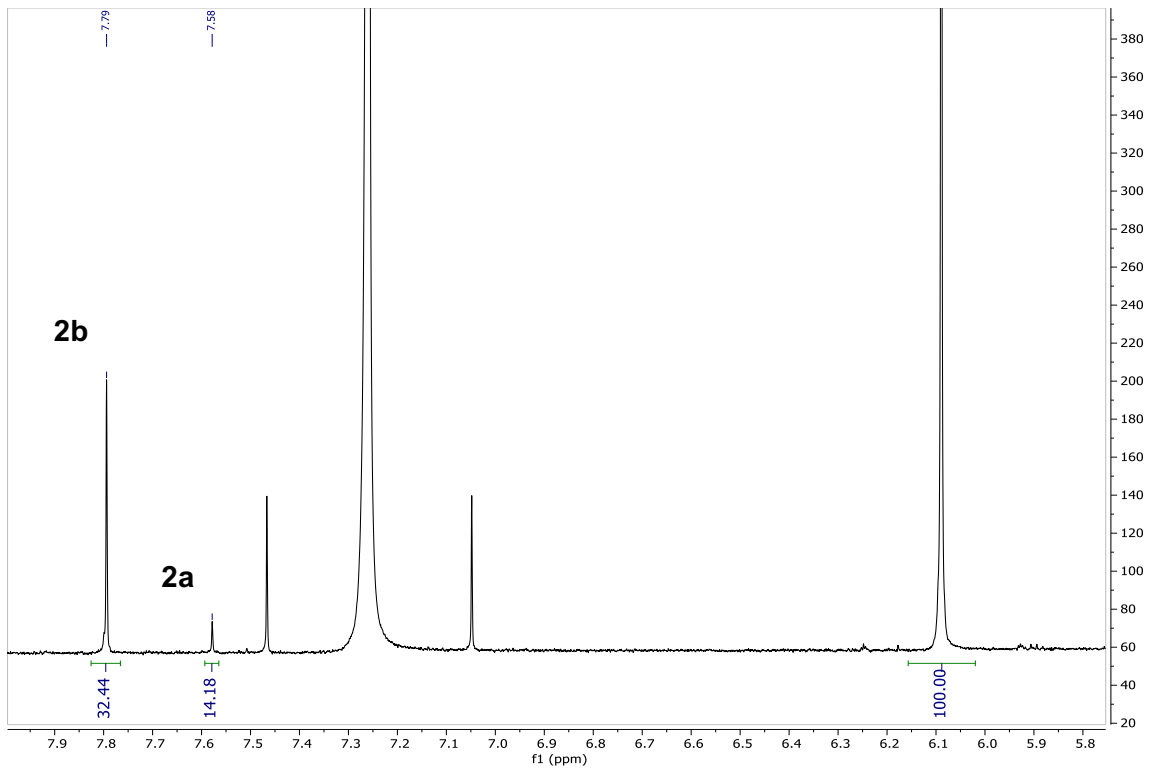
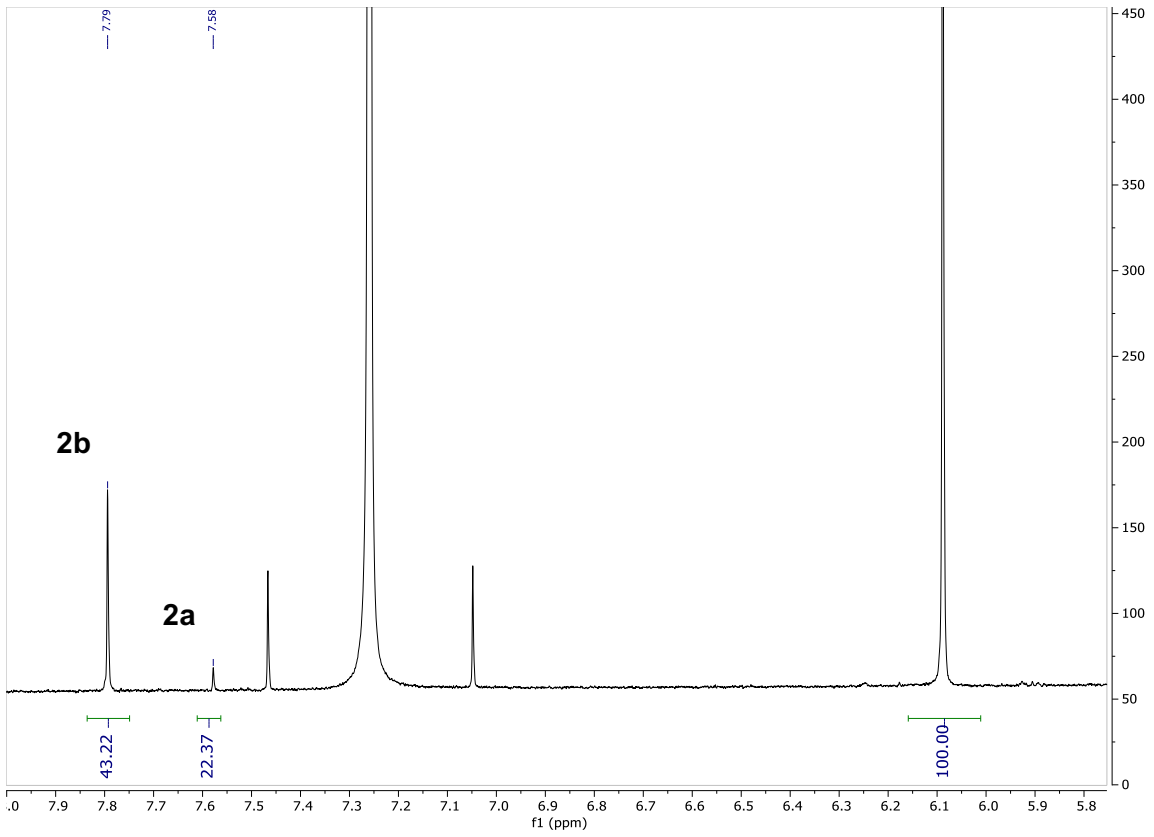


Figure S29: $^1\text{H-NMR}$ (500 MHz) spectra at 12 h with integrations. Top spectrum: CH_3OH quench. Bottom spectrum: CD_3OD quench. The integrations for **2a** and **2b** in the CD_3OD quench spectrum are suppressed relative to those from the CH_3OH quench indicating remaining active **2-MgBr**.

In ^1H NMR spectra, the D quench shows only deactivated species, as any proton signals come from monomer quenched by adventitious proton sources in the reaction. In contrast, the H quench would quantify both active and inactive species. The integrations of **2a** and **2b** at each time point are shown in table S3.

Based on this experiment, we determined that the polymerization of **2-MgBr** requires 18 h to reach full conversion.

Table S3: Integrations of **2a** and **2b** relative to the aromatic singlet of trimethoxybenzene internal standard, set to 100. The D quench integrations are lower than those of the H quench at early time points, indicating active Grignard monomer still present. At 18 h, the integrations for both quenches are the same and remain unchanged until the final time point at 22 h.

Time	H quench, 2a	D quench, 2a	H quench, 2b	D quench, 2b
12 h	43.42	32.42	22.37	14.18
14 h	38.20	31.09	21.86	14.53
16 h	33.28	27.79	23.61	15.46
18 h	29.49	29.20	21.22	21.54
20 h	29.70	29.78	21.43	21.45
22 h	29.69	29.71	21.39	21.39

Statistical copolymerization details

The statistical copolymer of **1-MgBr** and **2-MgBr** was prepared to provide UV-vis spectra to compare to that of the block copolymer described in the text.

1-MgBr was prepared through lithiation/magnesiumation as described in *general procedure A*. **2-MgBr** was prepared via Grignard metathesis listed in *general procedure B*. **1-MgBr** and **2-MgBr** were combined and subjected to the reaction conditions (Scheme **S5**). Copolymers were isolated via precipitation (MeOH 3X) before analysis.

The ratio of monomer incorporation was determined through ^1H NMR integration of the methylene protons of the respective monomers (figure **S30-31**).

Scheme S5.

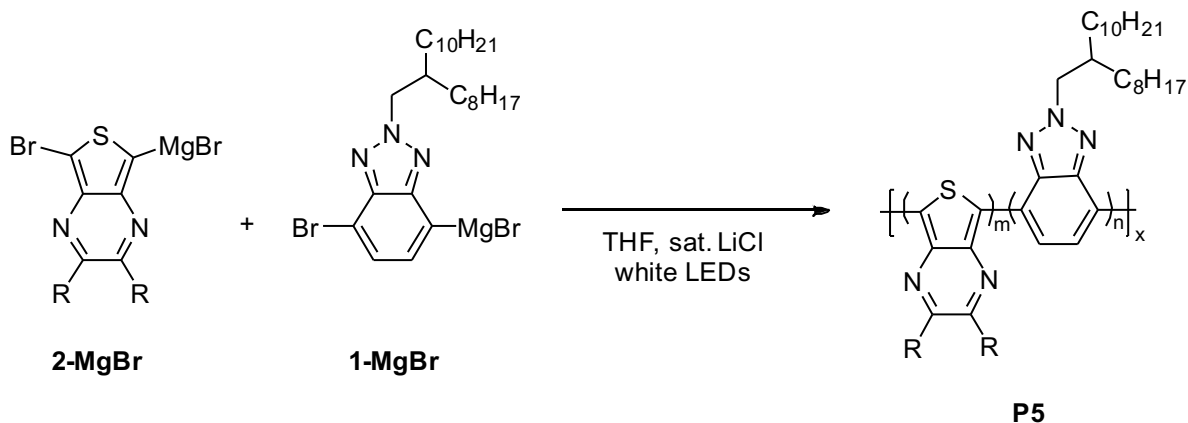


Table S4. Statistical copolymer characterization data. M_n and \bar{D} determined by GPC relative to polystyrene standards.

Stoichiometry (1-MgBr:2-MgBr)	Copolymer ratio (1-MgBr:2-MgBr)	M_n (kg/mol)	\bar{D}	Yield (%)
1:1	1.1:1	1.7	1.26	30
3:1	3.2:1	1.6	1.20	26

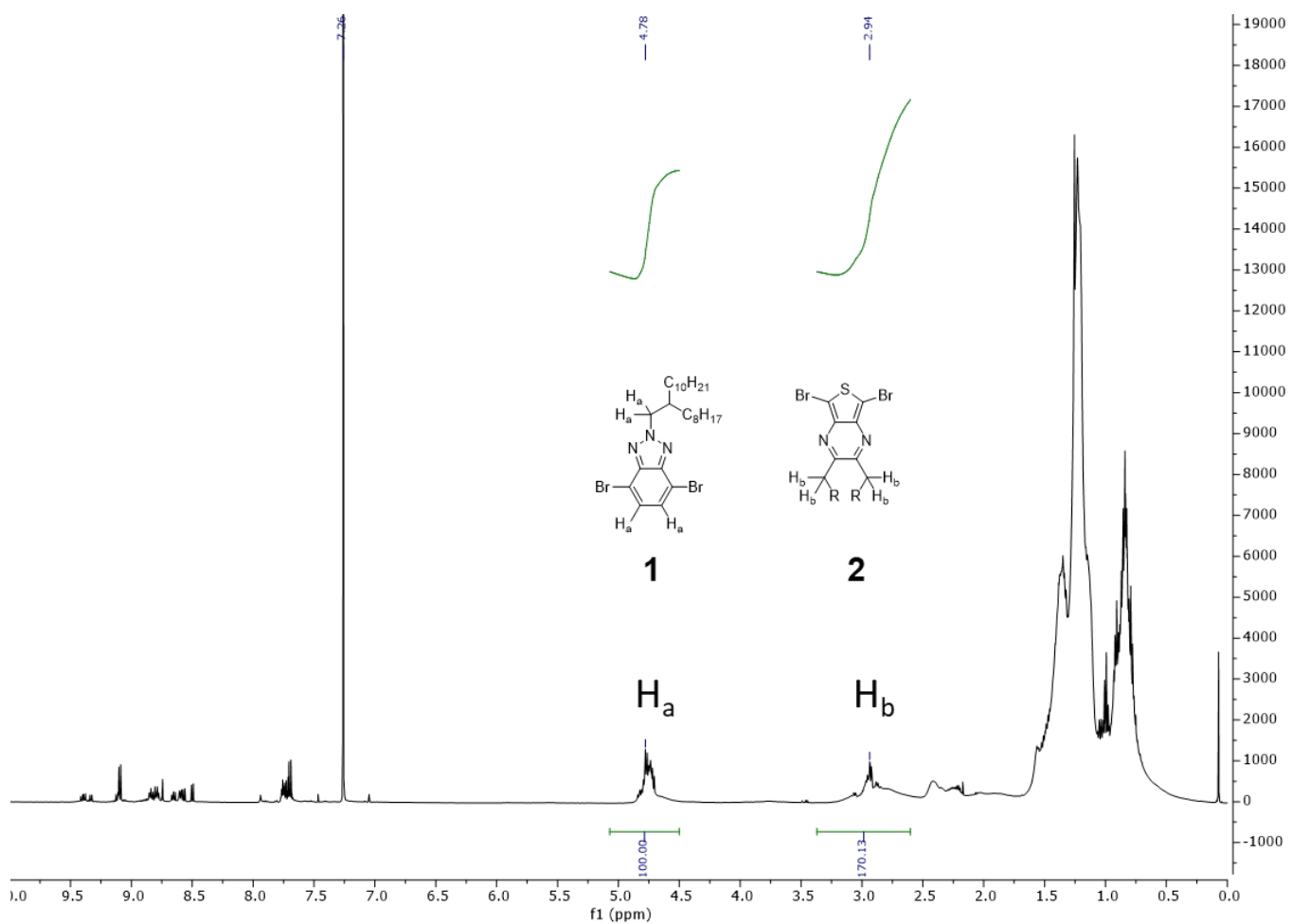


Figure S30. $^1\text{H-NMR}$ (500 MHz, CDCl_3) of 1:1 (**1-MgBr/2-MgBr**) stoichiometry copolymer

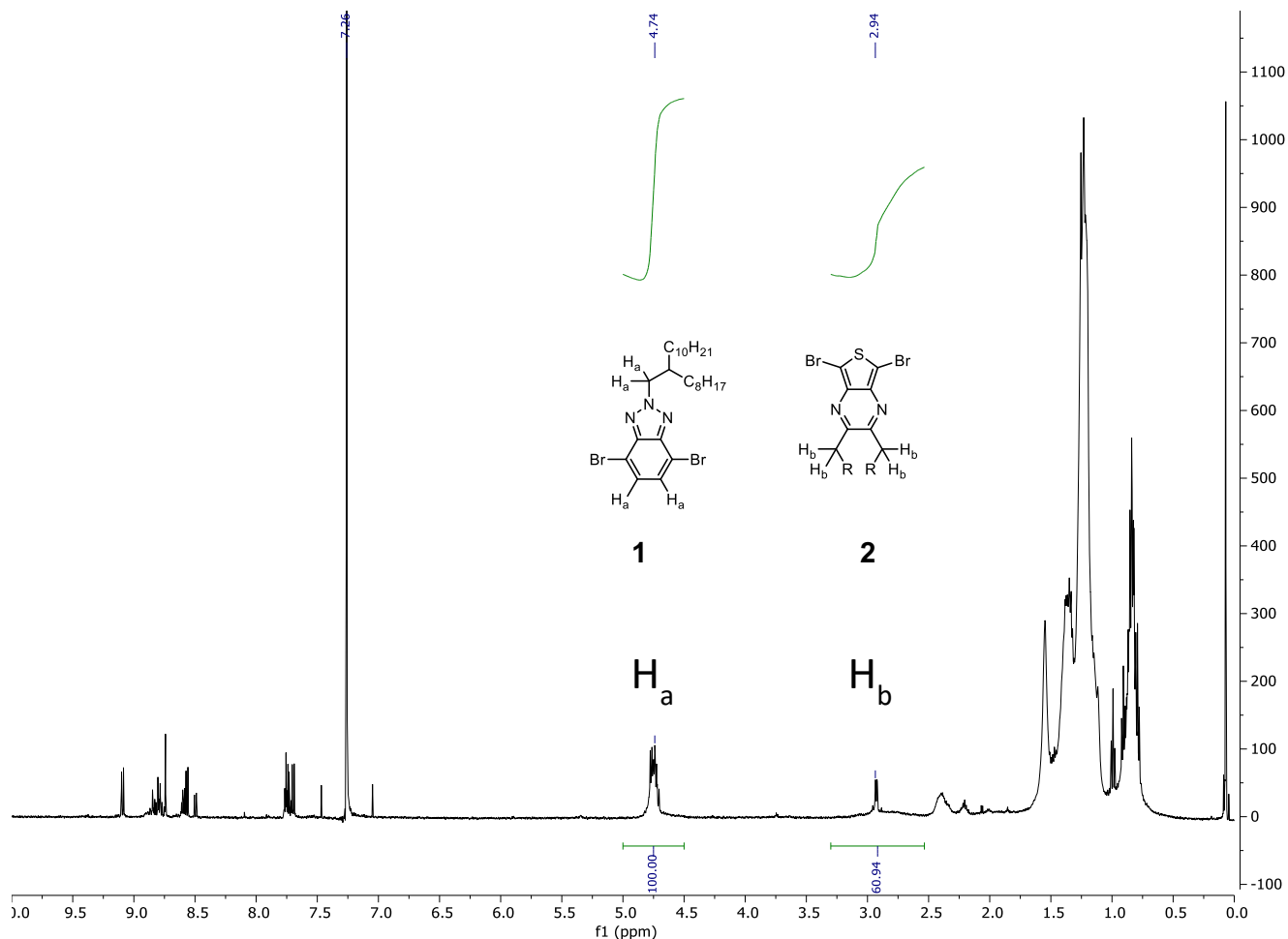


Figure S31. $^1\text{H-NMR}$ (500 MHz, CDCl_3) of 3:1 (**1-MgBr/2-MgBr**) stoichiometry copolymer

The low molecular weight of statistical copolymers for copolymerizations of **1-MgBr** has been previously observed. In the copolymerization of 4,4-bis(2-ethylhexyl)-4*H*-silolo[3,2-*b*:4,5-*b'*]dithiophene and **1**, Seferos and coworkers observed the production of low molecular weight statistical copolymers. The authors found that cross Grignard metathesis between the two monomers in solution resulted in bismetallated and dibrominated monomers in solution, which then terminated polymerization.¹²

To test whether the low molecular weights observed in copolymers of **1** and **2** are the result of Grignard exchange, a cross metathesis experiment was conducted (scheme **S6**). Grignards of **1** and **2** were prepared as described above for the copolymerization. The mixture was kept in the dark for one hour before quenching the reaction with methanol. The solution was concentrated *in vacuo* and monomer identities determined via $^1\text{H NMR}$ (figure **S32**). The ratios of monomer signals seen in the NMR shows a 5:1 ratio of bismetallated **2** to monometalated **2**. The enrichment

of bismetallated **2** comes at the apparent expense of **1-MgBr** which shows a 1:3.9 ratio of **1-MgBr** to **1**. This data would suggest that the low molecular weights observed are due to termination events resulting from cross Grignard metathesis of the monomers.

Scheme S6. Cross metathesis of Grignard monomers.

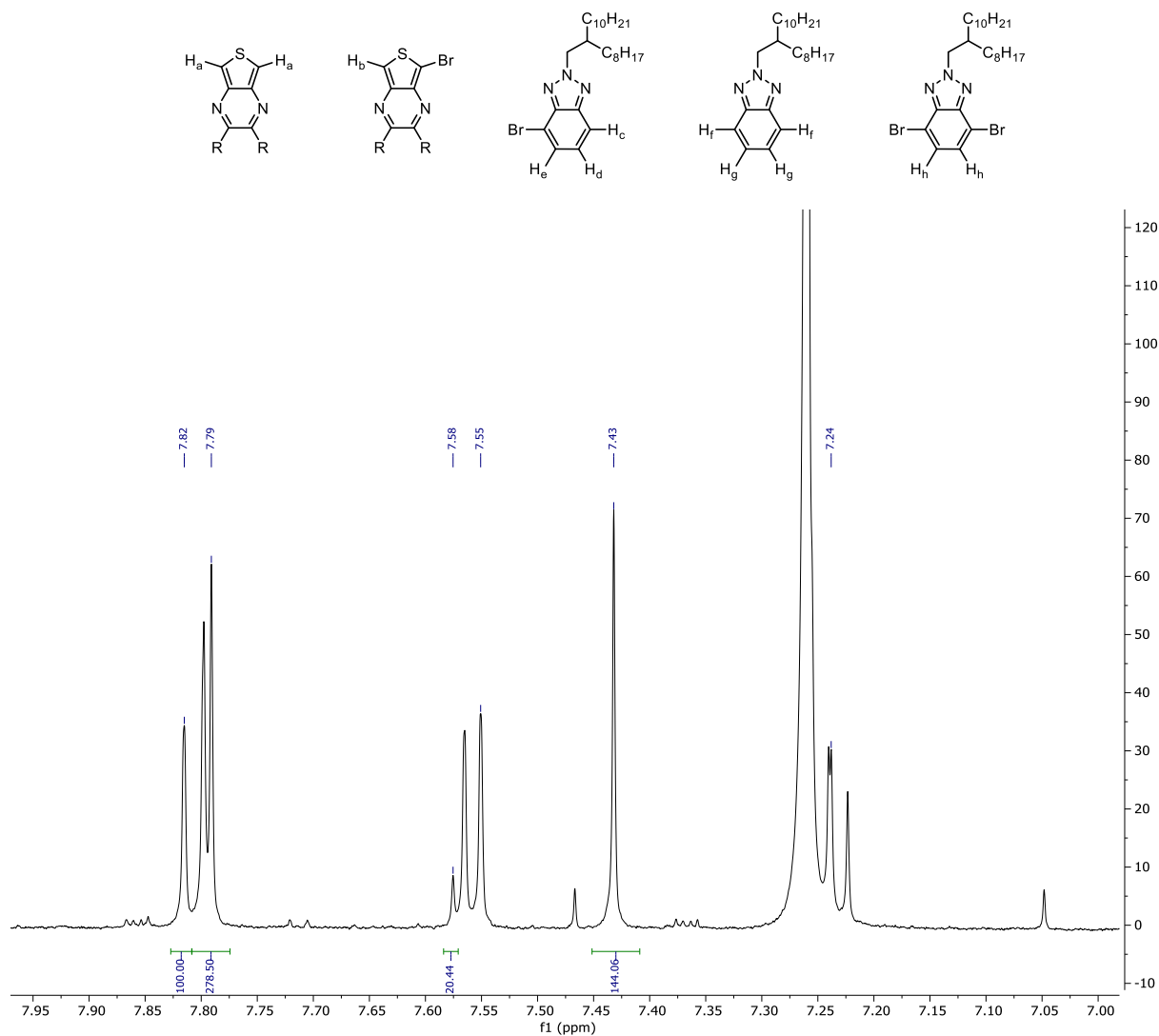
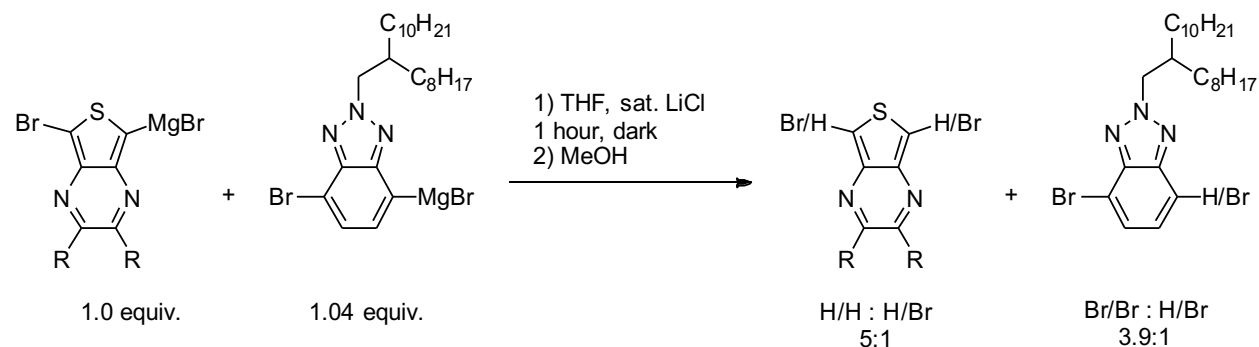


Figure S32. $^1\text{H-NMR}$ (500 MHz, CDCl_3) of Grignard metathesis experiment between **1-MgBr** and **2-MgBr**.

Block copolymerization details

The Grignard of **2** were prepared via Grignard metathesis listed in *general procedure B*. The solution was placed under dynamic argon and irradiated with 626 nm LEDs for 18 hours (informed by conversion assay of **P2**, see conversion assay details) before an aliquot was removed via an argon sparged syringe and precipitated into methanol. The precipitate was collected by centrifuge and submitted for THF GPC analysis. After the aliquot was removed, **1-MgBr**, prepared via lithiation/magnesiumation as described in *general procedure A*, was injected into the reaction. Irradiation with 626 nm LEDs was continued for 24 hours before the solution was quenched with methanol. **P5** was then isolated via precipitation into MeOH (2X) followed by precipitation into acetone (1X). **P5** was obtained in a 10% yield.

The low yield can be ascribed to termination pathways, which lead to the described uncontrolled chain-growth behavior, and result in **P2** homopolymer that is isolated in the acetone supernatant. Additionally, **P5** is unstable under ambient conditions and should be stored below -20°C under inert atmosphere. Even stored under these conditions, degradation of **P5** was observed within 48 hours.

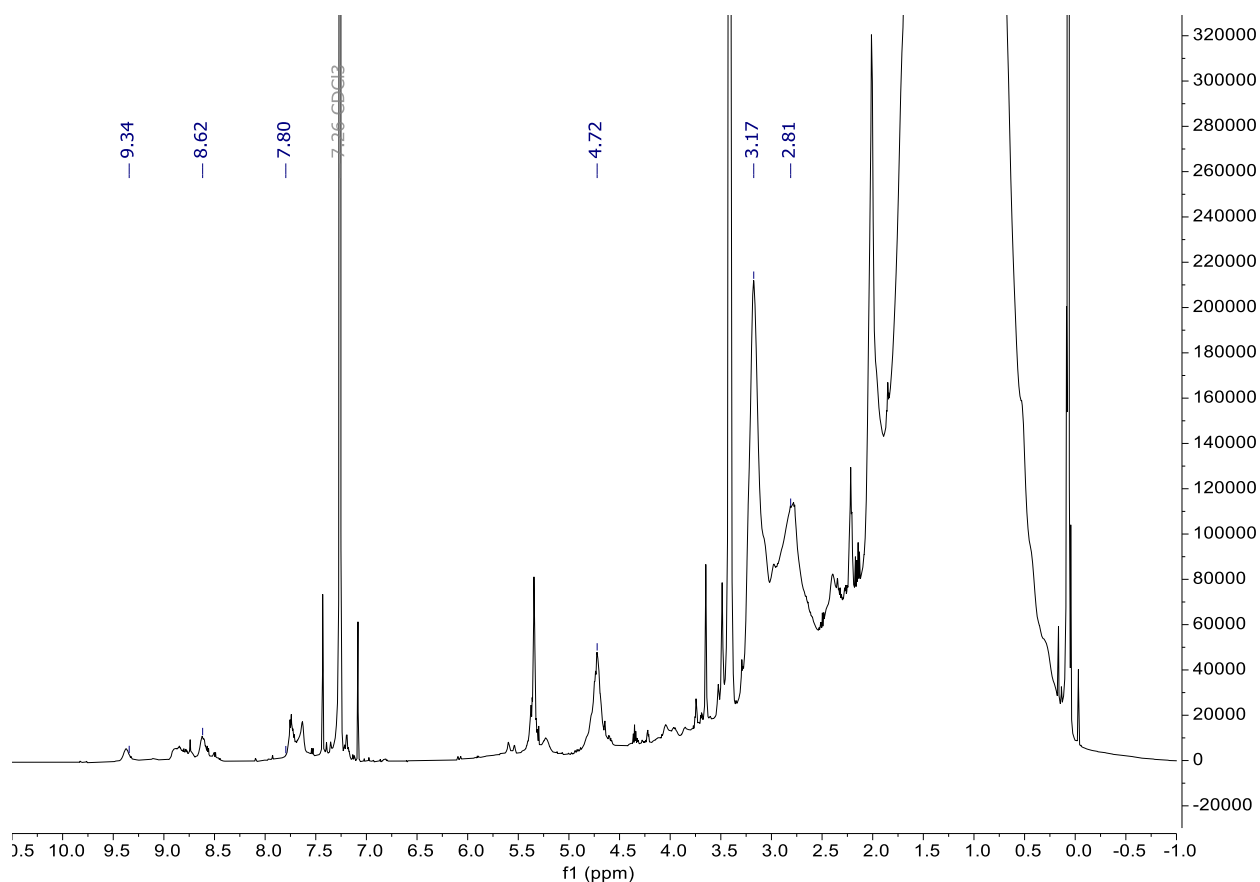


Figure S33. $^1\text{H-NMR}$ (600 MHz, CDCl_3) of **P2-b-P1** block copolymer

In order to further confirm connectivity between the signals of **P1** (9.34, 8.62, 7.80, 4.72 ppm) and **P2** (3.17, 2.81 ppm) signals seen in the $^1\text{H-NMR}$ of **P5** (figure **S33**) a $^1\text{H-DOSY}$ of **P5** was measured. The obtained diffusion values (Table S5) show good agreement between peaks corresponding to both blocks of **P5**. Differences in diffusion values are within expected variance as seen in previous DOSY studies of conjugated polymers.¹³

Table S5. Diffusion values extracted from $^1\text{H DOSY NMR}$ of **P5**. $^1\text{H DOSY}$ collected in CDCl_3 using a linear gradient ramp of 16 points (lowest amplitude gradient 2% and highest 95%) with a gradient pulse length (p30) of 1600 μs . Diffusion analysis was extracted from a mono-exponential peak intensity decay fitting of spectra via MNova. Diffusion of residual CHCl_3 solvent peak was measured to be $2.60 \times 10^{-5} \text{ cm}^2 \text{ s}^{-1}$.

Peak Shift	9.34 ppm	8.62 ppm	7.80 ppm	4.72 ppm	3.17 ppm	2.81 ppm
D ($\text{cm}^2 \text{ s}^{-1}$)	2.17×10^{-6}	2.23×10^{-6}	2.49×10^{-6}	2.79×10^{-6}	2.39×10^{-6}	2.52×10^{-6}
Error	4.4 %	4.3%	2.7%	2.2%	1.0%	2.2%

Polymerization wavelength variation details

Table S6. Molecular weight, dispersity, and yield data for irradiation variation for the polymerization of **1**. Molecular weight data Polymerization of **1** was conducted using polymerization *general procedure B*. While direct Grignard metathesis of **1** provides lower yields and molecular weights compared to *general procedure A*, we found that *general procedure B* provided more consistent results when different irradiation wavelengths were used. Molecular weight and dispersity values were determined via GPC relative polystyrene standards.

LED $h\nu$ (nm)	M_p (kg/mol)	M_n (kg/mol)	\bar{D}	Yield (%)
400 nm	9.3	6.1	1.42	<5%
470 nm	10.0	6.9	1.49	<5%
525 nm	25.8	10.3	2.04	<5%
626 nm	--	--	--	--
White 4000 K	14.7	9.6	1.60	11

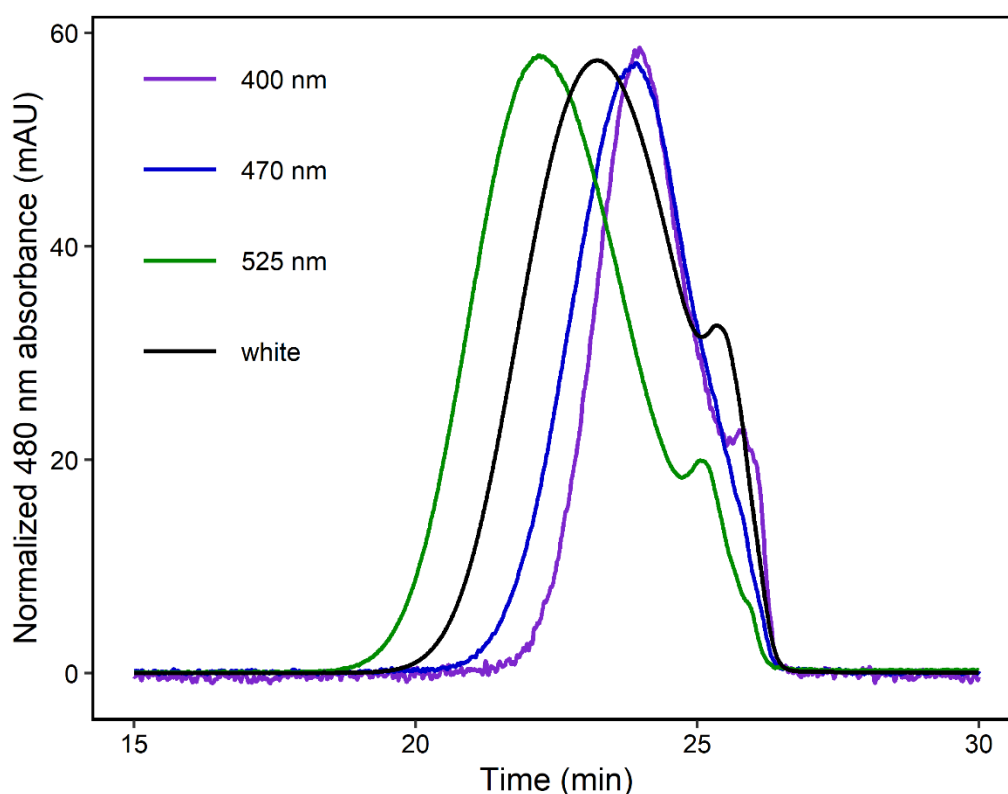


Figure S34. Replication of polymerization of **1-MgBr** using LEDs with different emission wavelengths.

Table S7. Replication of wavelength variation experiment for **1** (see figure S34 for GPC traces).

LED $h\nu$ (nm)	M_p (kg/mol)	M_n (kg/mol)	\bar{D}	Yield (%)
400 nm	8.3	6.1	1.36	<5%

470 nm	8.6	7.3	1.38	<5%
525 nm	20.5	12.3	1.64	<5%
626 nm	--	--	--	--
White 4000 K	13.7	8.7	1.62	16

To investigate whether the higher molecular weight polymer obtained using 525 nm LEDs could be obtained with in greater yield, **1** was polymerized using *general procedure A* with 525 nm LEDs (table S8 and figure S35). The use of *general procedure A* provided a slight increase in yield (table S8, entry 1). Additionally, we sought to confirm that the lower power of the 525 nm LEDs was not the underlying reason for the lower yield relative to the 4000 K white LEDs. Polymerization using 16 W 525 nm LEDs (table S8, entry 2) improved yield, but lowered the molecular weight of the obtained polymer. The temperature of the LEDs was monitored throughout the polymerization and exceeded 27 °C over the course of the reaction, ruling out overheating concerns with the higher-power LEDs.

Table S8. Molecular weight, dispersity, and yield data for polymerization of **1** using 525 nm LEDs of different wattage.

Entry	525 nm LED power	Measured intensity (lux)	M _p (kg/mol)	M _n (kg/mol)	Đ	Yield (%)
1	5.7 W	33,000	26.3	15	1.77	6%
2	16 W	85,000	11.6	9.5	1.45	11%

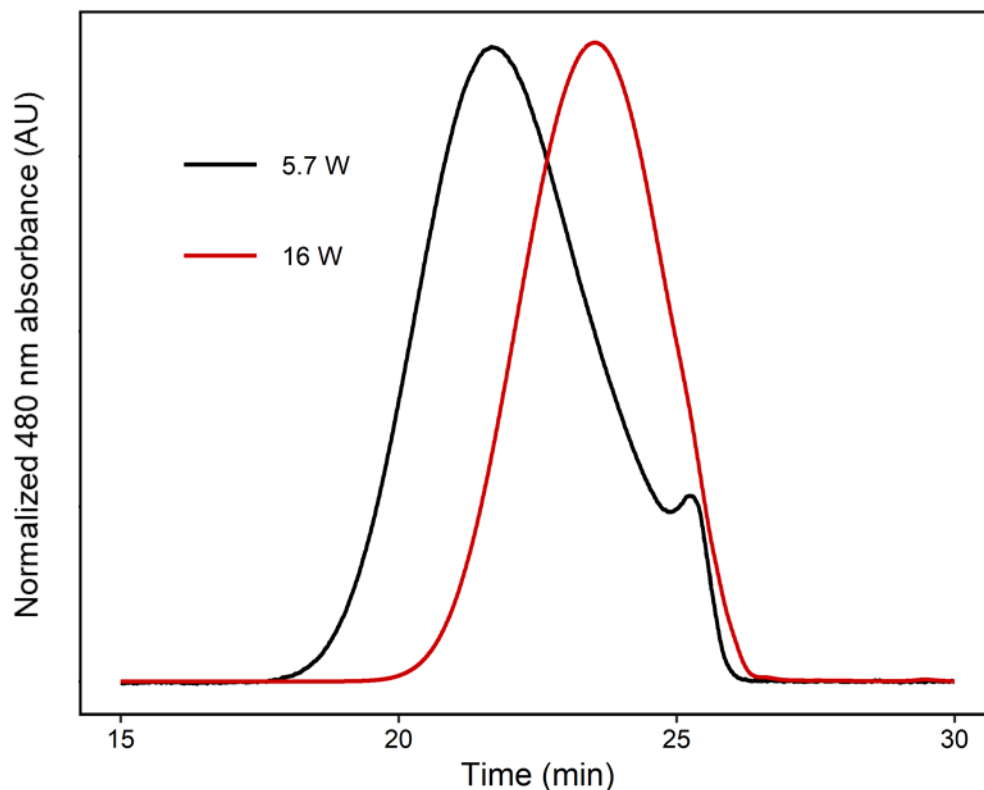


Figure S35. GPC of **P1** polymerized using green 5.7 W (black) and 16 W (red) LEDs

The polymerization of **2-MgBr** also shows wavelength dependence, albeit with more subtle differences (Figure S36). While the 400 nm LEDs clearly produced lower molecular weight polymer, many of the longer wavelengths of light produced polymers of similar number average molecular weight (M_n) but differing peak molecular weight (M_p). It is possible that a more pronounced difference would be observed if higher-molecular-weight species were soluble. **P2** absorbs light across the visible spectrum and into the NIR (Figure S45). This absorbance of longer wavelength light is likely the reason that **2-MgBr** can be polymerized using 626 nm LEDs while **1-MgBr** cannot.

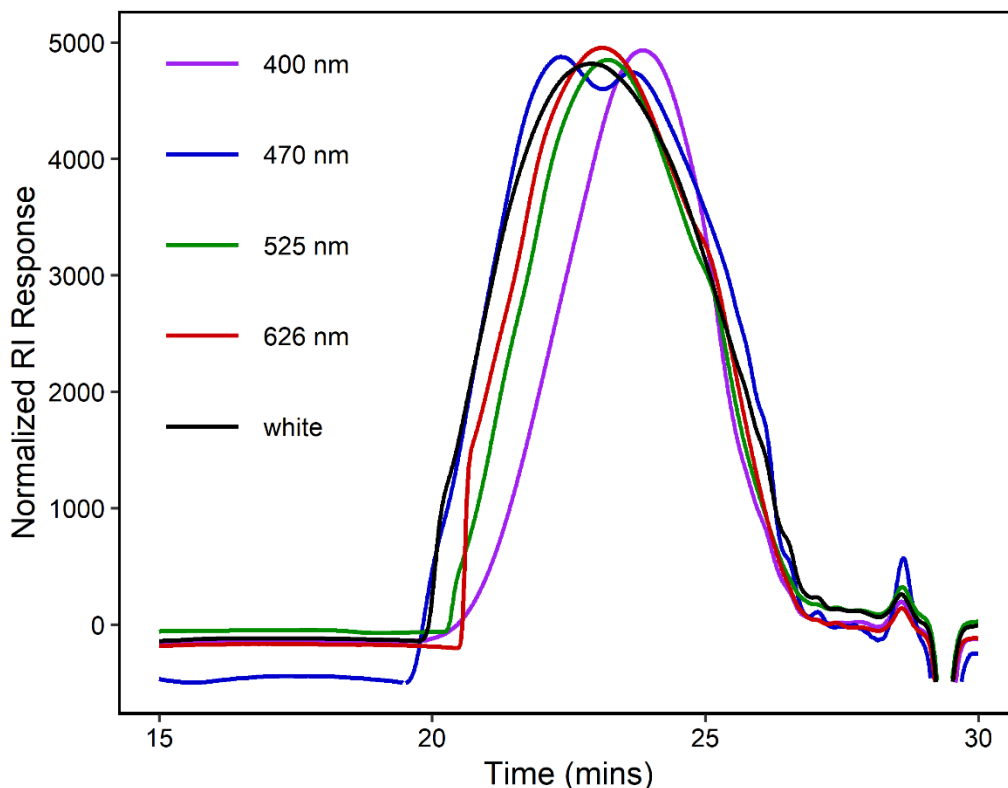


Figure S36. GPC traces of **2-MgBr** using LEDs with different emission wavelengths

Table S9. Molecular weight, dispersity, and yield data for irradiation variation for the polymerization of **2**. The polymerizations were conducted using *general procedure B*. Molecular weight and dispersity values were determined via GPC relative polystyrene standards.

LED $h\nu$ (nm)	M_p (kg/mol)	M_n (kg/mol)	\bar{D}	Yield (%)
400 nm	8.8	7.2	1.57	96
470 nm	19.1	7.6	2.06	68
525 nm	12.4	7.8	1.75	73
626 nm	13.1	7.9	1.77	67
White 4000 K	14.4	7.9	1.99	75

ICP-MS and control reaction details

Quantification of iron, nickel and palladium was accomplished using ICP-MS of acid digested samples. Specifically, dried samples were digested in 2.0 mL concentrated trace nitric acid (HNO_3 , > 69%, Thermo Fisher Scientific, Waltham, MA, USA), 0.5 mL hydrogen peroxide (H_2O_2 , > 30 %, for trace analysis, Sigma-Aldrich, St. Louis, MO, USA), and 0.25 mL concentrated hydrochloric acid (HCl , > 34%, Thermo Fisher Scientific, Waltham, MA, USA) via microwave digestion in a Milestone Ethos EZ Microwave Labstation operating at 1200 W. The microwave method included a 15-minute ramp to 220 °C, a 45-minute hold at 220 °C, and a 30-minute

exhaust to room temperature. A portion of the resulting digestate was diluted with concentrated hydrochloric acid and ultra-pure H₂O (18.2 MΩ·cm) to produce a final solution of 2.0% nitric acid and 2.0% hydrochloric acid (v/v) in a total sample volume of 10 mL. Quantitative standards were made using a custom multi-element standard containing Fe, Ni and Pd (Inorganic Ventures, Christiansburg, VA, USA) which was diluted to create a 100 ng/g mixed element standard in 2.0% nitric acid and 2.0% hydrochloric acid (v/v) in a total sample volume of 50 mL.

ICP-MS was performed on a computer-controlled (QTEGRA software) Thermo iCapQ ICP-MS (Thermo Fisher Scientific, Waltham, MA, USA) operating in KED mode and equipped with a ESI SC-2DX PrepFAST autosampler (Omaha, NE, USA). Internal standard was added inline using the prepFAST system and consisted of 1 ng/mL of a mixed element solution containing Bi, In, ⁶Li, Sc, Tb, Y (IV-ICPMS-71D from Inorganic Ventures). Online dilution was also carried out by the prepFAST system and used to generate calibration curves consisting of 100, 50, 25, 10, 5, 1, 0.5 ng/mL Fe, Ni and Pd. Each sample was acquired using 3 main (peak jumping) runs (100 sweeps). The isotopes selected for analysis were ⁵⁶Fe, ⁵⁷Fe, ⁵⁸Ni, ⁶⁰Ni, ⁶²Ni, ¹⁰⁵Pd, ¹⁰⁶Pd, ¹⁰⁸Pd and ⁸⁹Y and ¹¹⁵In (chosen as internal standards for data interpolation and machine stability). Instrument performance is optimized daily through autotuning followed by verification via a performance report (passing manufacturer specifications).

Table S10. ICP-MS results crude reaction mixture of **P1** polymerized *via general procedure A*. Experiments were performed in three independent reactions using new vials and stir bars.

Run	Fe	Ni	Pd
1	2.998 ppm	1.252 ppm	0.065 ppm
2	5.754 ppm	1.263 ppm	0.040 ppm
3	4.186 ppm	1.235 ppm	0.029 ppm

Table S11. ICP-MS results of crude reaction mixture of **P1** polymerized *via general procedure B*. Experiments were performed in three independent reactions using new vials and stir bars.

Run	Fe	Ni	Pd
1	1.430 ppm	1.377 ppm	0.019 ppm
2	1.932 ppm	8.638 ppm	0.038 ppm
3	2.777 ppm	1.088 ppm	0.029 ppm

Stir bar controls

To evaluate the effect of possible contamination of stir bars on observed reactivity, we compared the reactivity at early time points for three parallel reactions using a new stir bar, a piranha-washed stir bar (the standard cleaning protocol used in this work), and an acetone-washed stir bar. Grignard **1-MgBr** was prepared via *general procedure A* before being divided into three separate degassed vials containing the differently cleaned stir bars. Reactions were quenched at six hours with methanol before an aliquot was removed for GPC analysis and the remaining crude reaction mixture was submitted for ICP-MS analysis. Aliquots were precipitated once into methanol for GPC analysis.

Table S12 ICP-MS and GPC results of **P1** prepared via *general procedure A*, using different stir bars cleaned in various manners.

Stir bar	Fe	Ni	Pd	M_n (kg/mol)	\bar{D}	Yield (%)
New	1.649 ppm	0.912 ppm	0.150 ppm	5.1	1.97	12
Piranha washed	2.460 ppm	0.895 ppm	0.122 ppm	5.0	1.95	14
Acetone washed	24.099 ppm	1.030 ppm	0.113 ppm	4.8	1.96	11

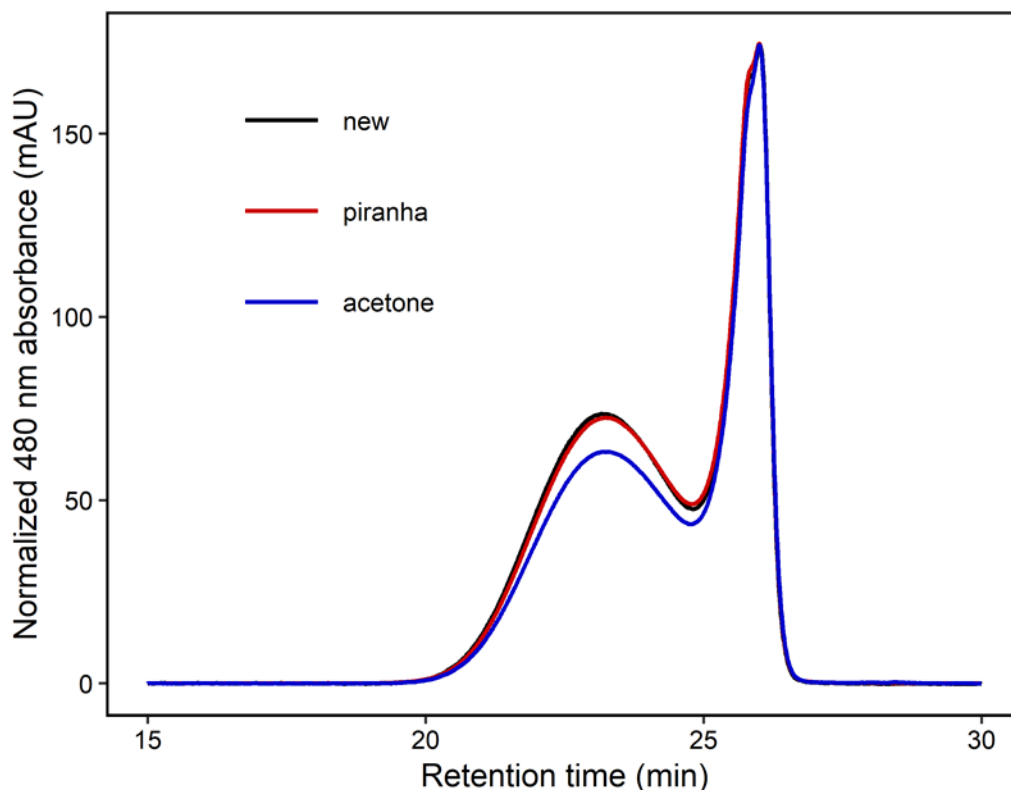


Figure S37. GPC traces of P1 polymerized using either a new (black), piranha washed (red), or acetone washed (blue) stir bar.

Metal doping studies

Trace metal analysis control reactions were performed using **1** using a variant of *via general procedure A*, wherein 5 mol% of the respective metal chloride salt was added into Vial 1 before generation of the Grignard.

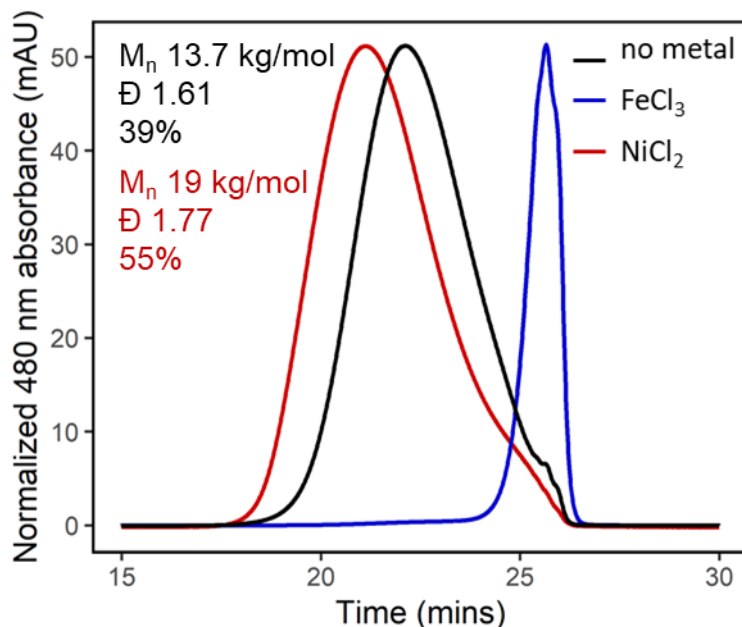


Figure S38. GPC traces of **P1** polymerized via preparation A with 5 mol % NiCl_2 (red) and 5 mol % FeCl_3 (blue).

Parts-per-million nickel: dark reactivity controls

To understand the possible contribution of parts per-million-nickel to the observed reactivity, we conducted a series of control reactions in which nickel was intentionally doped into the solvent prior to polymerization and left in the dark.

THF with different concentrations of nickel were prepared via serial dilution of stock nickel(II) bromide ethylene glycol dimethyl ether complex ($\text{NiBr}_2 \cdot \text{dme}$) in a nitrogen-filled glove box. This complex was used due to the low solubility of non-ligated NiX_2 salts. Monomer **1-MgBr** was prepared via *general procedure A* using the nickel-doped solvent. The polymerizations were performed in the dark and the reactions wrapped in aluminum foil over the course of the polymerization. Polymerizations were quenched with methanol prior to exposure to light.

Table S13. GPC results of **P1** polymerized in the dark with varying concentrations of $\text{Ni}(\text{glyme})\text{Br}_2$ added to the reaction. Molecular weights determined via refractive index traces.

Ni loading (ppm)	Yield (%)	M_n (kg/mol)	\bar{D}
1 ppm (no Ni added)	5 ^a	3.2	1.6
11 ppm (0.064 mol %)	10 ^a	2.1	3.9

28 ppm (0.16 mol %)	12	14.6	1.6
56 ppm (0.32 mol %)	23	17.1	1.6

^aSample could not be precipitated into methanol.

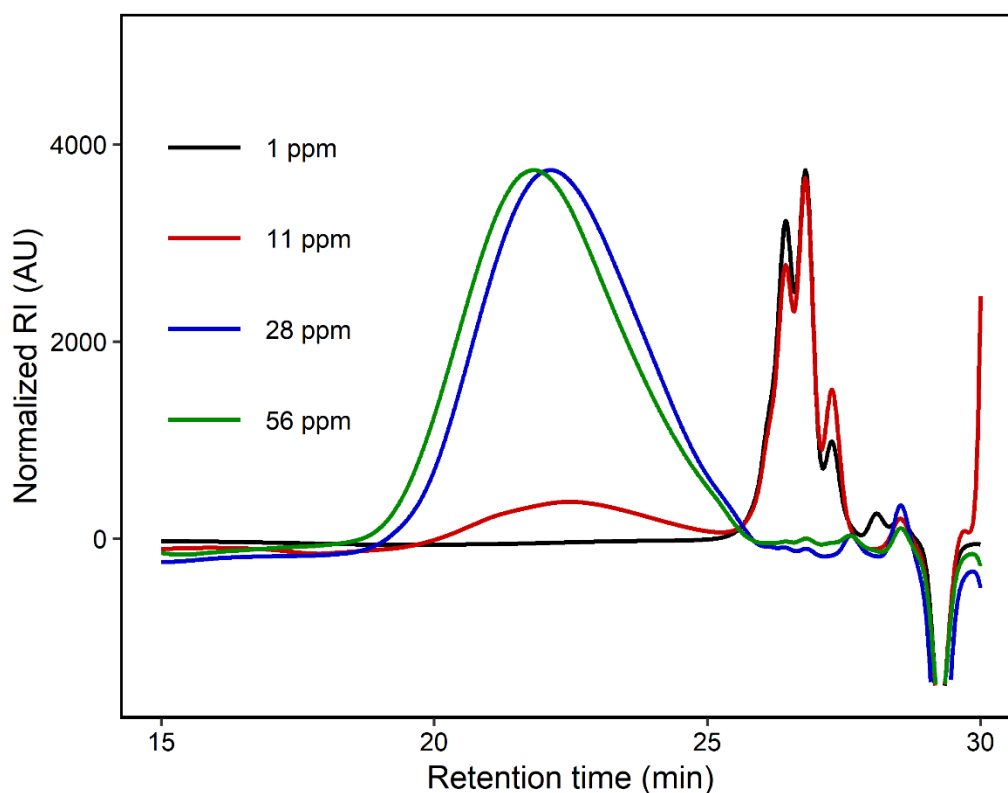


Figure S39 GPC traces of **P1** prepared via reaction of **1-MgBr** in the dark with solvent doped with varying concentrations of Ni(glyme)Br₂.

Donor-acceptor ABA dark control experiments

To determine background reactivity and the role of light for the ABA monomers, polymerizations were performed in the dark. **P6** and **P8** were polymerized using *general procedure A* and **P7** was polymerized using *general procedure B*, consistent with the light reactions. For all reactions, no material precipitated into acetone, so the acetone solution was concentrated. GPC RI traces were outside the calibration limit of the instrument (800 g/mol PS), indicating that only low-molecular-weight species (neither oligomer nor polymer) were obtained.

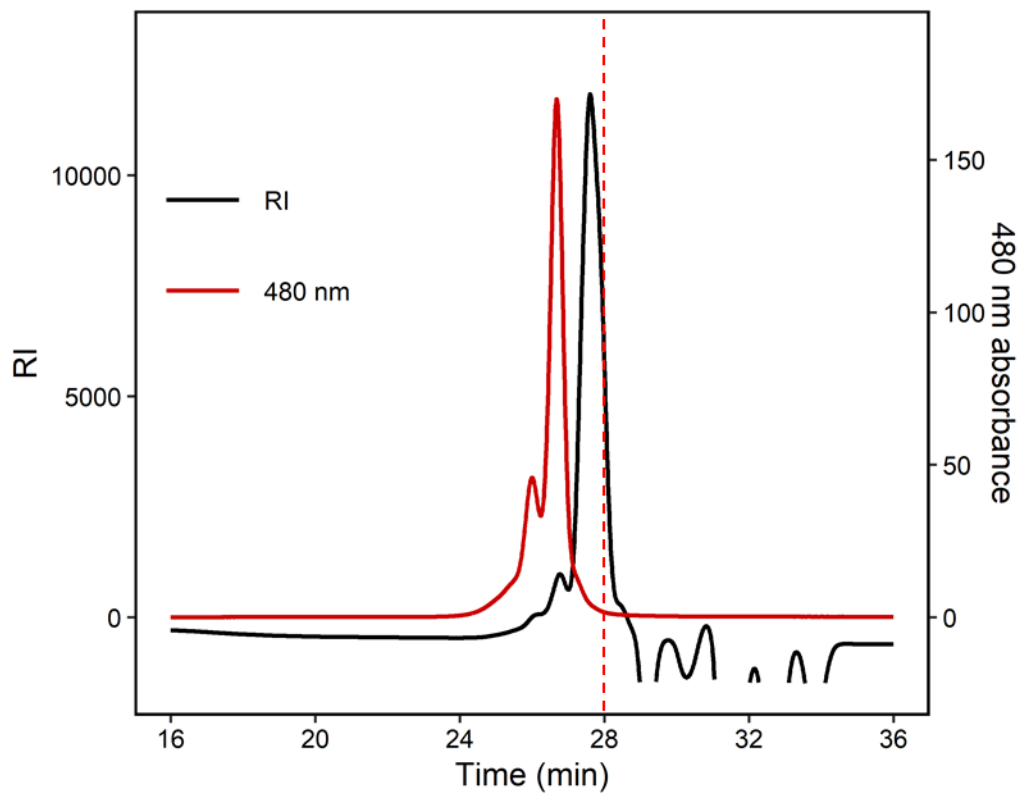


Figure S40 GPC trace of **P6** dark control reaction. Dashed red line shows lower calibration limit of polystyrene MW calibration curve.

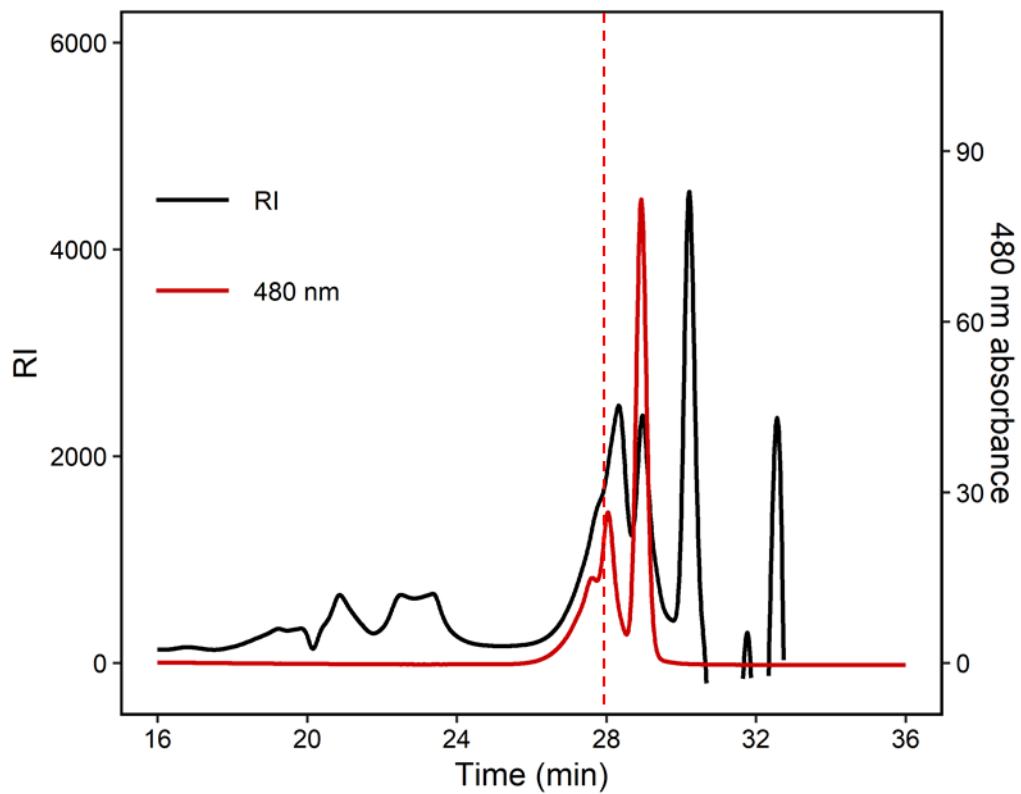


Figure S41 GPC trace of **P7** dark control reaction. Dashed red line shows lower calibration limit of polystyrene MW calibration curve.

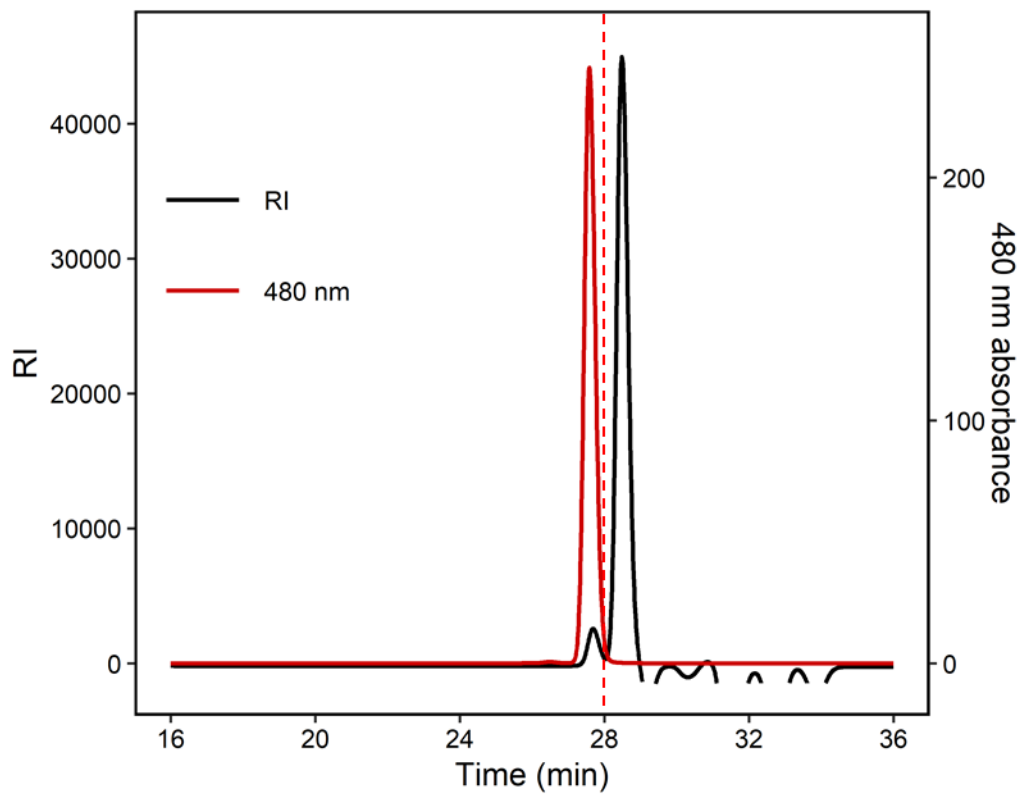


Figure S42 GPC trace of **P8** dark control reaction. Dashed red line shows lower calibration limit of polystyrene MW calibration curve.

UV-Vis spectra

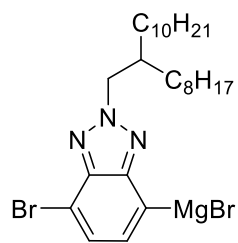
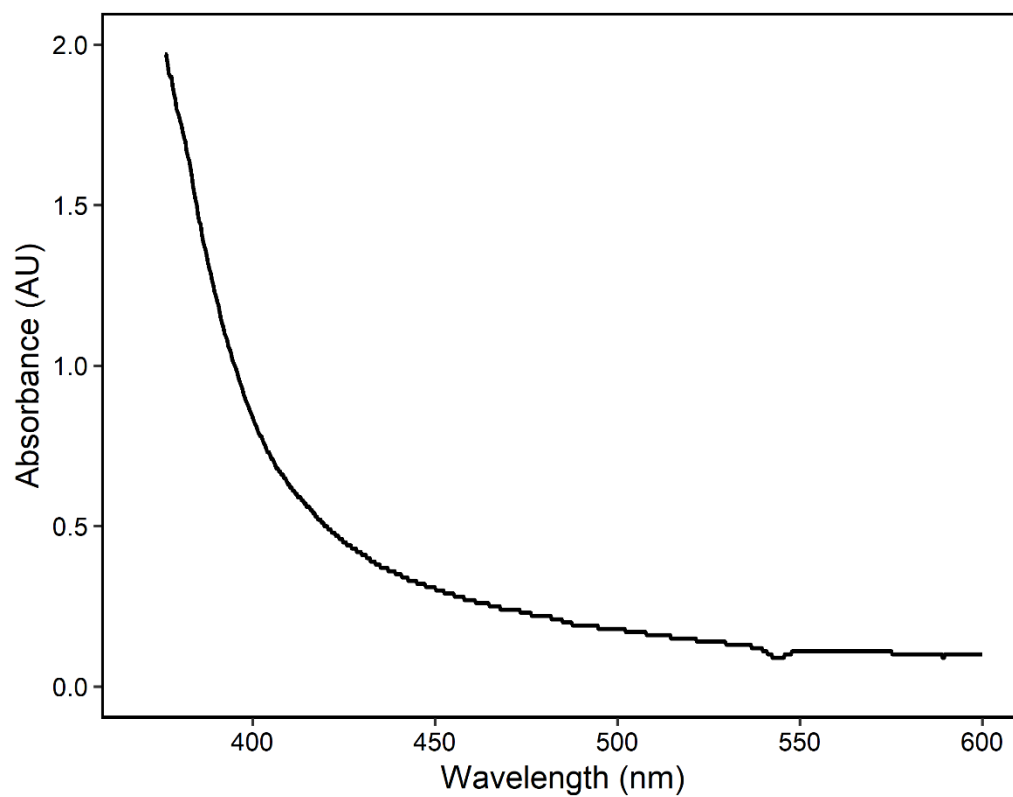


Figure S43. UV-Vis absorbance of **1-MgBr** (50 mM) in THF.

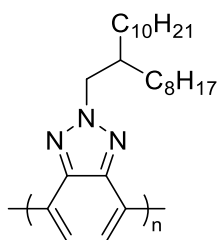
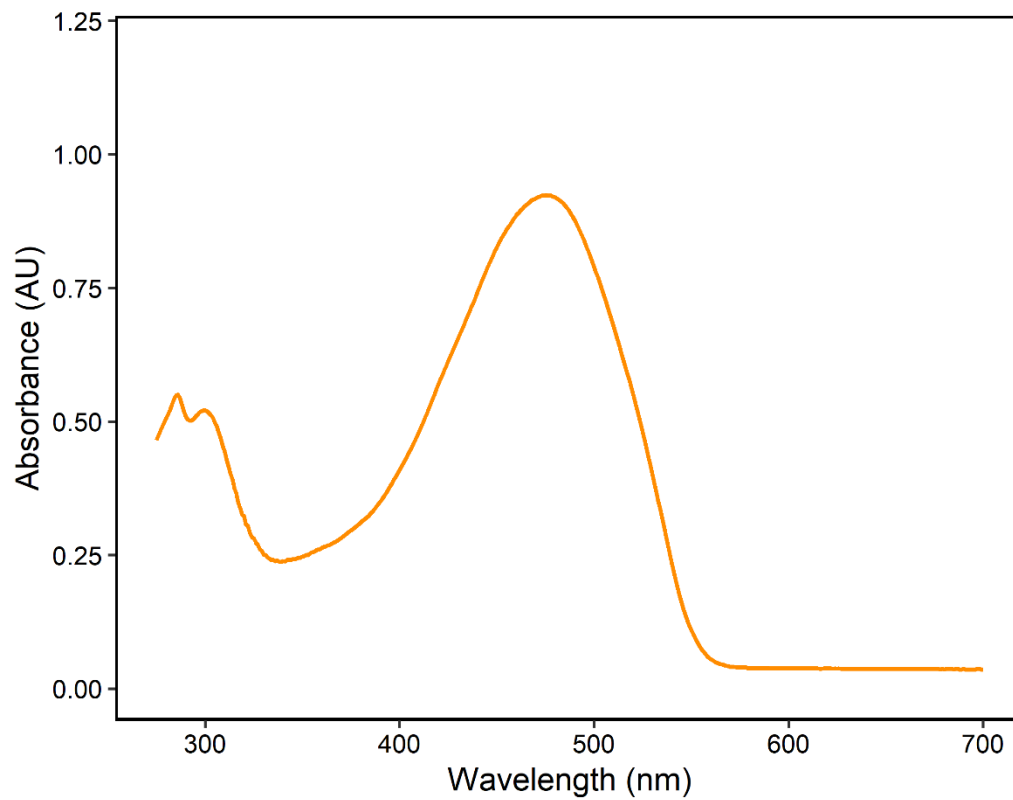


Figure S44. UV-Vis absorbance of **P1** in THF.

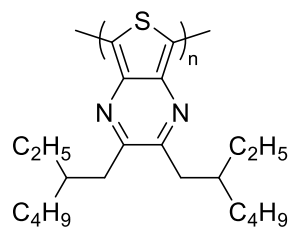
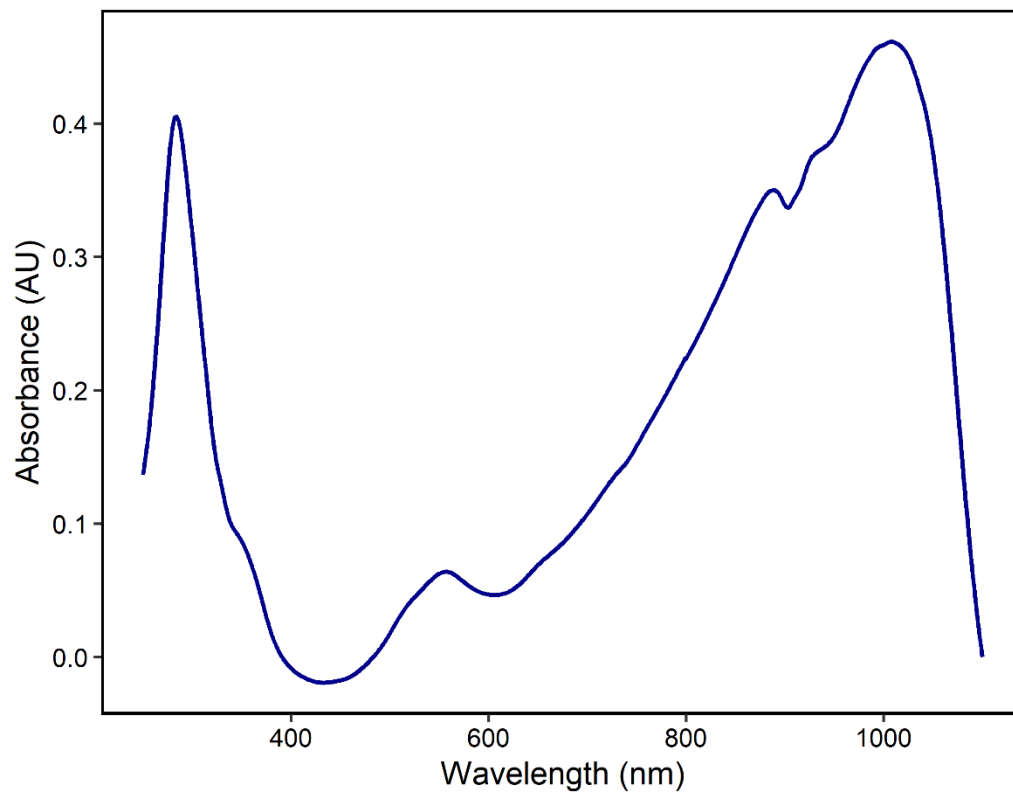


Figure S45. UV-Vis absorbance of **P2** in THF.

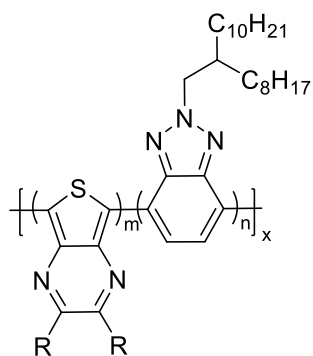
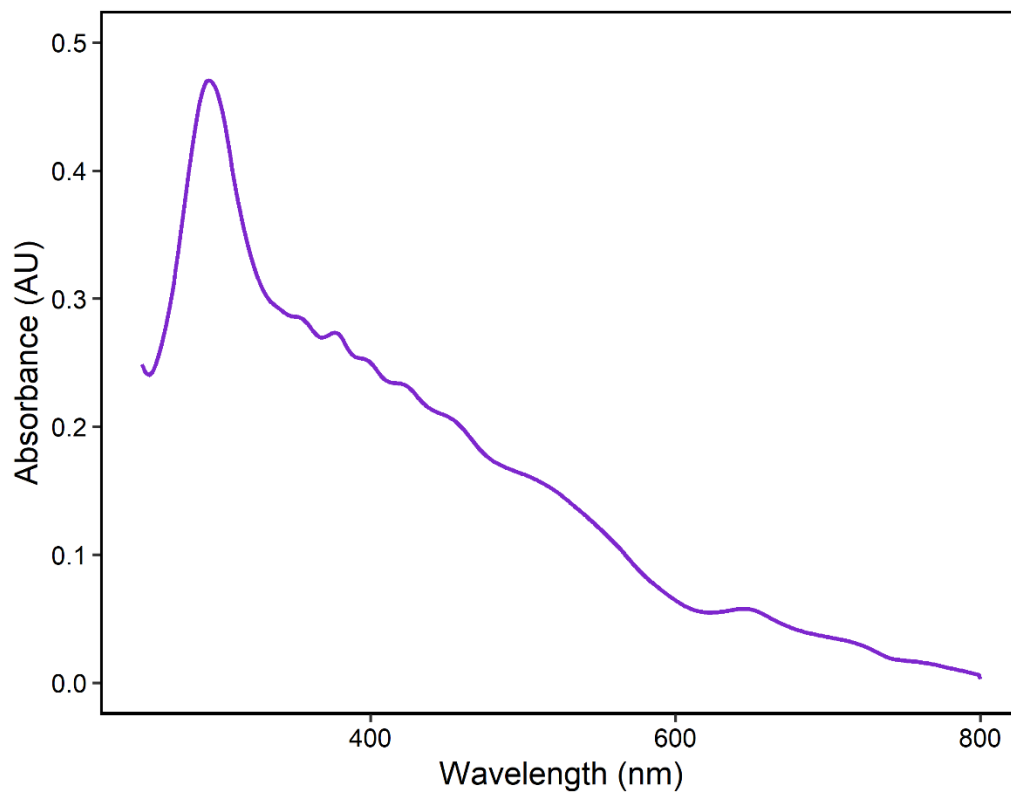


Figure S46. UV-Vis absorbance of statistical copolymer of **1** and **2** comprised of a 1.1:1 ratio of **1:2** in THF.

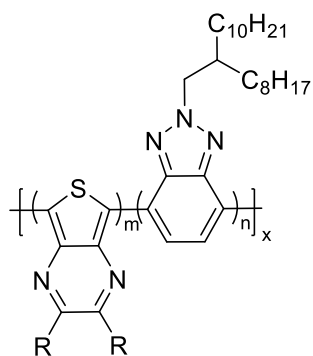
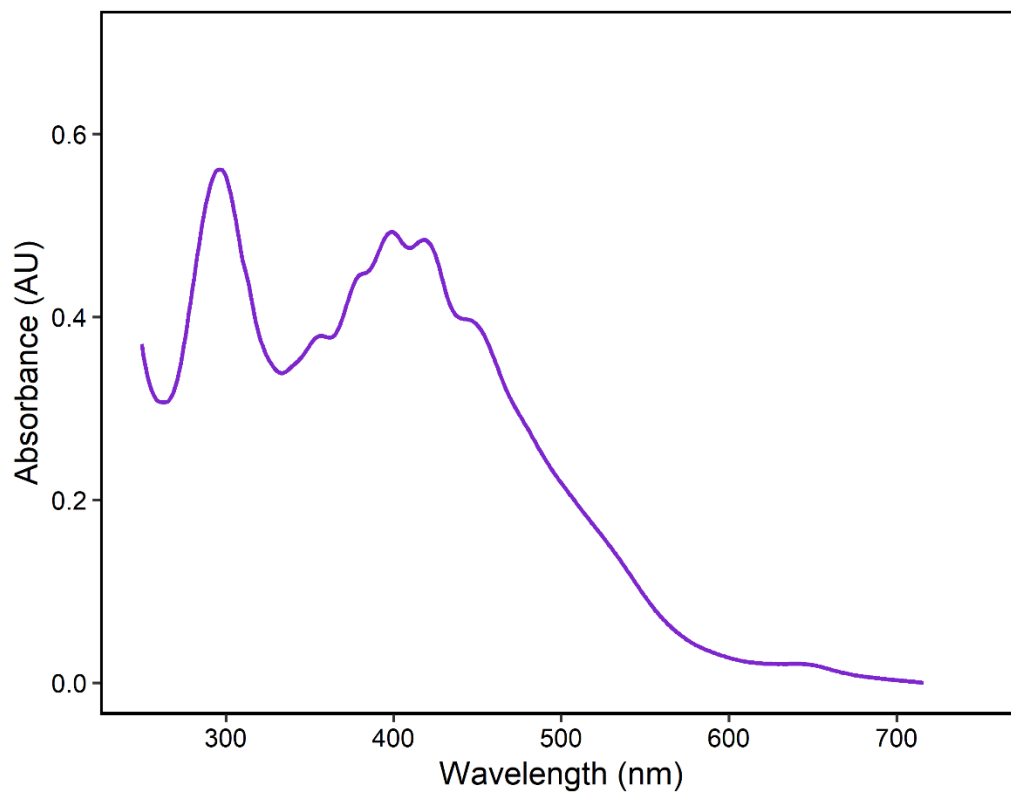


Figure S47. UV-Vis absorbance of statistical copolymer of **1** and **2** comprised of a 3.2:1 ratio of **1**:**2** in THF.

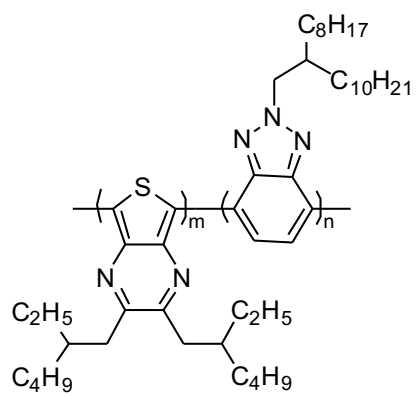
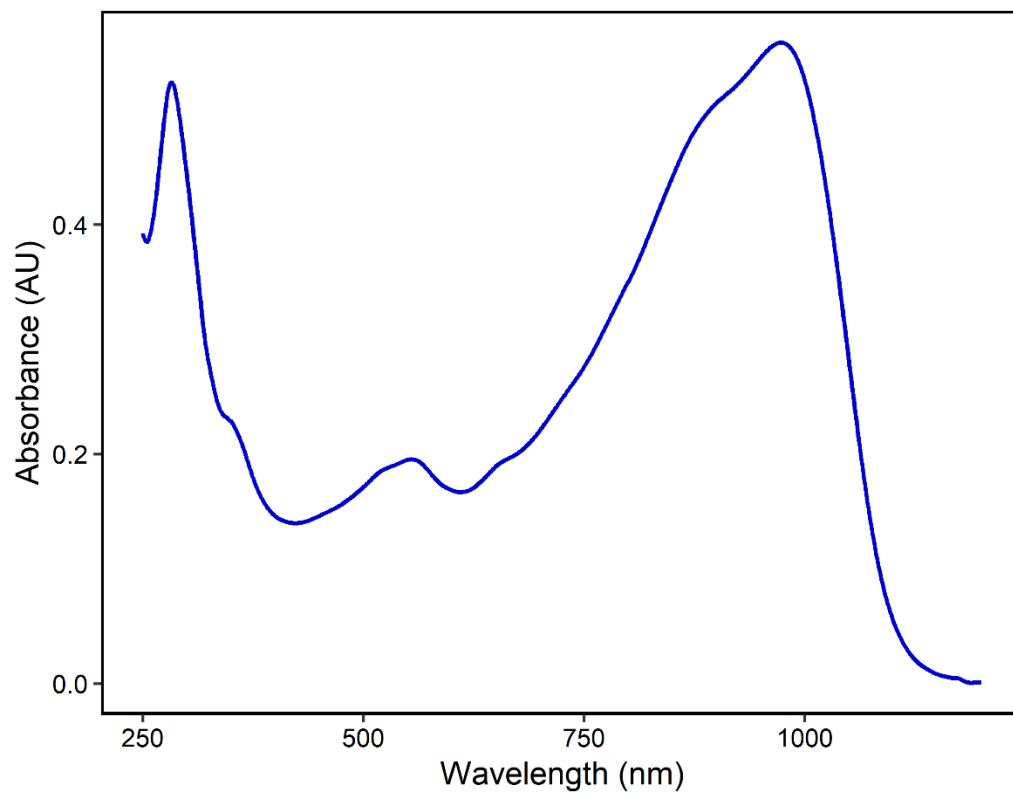


Figure S48. UV-Vis absorbance of **P5** in THF.

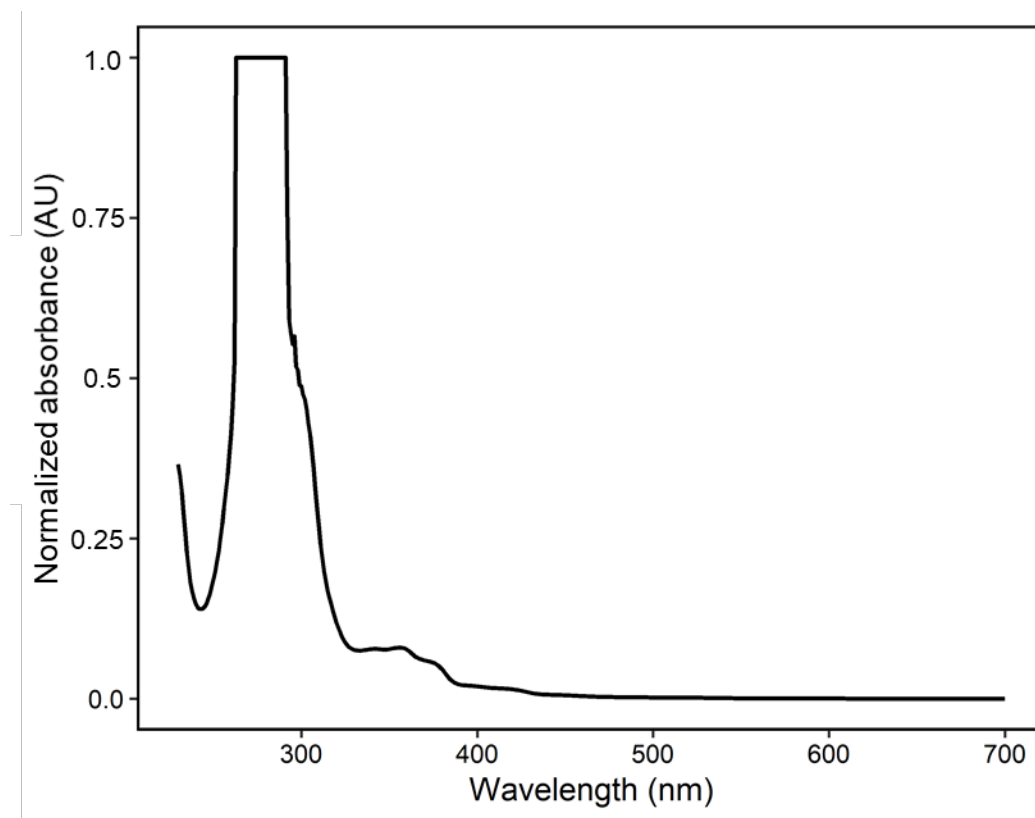


Figure S49. UV-Vis absorbance of crude reaction mixture for control dark reaction (table 1 entry 5) of **1-MgBr** generated via *general procedure A*. Absorbance of the solution at 550 nm is 0.006 AU.

NMR spectra

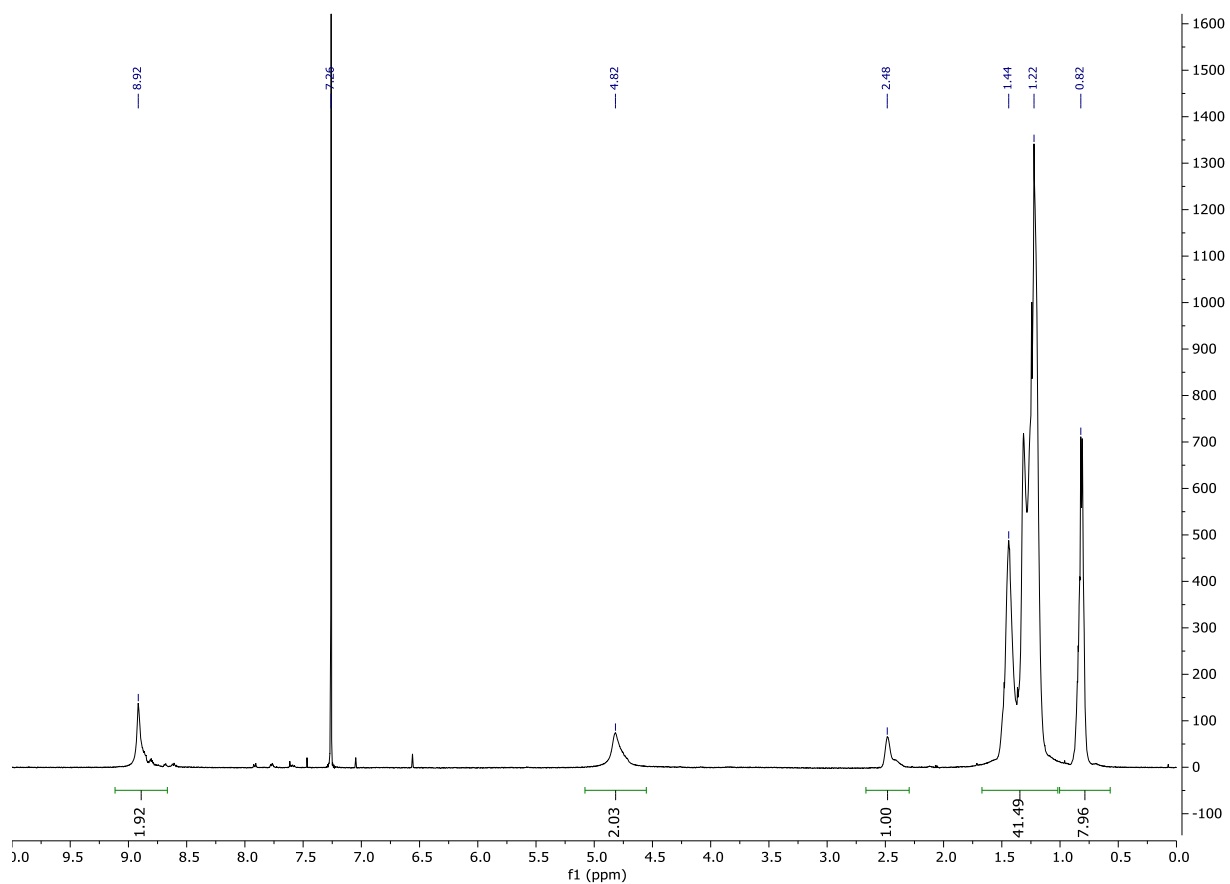
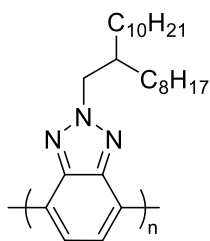


Figure S50. 1H -NMR (500 MHz, $CDCl_3$) **P1**

1H NMR (500 MHz, Chloroform-d) δ 8.92 (s, 2H), 4.82 (s, 2H), 2.48 (s, 1H), 1.33 (m, 32H), 0.82 (s, 6H).

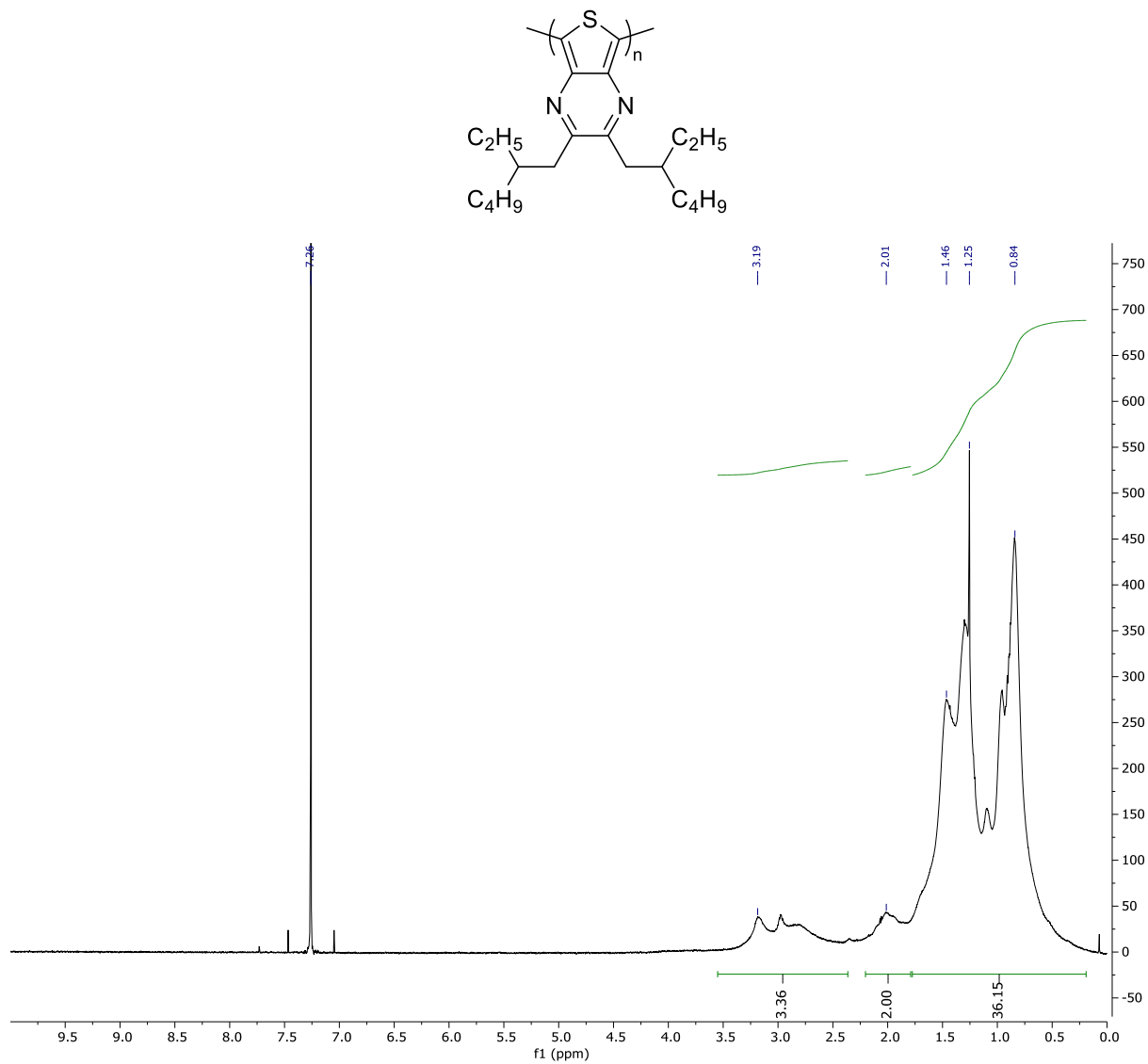


Figure S51. ¹H-NMR (500 MHz, CDCl₃) **P2**

¹H NMR (500 MHz, Chloroform-d) δ 3.19 (m), 2.01 (s), 1.77 – 0.29 (m).

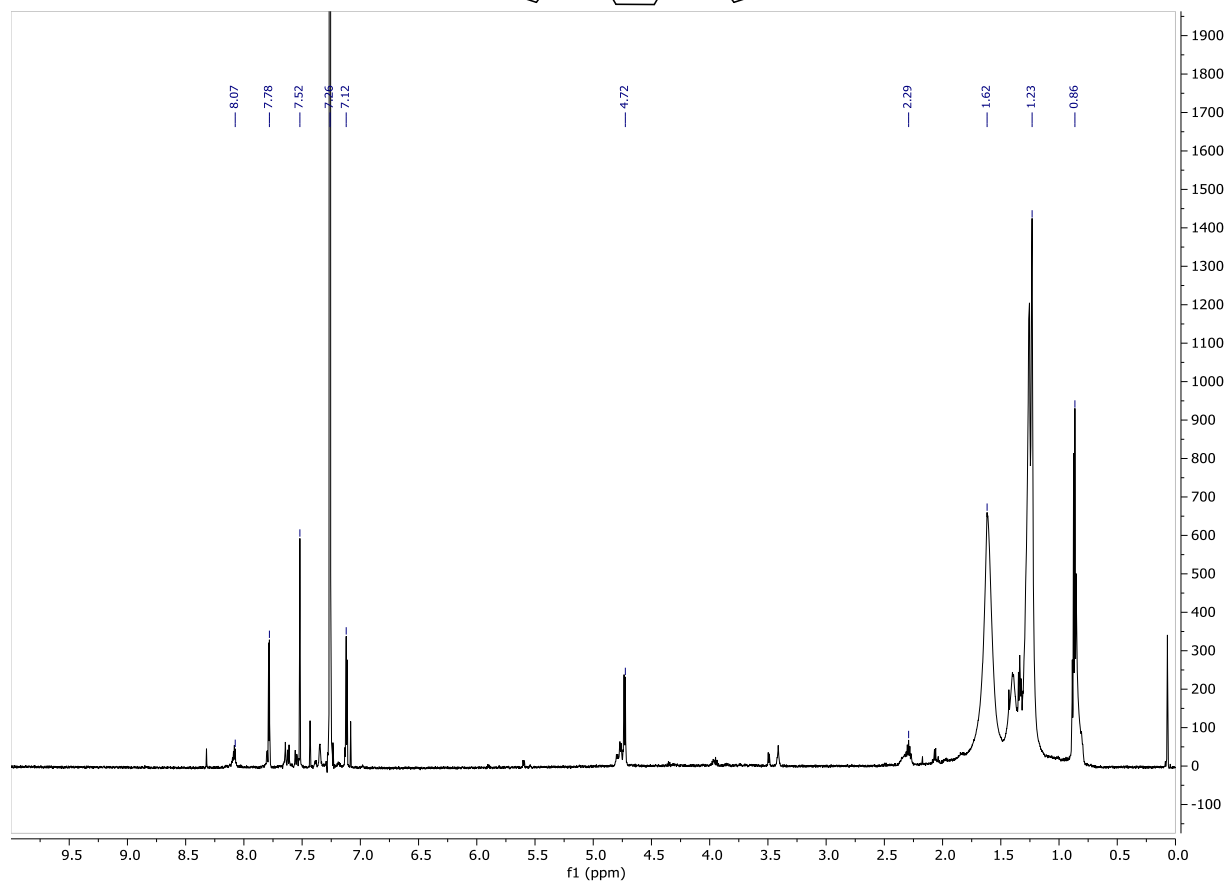
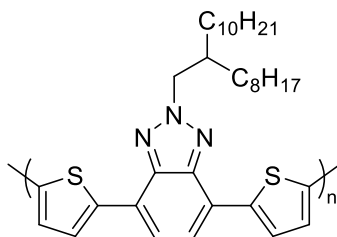


Figure S52. $^1\text{H-NMR}$ (600 MHz, CDCl_3) **P6**

$^1\text{H NMR}$ (600 MHz, Chloroform-d) δ 8.07 (s), 7.78 (s), 7.52 (s), 7.12 (s), 4.72 (s), 2.29 (s), 1.62 (s), 1.23 (s), 0.86 (s).

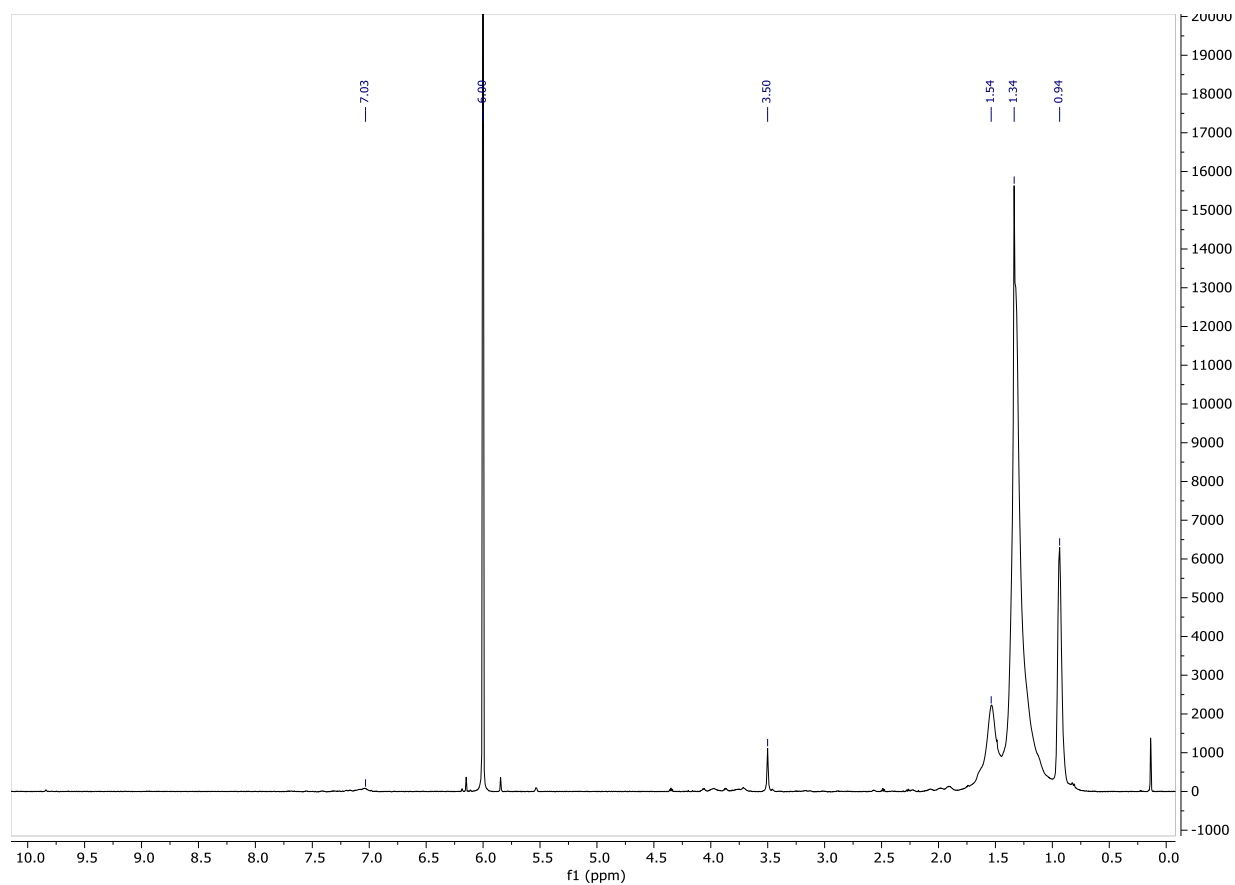
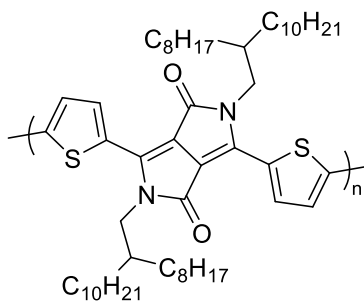


Figure S53. $^1\text{H-NMR}$ (600 MHz, $\text{C}_2\text{D}_2\text{Cl}_4$, 100°C) **P7**

$^1\text{H NMR}$ (600 MHz, Tetrachloroethane- d_2) δ 7.03 (s), 3.50 (s), 1.54 (s), 1.34 (s), 0.94 (s).

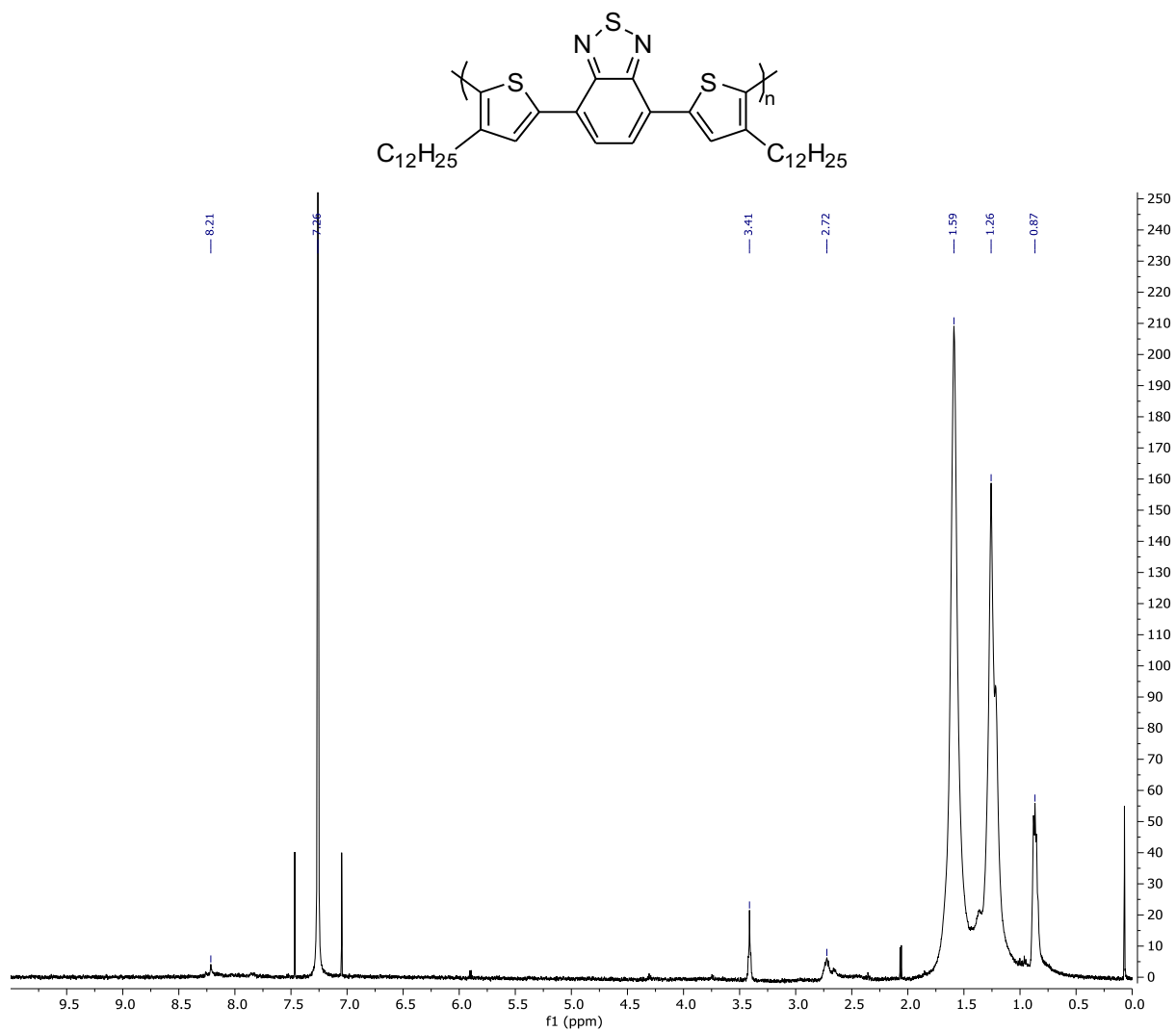


Figure S54. ¹H-NMR (500 MHz, CDCl₃) P8

¹H NMR (500 MHz, CDCl₃) δ 8.21(s), 3.41(s), 2.72(s), 1.59(s), 1.26(s), 0.87(s).

MALDI-TOF MS spectra

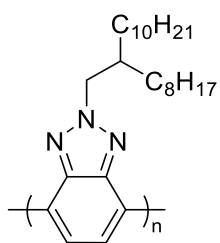
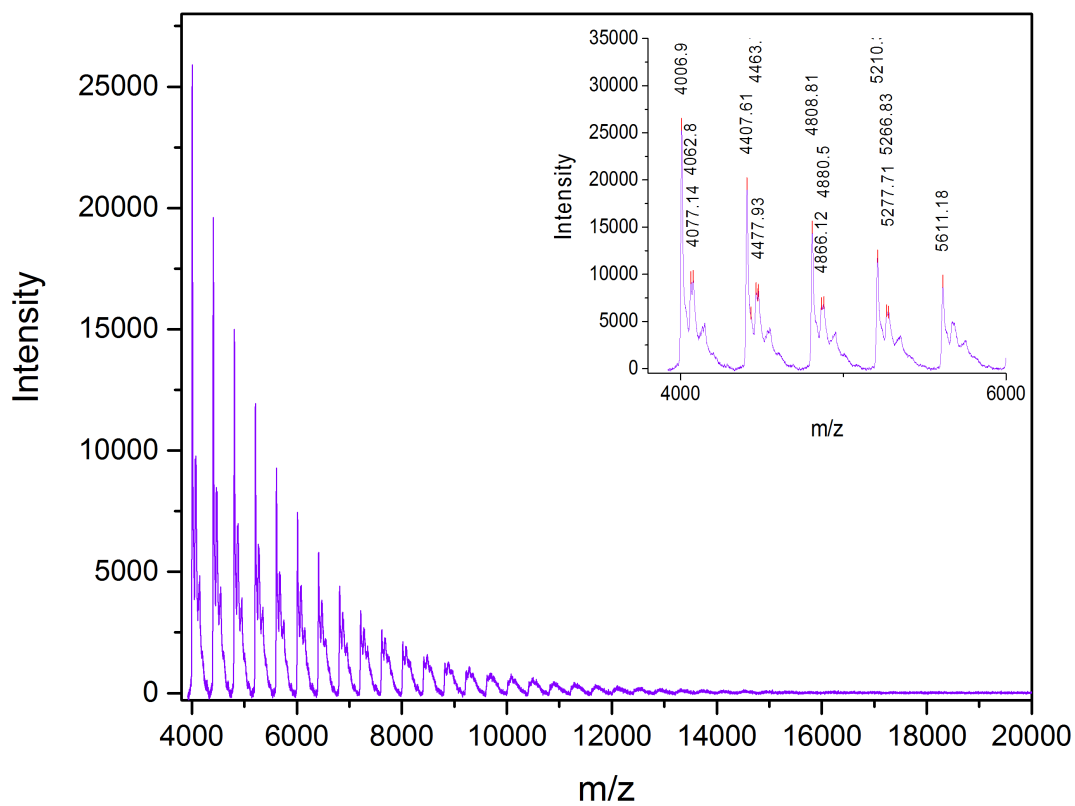


Figure S55. MALDI-TOF of P1.

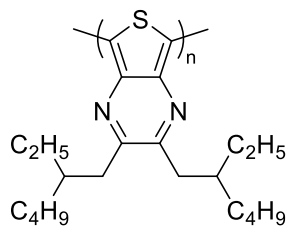
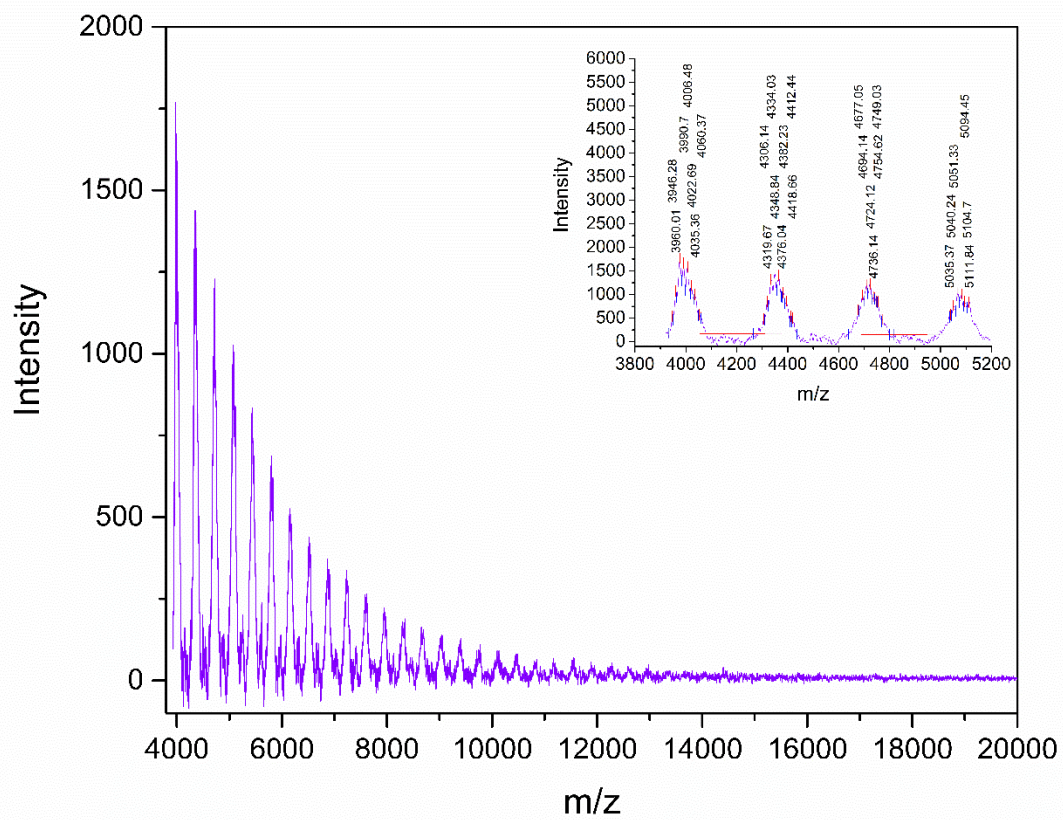


Figure S57. MALDI-TOF of P2.

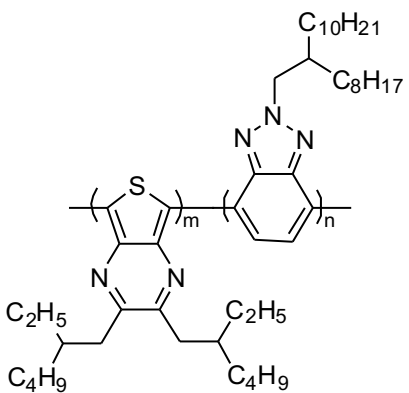
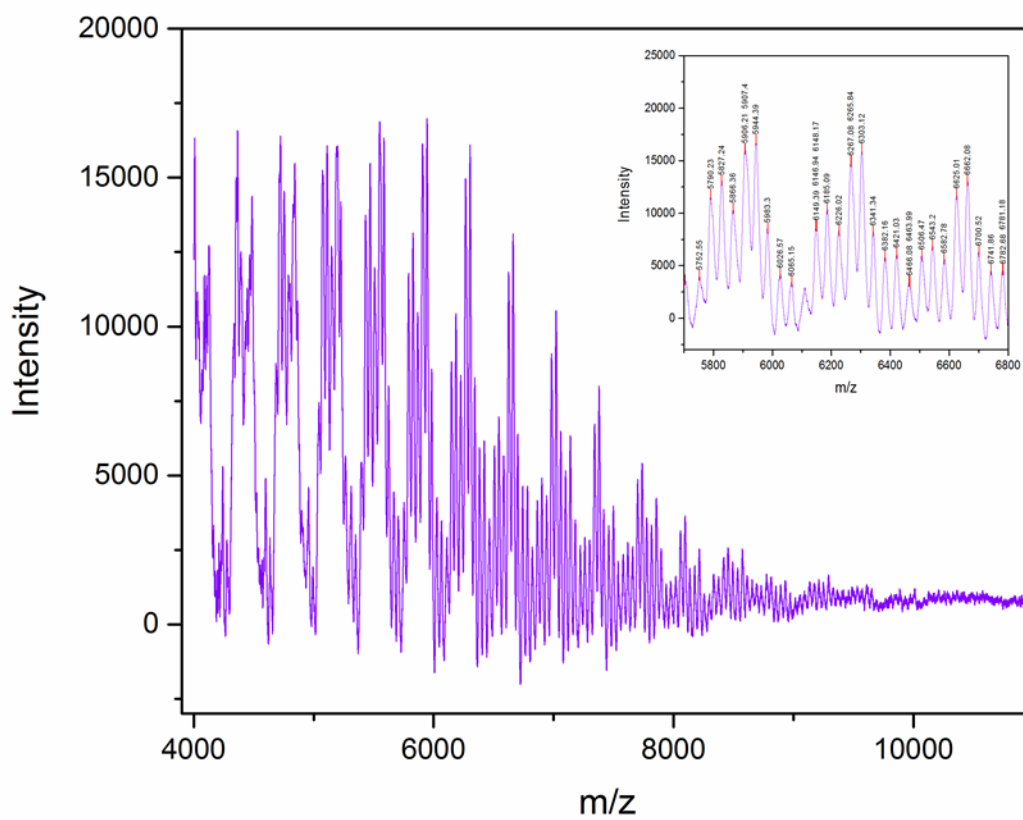


Figure S58. MALDI-TOF of P5.

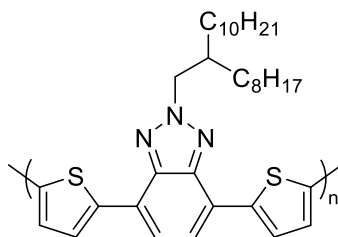
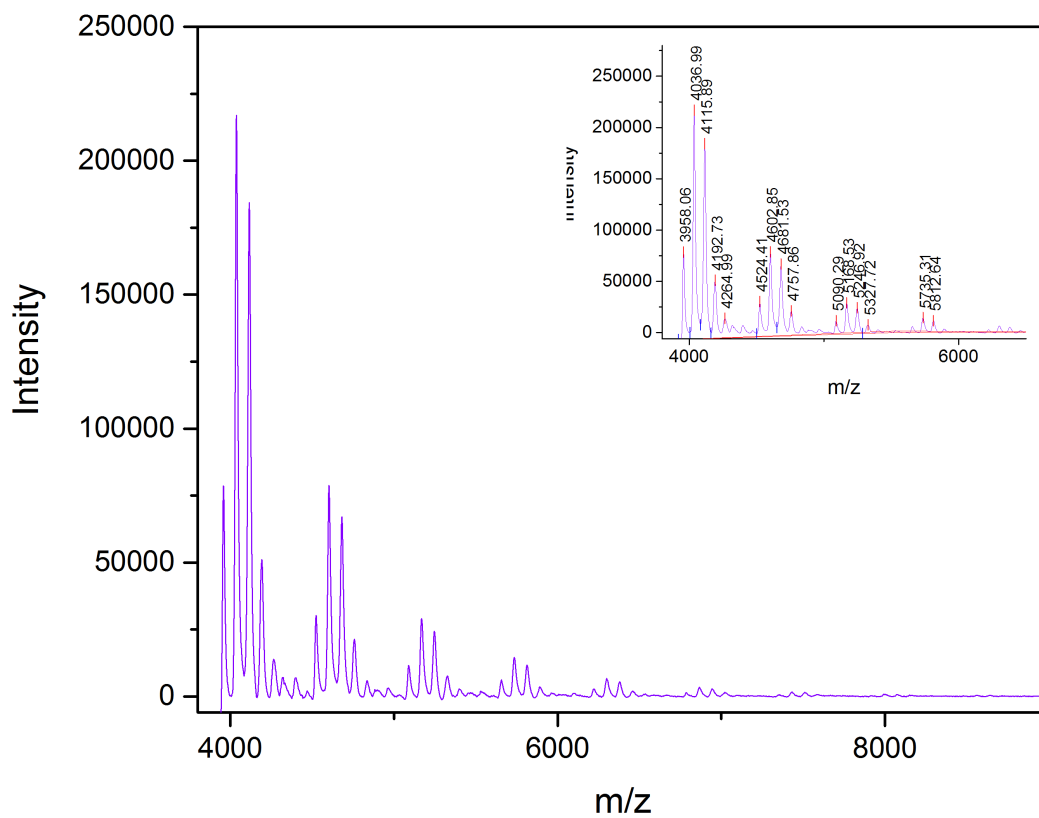


Figure S59. MALDI-TOF of P6.

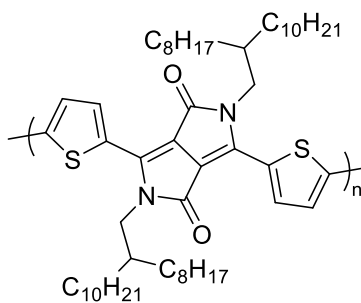
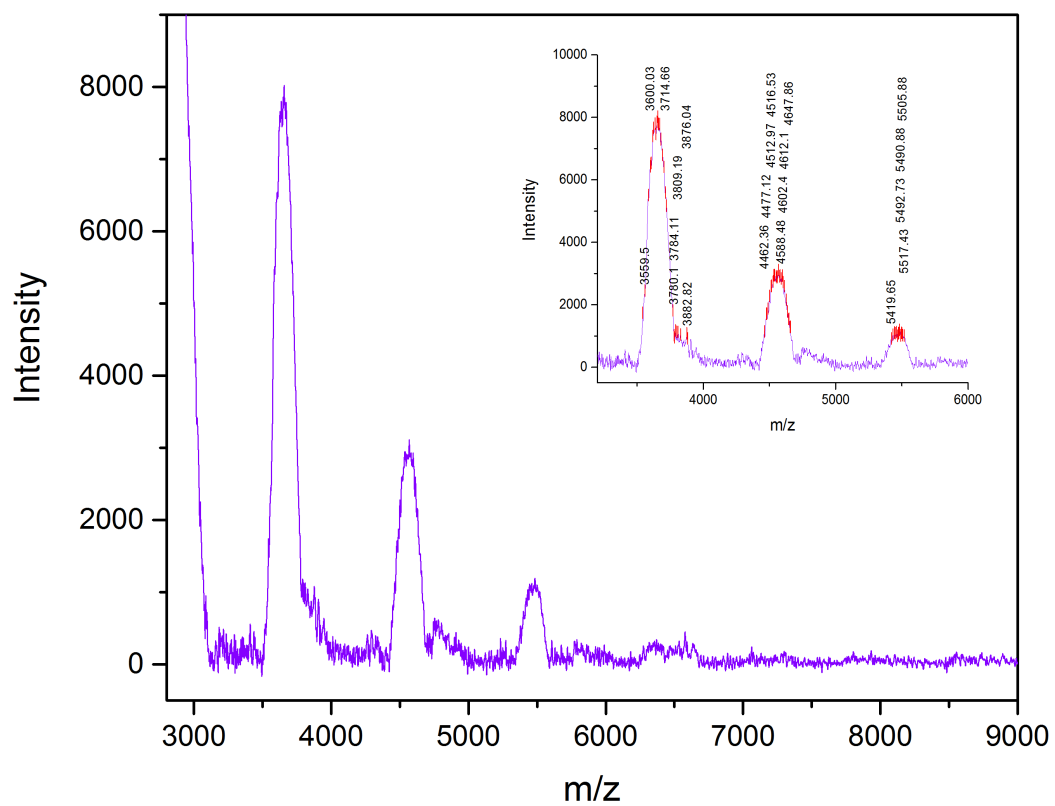


Figure S60. MALDI-TOF of P7.

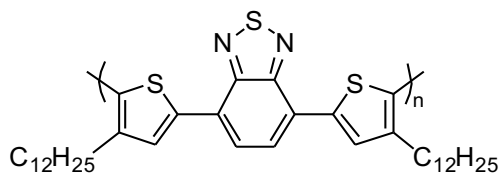
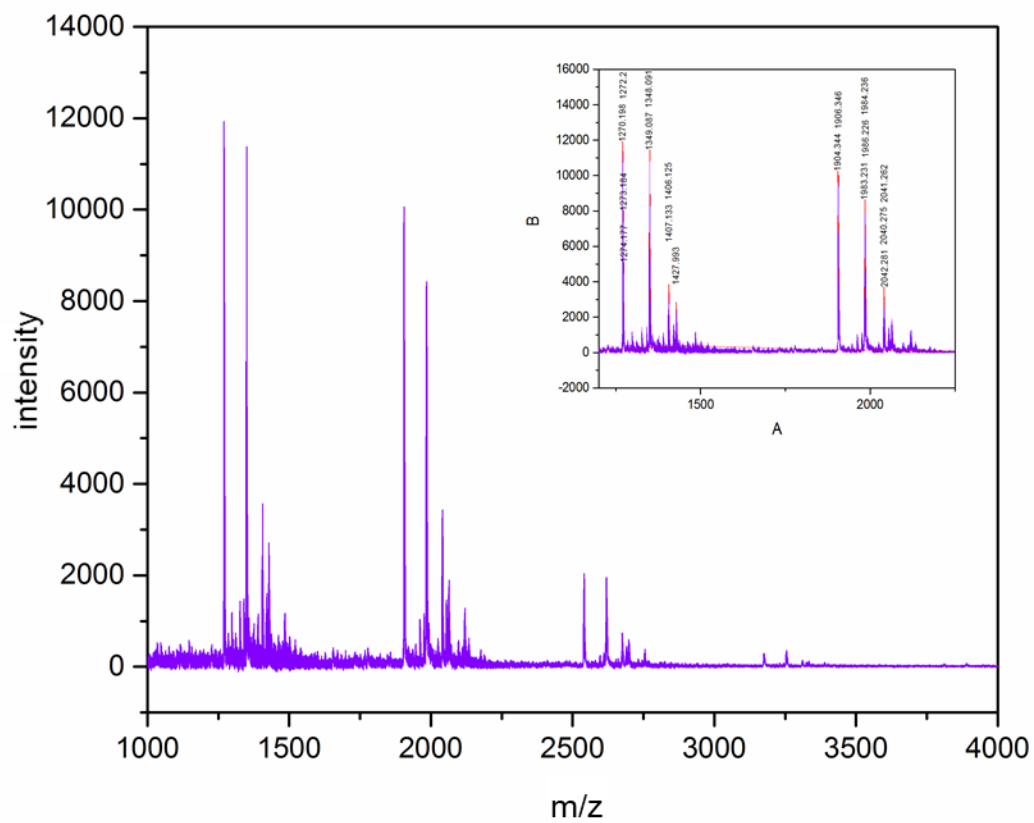


Figure S61. MALDI-TOF of P8.

References

- (1) Ozdemir, M.; Choi, D.; Kwon, G.; Zorlu, Y.; Kim, H.; Kim, M.-G.; Seo, S.; Sen, U.; Citir, M.; Kim, C.; Usta, H. Design, synthesis, and characterization of α,ω -disubstituted indeno[1,2-b]fluorene-6,12-dione-thiophene molecular semiconductors. Enhancement of ambipolar charge transport through synthetic tailoring of alkyl substituents. *RSC Advances* **2016**, *6*, 212-226.
- (2) Yang, R.; Tian, R.; Yan, J.; Zhang, Y.; Yang, J.; Hou, Q.; Yang, W.; Zhang, C.; Cao, Y. Deep-Red Electroluminescent Polymers: Synthesis and Characterization of New Low-Band-Gap Conjugated Copolymers for Light-Emitting Diodes and Photovoltaic Devices. *Macromolecules* **2005**, *38*, 244-253.
- (3) Bridges, C. R.; McCormick, T. M.; Gibson, G. L.; Hollinger, J.; Seferos, D. S. Designing and Refining Ni(II)diimine Catalysts Toward the Controlled Synthesis of Electron-Deficient Conjugated Polymers. *J. Am. Chem. Soc.* **2013**, *135*, 13212-13219.
- (4) Kenning, D. D.; Mitchell, K. A.; Calhoun, T. R.; Funfar, M. R.; Sattler, D. J.; Rasmussen, S. C. Thieno[3,4-b]pyrazines: Synthesis, Structure, and Reactivity. *J. Org. Chem.* **2002**, *67*, 9073-9076.
- (5) Karsten, B. P.; Janssen, R. A. J. Small Band Gap Oligothieno[3,4-b]pyrazines. *Org. Lett.* **2008**, *10*, 3513-3516.
- (6) Chen, C.-H.; Hsieh, C.-H.; Dubosc, M.; Cheng, Y.-J.; Hsu, C.-S. Synthesis and Characterization of Bridged Bithiophene-Based Conjugated Polymers for Photovoltaic Applications: Acceptor Strength and Ternary Blends. *Macromolecules* **2010**, *43*, 697-708.
- (7) Pasker, F. M.; Klein, M. F. G.; Sanyal, M.; Barrena, E.; Lemmer, U.; Colsmann, A.; Höger, S. Photovoltaic response to structural modifications on a series of conjugated polymers based on 2-aryl-2H-benzotriazoles. *J. Polym. Sci. A* **2011**, *49*, 5001-5011.
- (8) Lee, O. P.; Yiu, A. T.; Beaujuge, P. M.; Woo, C. H.; Holcombe, T. W.; Millstone, J. E.; Douglas, J. D.; Chen, M. S.; Fréchet, J. M. J. Efficient Small Molecule Bulk Heterojunction Solar Cells with High Fill Factors via Pyrene-Directed Molecular Self-Assembly. *Adv. Mater.* **2011**, *23*, 5359-5363.
- (9) Chen, D.; Zhao, Y.; Zhong, C.; Gao, S.; Yu, G.; Liu, Y.; Qin, J. Effect of polymer chain conformation on field-effect transistor performance: synthesis and properties of two arylene imide based D-A copolymers. *J. Mater. Chem.* **2012**, *22*, 14639-14644.
- (10) Zoombelt, A. P.; Mathijssen, S. G. J.; Turbiez, M. G. R.; Wienk, M. M.; Janssen, R. A. J. Small band gap polymers based on diketopyrrolopyrrole. *J. Mater. Chem.* **2010**, *20*, 2240-2246.
- (11) Jayakannan, M.; van Hal, P. A.; Janssen, R. A. J. Synthesis and structure-property relationship of new donor-acceptor-type conjugated monomers and polymers on the basis of thiophene and benzothiadiazole. *J. Polym. Sci. A* **2002**, *40*, 251-261.
- (12) Pollit, A. A.; Bridges, C. R.; Seferos, D. S. Evidence for the Chain-Growth Synthesis of Statistical π -Conjugated Donor-Acceptor Copolymers. *Macromol. Rapid Commun.* **2015**, *36*, 65-70.
- (13) Gu, K.; Onorato, J.; Xiao, S. S.; Luscombe, C. K.; Loo, Y.-L. Determination of the Molecular Weight of Conjugated Polymers with Diffusion-Ordered NMR Spectroscopy. *Chem. Mater.* **2018**, *30*, 570-576.